

Supporting information

# ***N*-Aryl substituents have the influence on photophysics of tetraaryl-pyrrolo[3,2-*b*]pyrroles**

**Wojciech D. Petrykowski<sup>a</sup>, Marzena Banasiewicz<sup>b</sup>, Olaf Morawski<sup>b</sup>, Cristina A. Barboza<sup>\*b</sup> and Daniel T. Gryko<sup>\*a</sup>**

*a. Institute of Organic Chemistry, Polish Academy of Sciences, Kasprzaka 44/52, 01-224 Warsaw, Poland.*

*E-mail: dtgryko@icho.edu.pl*

*b. Institute of Physics, Polish Academy of Sciences, Al. Lotników 32/46, 02-668 Warsaw, Poland.*

*E-mail: crissetubal@gmail.com*

## **Table of contents**

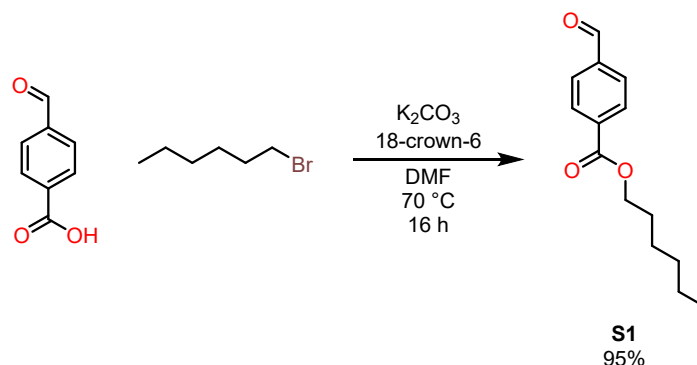
1. Instrumentation and materials .....	2
2. Synthesis .....	3
3. Computational details .....	14
4. Theoretical Data .....	15
5. UV/Vis spectra .....	29
6. NMR spectra .....	78
7. References .....	93

## 1. Instrumentation and materials

All chemicals were used as received unless noted otherwise. Dry and degassed solvents were obtained using MBRAUN Solvent Purification System. All NMR spectra were collected with 500 MHz and 600 MHz Varian spectrometers. Chemical shifts ( $\delta$ , ppm) were determined with tetramethylsilane as the internal reference.  $J$  values are given in Hz. All the mass spectra were obtained by atmospheric pressure chemical ionization (APCI-MS) or electrospray ionization (ESI-MS). All melting points were measured with an automated melting point apparatus. Chromatography was performed on silica gel (230-400 mesh).

## 2. Synthesis

### Hexyl 4-formylbenzoate (S1)

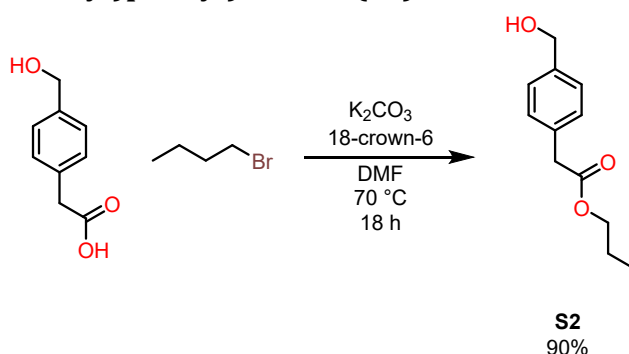


The compound was obtained according to previously reported procedure for a similar compound with minor modifications.<sup>1</sup>

4-Formylbenzoic acid (2.00 g, 13.3 mmol, 1 equiv.), potassium carbonate (3.68 g, 26.6 mmol, 2 equiv.) and 18-crown-6 (a single crystal) were added into a 250 mL Schlenk flask. The flask was evacuated and filled with argon three times. Dry and degassed DMF (40 mL) and 1-bromohexane (2.20 g, 1.86 mL, 13.3 mmol, 1 equiv.) were added, the flask was connected into a bubbler and flushed with argon. The mixture was stirred at 70 °C for 16 hours. DMF was evaporated under reduced pressure and 30 mL of water were added. The product was extracted 5 times with 30 mL of hexane and dried with sodium sulfate. The solvent was evaporated and the liquid yellow product was dried in vacuum at room temperature for one hour. Yield: 2.96 g (12.7 mmol, 95%).

$^1\text{H NMR}$  (600 MHz,  $\text{CDCl}_3$ )  $\delta_{\text{CDCl}_3}$ : 10.11 (s, 1H), 8.20 (d,  $J = 8.2$  Hz, 2H), 7.96 (d,  $J = 8.5$  Hz, 2H), 4.36 (t,  $J = 6.7$  Hz, 2H), 1.92 – 1.69 (m, 2H), 1.50 – 1.41 (m, 2H), 1.40 – 1.27 (m, 4H), 1.02 – 0.76 (t,  $J = 7.4$  Hz, 3H).

### Butyl 2-(4-(hydroxymethyl)phenyl)acetate (S2)



The compound was obtained according to previously reported procedure for a similar compound with minor modifications.<sup>1</sup>

2-(4-(Hydroxymethyl)phenyl)acetic acid (3.50 g, 21.1 mmol, 1 equiv.), potassium carbonate (5.82 g, 42.1 mmol, 2 equiv.) and 18-crown-6 (a single crystal) were added into a 250 mL Schlenk flask. The flask was evacuated and filled with argon three times. Dry and degassed DMF (70 mL) and 1-bromobutane (2.89 g, 2.27 mL, 21.1 mmol, 1 equiv.) were added, the flask was connected into a

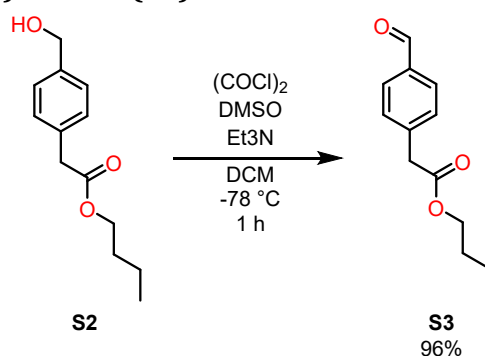
bubbler and flushed with argon. The mixture was stirred at 70 °C for 18 hours. DMF was evaporated under reduced pressure and 70 mL of water were added. The product was extracted 5 times with 70 mL of hexane/diethyl ether 1:1 and dried with sodium sulfate. The solvent was evaporated and the liquid yellow product was dried in vacuum at room temperature for one hour. Yield: 4.23 g (19.2 mmol, 90%).

**<sup>1</sup>H NMR** (500 MHz, CDCl<sub>3</sub>)  $\delta_{CDCl_3}$ : 7.32 (d, *J* = 8.1 Hz, 2H), 7.27 (d, *J* = 8.1 Hz, 2H), 4.67 (s, 2H), 4.09 (t, *J* = 6.7 Hz, 2H), 3.61 (s, 2H), 1.67 – 1.47 (m, 2H), 1.35 (h, *J* = 7.4 Hz, 2H), 0.91 (t, *J* = 7.4 Hz, 3H).

**<sup>13</sup>C NMR** (151 MHz, CDCl<sub>3</sub>)  $\delta_{CDCl_3}$ : 171.65, 139.67, 133.57, 129.43, 127.19, 65.05, 64.79, 41.11, 30.57, 19.05, 13.65.

**HR MS** (ESI<sup>+</sup>): calculated for C<sub>13</sub>H<sub>18</sub>O<sub>3</sub>Na [M+Na]<sup>+</sup>: 245.1154; found 245.1159.

### Butyl 2-(4-formylphenyl)acetate (S3)



The compound was obtained according to the original procedure for Swern oxidation with minor modifications.<sup>2</sup>

A 250 mL Schlenk flask was evacuated and heated with a heatgun, then it was filled with argon. The flask was again evacuated and filled with argon three times. Dry, degassed DCM (55 mL) and oxalyl chloride (2.57 g, 1.73 mL, 20.2 mmol, 1.1 equiv.) were added. The solution was cooled down to -78 °C with a dry ice/isopropanol bath. Dry DMSO (3.45 g, 3.1 mL, 44.1 mmol, 2.4 equiv.) was added dropwise. The solution was stirred for 10 minutes. **S2** (4.08 g, 18.4 mmol, 1 equiv.) was separately dissolved in dry and degassed DCM (18 mL) under argon. It was added into the reaction mixture dropwise. After 15 minutes of stirring, dry triethylamine (9.30 g, 13 mL, 91.9 mmol, 5 equiv.) was added and the cooling bath was removed. After one hour of stirring 50 mL of water was added. The phases were separated and the water phase was extracted three times with 50 mL of DCM. The combined organic phases were dried with magnesium sulfate. 50 mL of hexane were added. Dimethyl sulfide with DCM were distilled out of the mixture. 50 mL of water and 20 mL of hexane were added. The phases were separated and the water phase was extracted with 20 mL of hexane/diethyl ether 1:1 3 times. The combined organic phases were dried with magnesium sulfate. The solvents were evaporated and the liquid yellow product was dried in vacuum at room temperature for one hour. Yield: 3.87 g (17.6 mmol, 96%).

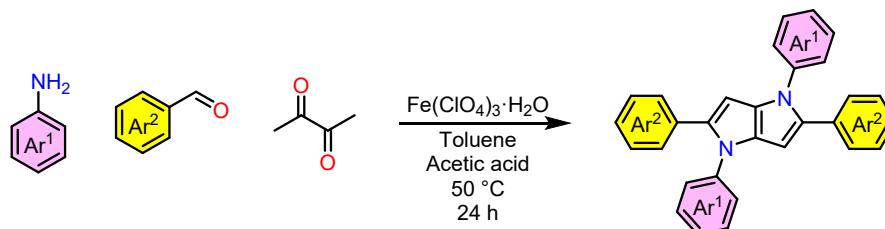
**<sup>1</sup>H NMR** (500 MHz, CDCl<sub>3</sub>)  $\delta_{CDCl_3}$ : 10.00 (s, 1H), 7.85 (d, *J* = 8.1 Hz, 2H), 7.46 (d, *J* = 8.0 Hz, 2H), 4.11 (t, *J* = 6.7 Hz, 2H), 3.70 (s, 2H), 1.69 – 1.57 (m, 2H), 1.34 (h, *J* = 7.4 Hz, 2H), 0.91 (t, *J* = 7.4 Hz, 3H).



$^{13}\text{C}$  NMR (126 MHz,  $\text{CDCl}_3$ )  $\delta_{\text{CDCl}_3}$ : 191.83, 170.65, 141.04, 135.34, 130.01, 65.09, 41.52, 30.53, 19.04, 13.63.

HR MS (APCI+): (ESI+): calculated for  $\text{C}_{13}\text{H}_{15}\text{O}_3$   $[\text{M}+\text{H}]^+$ : 219.1021; found 219.1023.

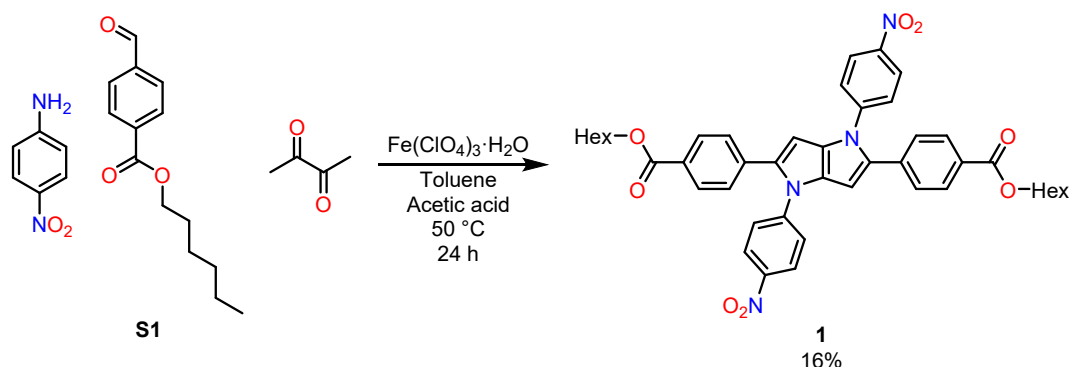
## General procedure for the synthesis of TAPPs



TAPPs were prepared according to previously reported procedure with modified purification protocols in order to assure sufficient purity of the products for UV/Vis spectroscopy.<sup>3</sup>

The amine (2.13 mmol, 2 equiv.) and the aldehyde (2.13 mmol, 2 equiv.) were dissolved in a mixture of toluene (1.7 mL) and acetic acid (1.7 mL) and stirred at 50 °C in an open 50 mL flask for one hour. Iron(III) perchlorate (24 mg, 64  $\mu\text{mol}$ , 0.06 equiv.) and butanedione (92 mg, 94  $\mu\text{L}$ , 1.1  $\mu\text{mol}$ , 1 equiv.) were added and the resulting dark solution was stirred at 50 °C in an open flask for 24 hours. The purification procedures are described below for each TAPP individually.

## Purification of 1



Prepared from 4-nitroaniline (295 mg) and **S1** (500 mg).

The solvents were evaporated. 10 mL of diethyl ether were added, the precipitate was filtered and washed with diethyl ether and acetonitrile. It was recrystallized from 27 mL of ethyl acetate. The red product was dried in vacuum at 70 °C for 8 hours. Yield: 128 mg (170  $\mu\text{mol}$ , 16%).

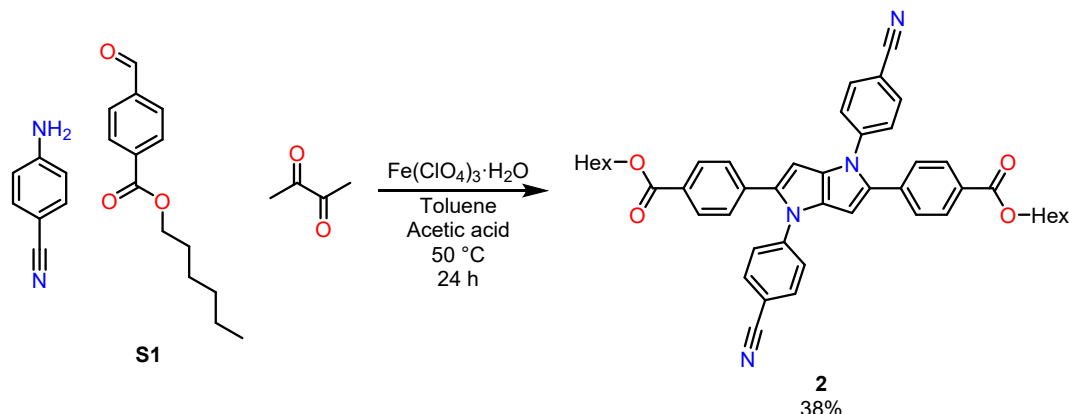
$^1\text{H}$  NMR (500 MHz,  $\text{CDCl}_3$ )  $\delta_{\text{CDCl}_3}$ : 8.27 (d,  $J$  = 9.0 Hz, 4H), 7.97 (d,  $J$  = 8.5 Hz, 4H), 7.40 (d,  $J$  = 9.0 Hz, 4H), 7.28 (d,  $J$  = 8.5 Hz, 4H), 6.61 (s, 2H), 4.31 (t,  $J$  = 6.7 Hz, 4H), 1.92 – 1.68 (m, 4H), 1.44 (p,  $J$  = 7.2 Hz, 4H), 1.38 – 1.28 (m, 8H), 0.90 (t,  $J$  = 7.4 Hz, 6H).

$^{13}\text{C}$  NMR (126 MHz,  $\text{CDCl}_3$ )  $\delta_{\text{CDCl}_3}$ : 166.14, 145.21, 144.68, 136.50, 136.03, 132.22, 129.94, 129.08, 127.82, 125.12, 124.86, 98.22, 65.32, 31.44, 28.67, 25.69, 22.53, 13.99.

HR MS (APCI+): calculated for  $\text{C}_{44}\text{H}_{45}\text{N}_4\text{O}_8$   $[\text{M}+\text{H}]^+$ : 757.3237; found 757.3226.

Melting point: 243.5 - 244.1 °C

## Purification of 2



Prepared from 4-aminobenzonitrile (252 mg) and **S1** (500 mg).

The solvents were evaporated. 10 mL of diethyl ether were added, the precipitate was filtered and washed with diethyl ether and acetonitrile. The product was recrystallized from 26 mL of toluene. The yellow product was dried in vacuum at 70 °C for 8 hours. Yield: 288 mg (401  $\mu\text{mol}$ , 38%).

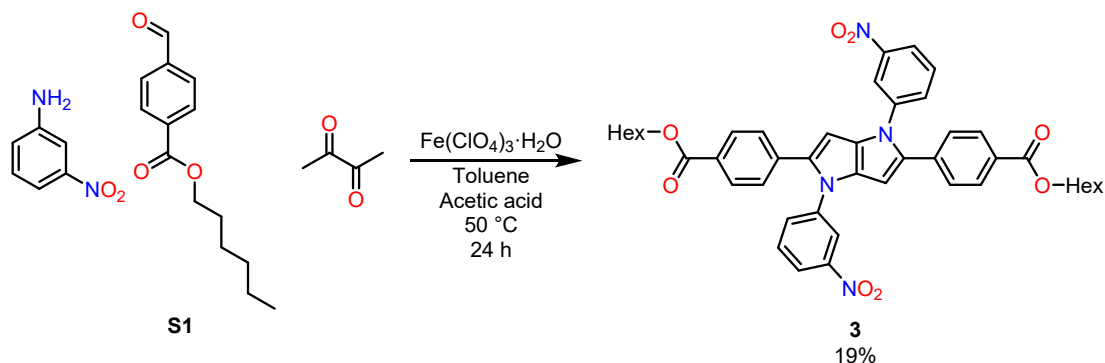
$^1\text{H NMR}$  (600 MHz,  $\text{CDCl}_3$ )  $\delta_{\text{CDCl}_3}$ : 7.95 (d,  $J = 8.3$  Hz, 4H), 7.69 (d,  $J = 8.5$  Hz, 4H), 7.36 (d,  $J = 8.5$  Hz, 4H), 7.26 (d,  $J = 8.0$  Hz, 4H), 6.56 (s, 2H), 4.31 (t,  $J = 6.7$  Hz, 4H), 1.76 (p,  $J = 6.8$  Hz, 4H), 1.44 (p,  $J = 7.0$  Hz, 4H), 1.38 – 1.27 (m, 8H), 0.90 (t,  $J = 7.0$  Hz, 6H).

$^{13}\text{C NMR}$  (151 MHz,  $\text{CDCl}_3$ )  $\delta_{\text{CDCl}_3}$ : 166.19, 143.09, 136.61, 135.81, 133.46, 132.19, 129.86, 128.91, 127.75, 125.21, 118.24, 109.60, 97.79, 65.29, 31.45, 28.67, 25.69, 22.53, 14.00.

**HR MS** (APCI<sup>+</sup>): calculated for  $\text{C}_{46}\text{H}_{45}\text{N}_4\text{O}_4$   $[\text{M}+\text{H}]^+$ : 717.3441; found 717.3442.

**Melting point:** 261.7 - 263.3 °C

## Purification of 3



Prepared from 3-nitroaniline (295 mg) and **S1** (500 mg).

The solvents were evaporated. 10 mL of diethyl ether were added, the precipitate was filtered and washed with diethyl ether and acetonitrile. The product was recrystallized from 10 mL of acetonitrile. The yellow product was dried in vacuum at 70 °C for 8 hours. Yield: 157 mg (207  $\mu\text{mol}$ , 19%).

$^1\text{H NMR}$  (600 MHz,  $\text{CDCl}_3$ )  $\delta_{\text{CDCl}_3}$ : 8.26 (t,  $J = 2.0$  Hz, 2H), 8.15 (d,  $J = 8.2$  Hz, 2H), 7.94 (d,  $J = 8.4$  Hz, 4H), 7.54 (t,  $J = 8.1$  Hz, 2H), 7.48 (d,  $J = 8.0$  Hz, 2H), 7.28 (d,  $J = 8.4$  Hz, 4H), 6.58 (s, 2H),

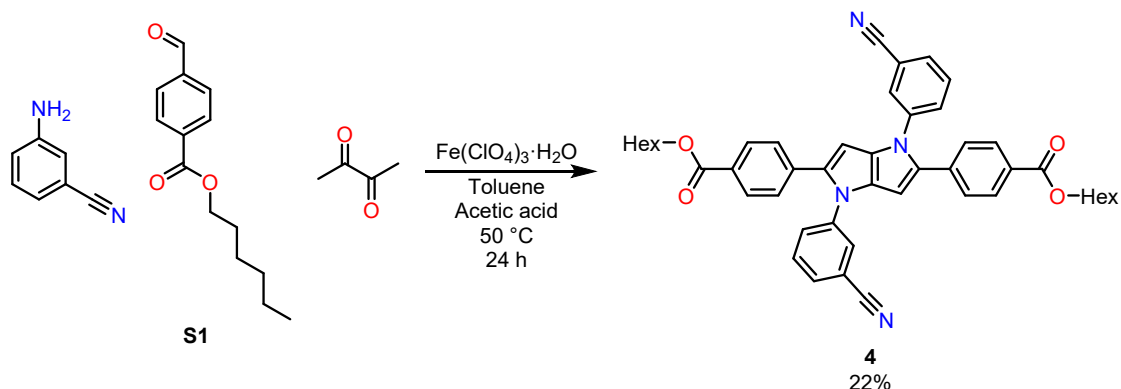
4.30 (t,  $J = 6.7$  Hz, 4H), 1.88 – 1.68 (m, 4H), 1.43 (p,  $J = 7.1$  Hz, 4H), 1.38 – 1.26 (m, 8H), 0.90 (t,  $J = 7.4$  Hz, 6H).

$^{13}\text{C}$  NMR (151 MHz,  $\text{CDCl}_3$ )  $\delta_{\text{CDCl}_3}$ : 166.21, 148.92, 140.59, 136.47, 136.00, 132.38, 131.06, 130.23, 129.89, 128.84, 127.77, 120.93, 119.51, 97.08, 65.26, 31.45, 28.66, 25.69, 22.53, 13.99.

HR MS (APCI<sup>+</sup>): calculated for  $\text{C}_{44}\text{H}_{44}\text{N}_4\text{O}_8$   $[\text{M}]^+$ : 756.3159; found 756.3155.

Melting point: 178.7 - 179.1 °C

### Purification of 4



Prepared from 4-aminobenzonitrile (252 mg) and S1 (500 mg).

The solvents were evaporated. 10 mL of diethyl ether were added, the precipitate was filtered and washed with diethyl ether and acetonitrile. The product was recrystallized from 17 mL of acetonitrile. The yellow product was dried in vacuum at 70 °C for 8 hours. Yield: 167 mg (233  $\mu\text{mol}$ , 22%).

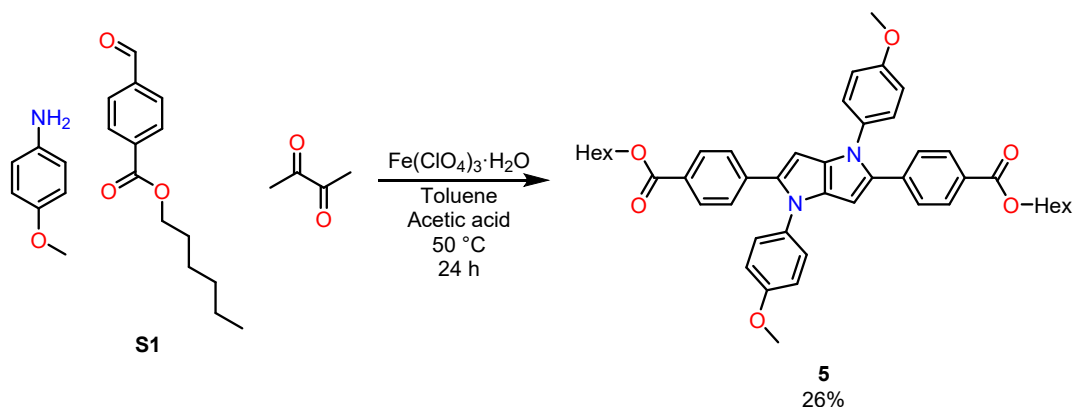
$^1\text{H}$  NMR (600 MHz,  $\text{CDCl}_3$ )  $\delta_{\text{CDCl}_3}$ : 7.94 (d,  $J = 8.5$  Hz, 4H), 7.62 (s, 2H), 7.58 (d,  $J = 7.7$  Hz, 2H), 7.50 (t,  $J = 7.9$  Hz, 2H), 7.44 (d,  $J = 9.0$  Hz, 2H), 7.25 (d,  $J = 8.5$  Hz, 4H), 6.53 (s, 2H), 4.31 (t,  $J = 6.7$  Hz, 4H), 1.89 – 1.69 (m, 4H), 1.44 (p,  $J = 7.2$  Hz, 4H), 1.39 – 1.27 (m, 8H), 0.90 (t,  $J = 7.4$  Hz, 6H).

$^{13}\text{C}$  NMR (151 MHz,  $\text{CDCl}_3$ )  $\delta_{\text{CDCl}_3}$ : 166.22, 140.40, 136.48, 135.87, 132.39, 130.41, 129.87, 129.75, 129.63, 128.78, 128.00, 127.66, 117.87, 113.72, 96.87, 65.25, 31.45, 28.67, 25.70, 22.53, 14.00.

HR MS (APCI<sup>+</sup>): calculated for  $\text{C}_{46}\text{H}_{44}\text{N}_4\text{O}_4$   $[\text{M}]^+$ : 716.3363; found 716.3362.

Melting point: 173.9 - 174.6 °C

## Purification of 5



Prepared from 4-methoxyaniline (263 mg) and **S1** (500 mg).

The solvents were evaporated. 10 mL of acetonitrile were added, the precipitate was filtered and washed with acetonitrile. The product was recrystallized from 15 mL of acetonitrile. The yellow product was dried in vacuum at 70 °C for 8 hours. Yield: 205 mg (282  $\mu\text{mol}$ , 26%).

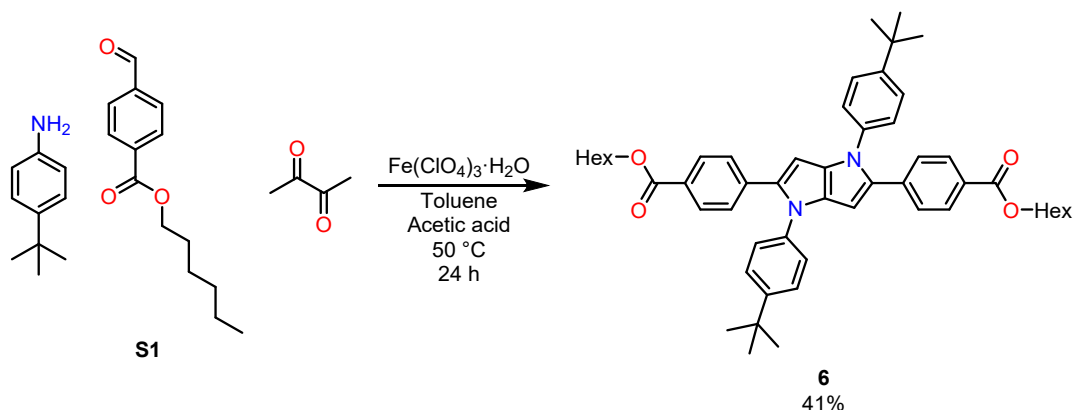
$^1\text{H NMR}$  (500 MHz,  $\text{CDCl}_3$ )  $\delta_{\text{CDCl}_3}$ : 7.87 (d,  $J = 8.5$  Hz, 4H), 7.26 (d,  $J = 8.5$  Hz, 5H), 7.21 (d,  $J = 8.9$  Hz, 4H), 6.92 (d,  $J = 8.9$  Hz, 4H), 6.42 (s, 2H), 4.28 (t,  $J = 6.7$  Hz, 4H), 3.84 (s, 6H), 1.74 (p,  $J = 6.8$  Hz, 4H), 1.51 – 1.38 (m, 4H), 1.37 – 1.20 (m, 8H), 0.90 (t,  $J = 7.4$  Hz, 6H).

$^{13}\text{C NMR}$  (126 MHz,  $\text{CDCl}_3$ )  $\delta_{\text{CDCl}_3}$ : 166.57, 157.93, 137.77, 135.74, 133.07, 132.79, 129.44, 127.60, 127.35, 126.66, 114.57, 94.80, 65.03, 55.48, 31.47, 28.71, 25.71, 22.54, 14.00.

HR MS (APCI+): calculated for  $\text{C}_{46}\text{H}_{51}\text{N}_2\text{O}_6$   $[\text{M}+\text{H}]^+$ : 727.3747; found 727.3746.

Melting point: 156.2 - 157.1 °C

## Purification of 6



Prepared from 4-*tert*-butylaniline (318 mg, 340  $\mu\text{L}$ ) and **S1** (500 mg).

The solvents were evaporated. 10 mL of diethyl ether were added, the precipitate was filtered and washed with diethyl ether and acetonitrile. The product was recrystallized from 27 mL of ethyl acetate. The yellow product was dried in vacuum at 70 °C for 8 hours. Yield: 343 mg (441  $\mu\text{mol}$ , 41%).

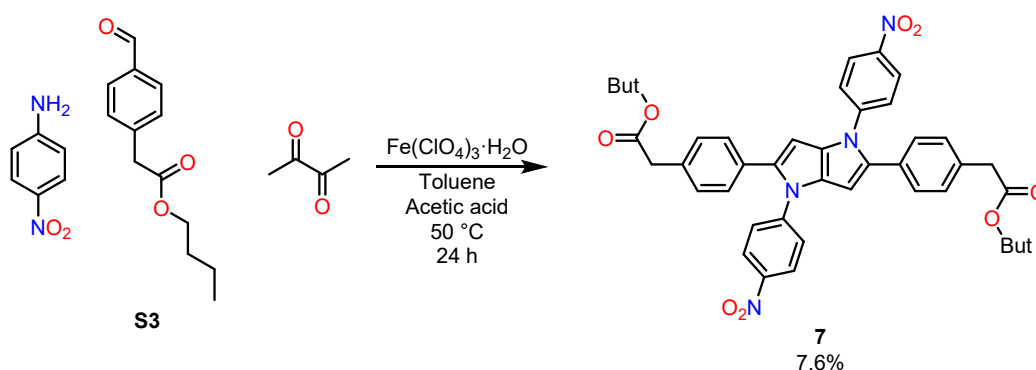
**$^1\text{H}$  NMR** (600 MHz,  $\text{CDCl}_3$ )  $\delta_{\text{CDCl}_3}$ : 7.87 (d,  $J = 8.4$  Hz, 4H), 7.39 (d,  $J = 8.5$  Hz, 4H), 7.28 (d,  $J = 8.4$  Hz, 4H), 7.20 (d,  $J = 8.4$  Hz, 4H), 6.49 (s, 2H), 4.28 (t,  $J = 6.7$  Hz, 4H), 1.74 (p,  $J = 6.8$  Hz, 4H), 1.48 – 1.39 (m, 4H), 1.38 – 1.27 (m, 26H), 0.89 (t,  $J = 6.9$  Hz, 6H).

**$^{13}\text{C}$  NMR** (151 MHz,  $\text{CDCl}_3$ )  $\delta_{\text{CDCl}_3}$ : 166.63, 149.12, 137.90, 137.05, 135.52, 132.97, 129.40, 127.57, 127.40, 126.18, 124.74, 95.69, 65.03, 34.57, 31.45, 31.37, 28.69, 25.70, 22.53, 13.98.

**HR MS** (APCI+): calculated for  $\text{C}_{52}\text{H}_{63}\text{N}_2\text{O}_4$   $[\text{M}+\text{H}]^+$ : 779.4788; found 779.4790.

**Melting point**: 223.1 – 223.6 °C

### Purification of 7



Prepared from 4-nitroaniline (294 mg) and **S3** (469 mg).

The solvents were evaporated. 10 mL of methanol were added and the resulting precipitate was filtered and washed with methanol. The product was purified by column chromatography on silica gel. The eluent was toluene/ethyl acetate 99:1 to 19:1. The solvents were evaporated and the product was recrystallized from a mixture of 13 mL of acetonitrile and 5 mL of methanol. It was recrystallized again from a mixture of 5 mL of ethyl acetate and 10 mL of hexane. The yellow product was dried in vacuum at 70 °C for 8 hours. Yield: 58.8 mg (80.7  $\mu\text{mol}$ , 7.6%).

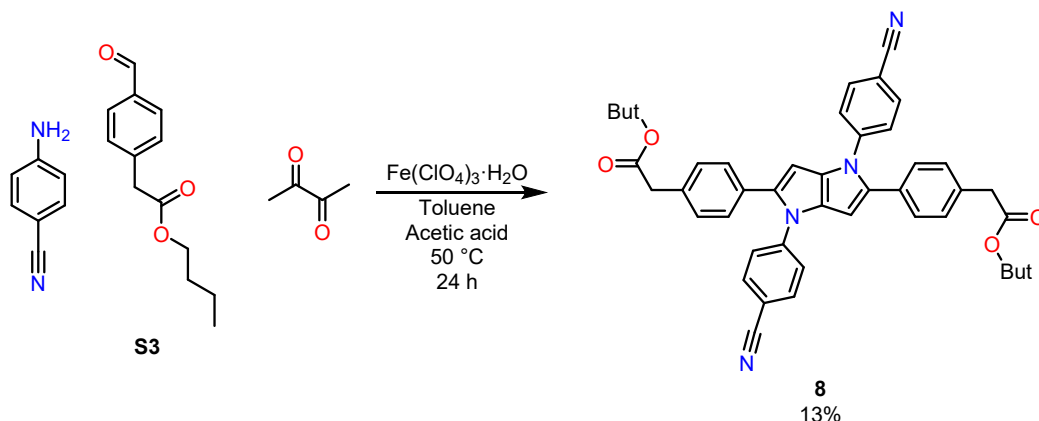
**$^1\text{H}$  NMR** (500 MHz,  $\text{CDCl}_3$ )  $\delta_{\text{CDCl}_3}$ : 8.23 (d,  $J = 8.9$  Hz, 4H), 7.38 (d,  $J = 8.9$  Hz, 4H), 7.23 (d,  $J = 8.1$  Hz, 4H), 7.17 (d,  $J = 8.0$  Hz, 4H), 6.49 (s, 2H), 4.11 (t,  $J = 6.7$  Hz, 4H), 3.61 (s, 4H), 1.72 – 1.49 (m, 4H), 1.36 (h,  $J = 7.4$  Hz, 4H), 0.92 (t,  $J = 7.4$  Hz, 6H).

**$^{13}\text{C}$  NMR** (126 MHz,  $\text{CDCl}_3$ )  $\delta_{\text{CDCl}_3}$ : 171.38, 145.04, 144.83, 136.08, 133.40, 131.27, 131.13, 129.64, 128.43, 124.92, 124.62, 97.42, 64.88, 41.01, 30.58, 19.06, 13.65.

**HR MS** (APCI+): calculated for  $\text{C}_{42}\text{H}_{41}\text{N}_4\text{O}_8$   $[\text{M}+\text{H}]^+$ : 729.2924; found 729.2927.

**Melting point**: 213.5 - 215.2 °C

## Purification of 8



Prepared from 4-aminobenzonitrile (252 mg) and **S3** (469 mg).

The solvents were evaporated. 10 mL of diethyl ether were added. The precipitate was filtered and washed with diethyl ether and methanol. The product was recrystallized from a mixture of 9 mL of acetonitrile and 10 mL of methanol. It was recrystallized again from a mixture of 9 mL of acetonitrile and 13 mL of methanol. The pale product was dried in vacuum at 70 °C for 8 hours. Yield: 97.1 mg (141  $\mu$ mol, 13%).

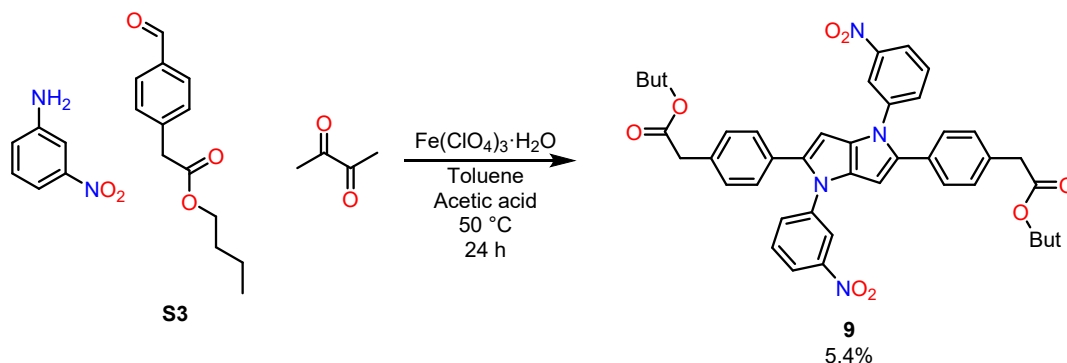
**$^1\text{H}$  NMR** (500 MHz,  $\text{CDCl}_3$ )  $\delta_{\text{CDCl}_3}$ : 7.64 (d,  $J$  = 8.7 Hz, 4H), 7.34 (d,  $J$  = 8.7 Hz, 4H), 7.21 (d,  $J$  = 8.2 Hz, 4H), 7.15 (d,  $J$  = 8.2 Hz, 4H), 6.45 (s, 2H), 4.11 (t,  $J$  = 6.7 Hz, 4H), 3.61 (s, 4H), 1.71 – 1.58 (m, 4H), 1.36 (h,  $J$  = 7.4 Hz, 4H), 0.92 (t,  $J$  = 7.4 Hz, 6H).

**$^{13}\text{C}$  NMR** (126 MHz,  $\text{CDCl}_3$ )  $\delta_{\text{CDCl}_3}$ : 171.41, 143.41, 135.82, 133.22, 133.18, 131.37, 131.06, 129.54, 128.36, 125.01, 118.45, 108.96, 96.92, 64.85, 41.00, 30.57, 19.06, 13.66.

**HR MS** (APCI<sup>+</sup>): calculated for  $\text{C}_{44}\text{H}_{41}\text{N}_4\text{O}_4$   $[\text{M}+\text{H}]^+$ : 689.3128; found 689.3126.

**Melting point:** 191.2 - 193.9 °C

## Purification of 9



Prepared from 3-nitroaniline (294 mg) and **S3** (469 mg).

The solvents were evaporated. 10 mL of methanol were added and the precipitate was filtered and washed with methanol. The product was recrystallized from a mixture of 10 mL of acetonitrile and 15 mL of methanol. It was recrystallized again from a mixture of 7 mL of acetonitrile and 10 mL of

methanol. The yellow product was dried in vacuum at 70 °C for 8 hours. Yield: 41.7 mg (57.2  $\mu$ mol, 5.4%).

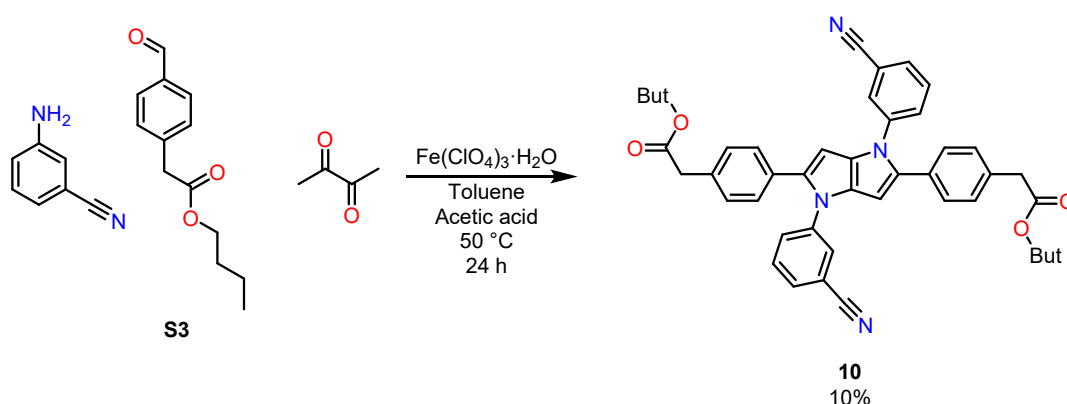
**$^1\text{H}$  NMR** (500 MHz,  $\text{CDCl}_3$ )  $\delta_{\text{CDCl}_3}$ : 8.24 (s, 2H), 8.10 (d,  $J = 7.4$  Hz, 2H), 7.56 – 7.42 (m, 4H), 7.23 – 7.08 (m, 8H), 6.47 (s, 2H), 4.09 (t,  $J = 6.7$  Hz, 4H), 3.59 (s, 4H), 1.65 – 1.54 (m, 4H), 1.35 (h,  $J = 7.4$  Hz, 4H), 0.91 (t,  $J = 7.4$  Hz, 6H).

**$^{13}\text{C}$  NMR** (126 MHz,  $\text{CDCl}_3$ )  $\delta_{\text{CDCl}_3}$ : 171.40, 148.80, 140.88, 135.97, 133.17, 131.24, 130.92, 129.92, 129.56, 128.44, 120.39, 119.32, 96.16, 64.84, 41.08, 30.56, 19.06, 13.66.

**HR MS** (APCI+): calculated for  $\text{C}_{42}\text{H}_{41}\text{N}_4\text{O}_8$   $[\text{M}+\text{H}]^+$ : 729.2924; found 729.2934.

**Melting point:** 175.0 - 176.8 °C

### Purification of 10



Prepared from 3-aminobenzonitrile (252 mg) and **S3** (469 mg).

The solvents were evaporated. 10 mL of methanol were added and the precipitate was filtered and washed with methanol. The product was recrystallized from a mixture of 8 mL of acetonitrile and 10 mL of methanol. It was recrystallized again from a mixture of 8 mL of acetonitrile and 12 mL of methanol. The pale product was dried in vacuum at 70 °C for 8 hours. Yield: 74.9 mg (109  $\mu$ mol, 10%).

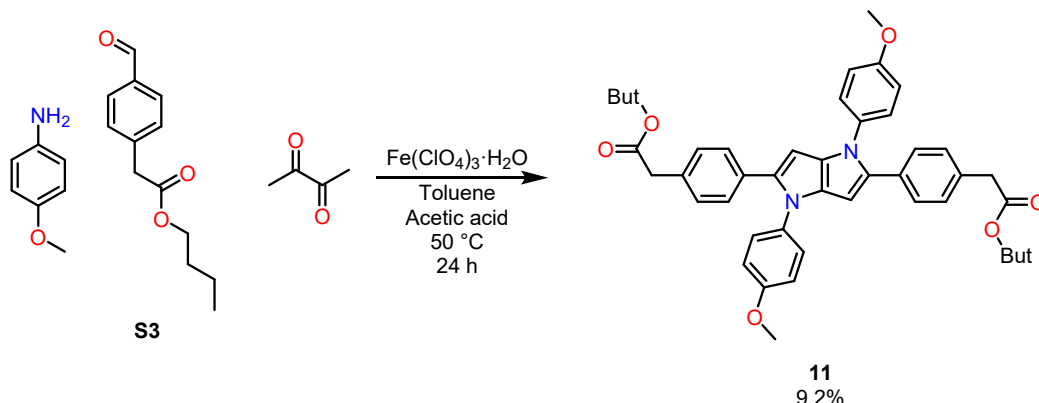
**$^1\text{H}$  NMR** (500 MHz,  $\text{CDCl}_3$ )  $\delta_{\text{CDCl}_3}$ : 7.60 (s, 2H), 7.56 – 7.49 (m, 2H), 7.49 – 7.37 (m, 4H), 7.20 (d,  $J = 8.2$  Hz, 4H), 7.14 (d,  $J = 8.1$  Hz, 4H), 6.41 (s, 2H), 4.10 (t,  $J = 6.7$  Hz, 4H), 3.60 (s, 4H), 1.66 – 1.54 (m, 4H), 1.35 (h,  $J = 7.4$  Hz, 4H), 0.91 (t,  $J = 7.4$  Hz, 6H).

**$^{13}\text{C}$  NMR** (126 MHz,  $\text{CDCl}_3$ )  $\delta_{\text{CDCl}_3}$ : 171.42, 140.69, 135.84, 133.07, 131.22, 130.14, 129.52, 129.51, 129.25, 128.31, 127.88, 118.05, 113.40, 95.90, 64.84, 41.07, 30.57, 19.06, 13.67.

**HR MS** (APCI+): calculated for  $\text{C}_{44}\text{H}_{41}\text{N}_4\text{O}_4$   $[\text{M}+\text{H}]^+$ : 689.3128; found 689.3131.

**Melting point:** 188.3 - 190.3 °C

## Purification of 11



Prepared from 4-methoxyaniline (262 mg) and **S3** (469 mg).

The solvents were evaporated. The product was purified by column chromatography on silica gel. The eluent was hexane/ethyl acetate 9:1 to 2:1. The solvents were evaporated. The product was recrystallized from 15 mL of ethanol. The yellow product was dried in vacuum at 70 °C for 8 hours. Yield: 68.3 mg (97.7  $\mu$ mol, 9.2%).

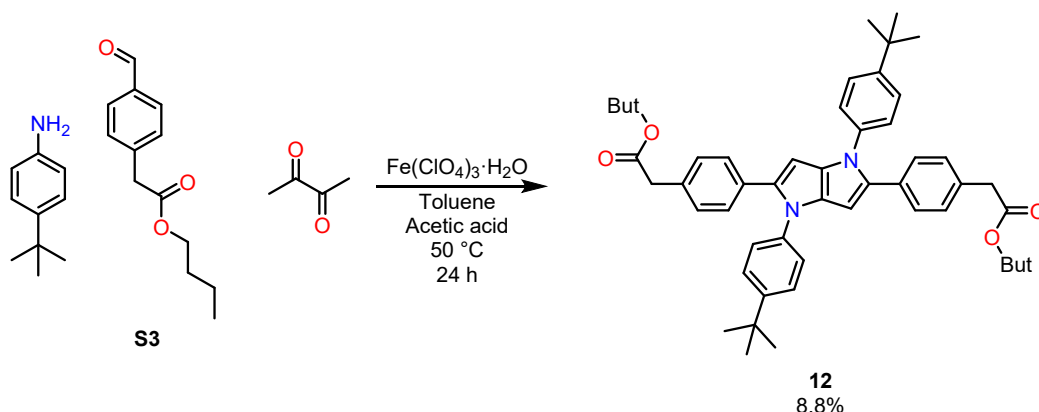
**$^1\text{H}$  NMR** (500 MHz,  $\text{CDCl}_3$ )  $\delta_{\text{CDCl}_3}$ : 7.21 (d,  $J$  = 8.9 Hz, 4H), 7.16 (d,  $J$  = 8.3 Hz, 4H), 7.12 (d,  $J$  = 8.3 Hz, 4H), 6.89 (d,  $J$  = 8.9 Hz, 4H), 6.32 (s, 2H), 4.09 (t,  $J$  = 6.7 Hz, 4H), 3.83 (s, 6H), 3.56 (s, 4H), 1.64 – 1.55 (m, 4H), 1.34 (h,  $J$  = 7.4 Hz, 4H), 0.90 (t,  $J$  = 7.4 Hz, 6H).

**$^{13}\text{C}$  NMR** (126 MHz,  $\text{CDCl}_3$ )  $\delta_{\text{CDCl}_3}$ : 171.65, 157.52, 135.58, 133.18, 132.46, 131.78, 129.00, 128.10, 126.55, 114.31, 93.74, 64.71, 55.42, 41.09, 30.57, 19.05, 13.65.

**HR MS** (APCI<sup>+</sup>): calculated for  $\text{C}_{44}\text{H}_{47}\text{N}_2\text{O}_6$   $[\text{M}+\text{H}]^+$ : 699.3434; found 699.3430.

**Melting point:** 148.8 - 149.6 °C

## Purification of 12



Prepared from 4-*tert*-butylaniline (318 mg) and **S3** (469 mg).

The solvents were evaporated. 10 mL of methanol were added and the precipitate was filtered and washed with methanol. The product was recrystallized from a mixture of 11 mL of acetonitrile and 10 mL of methanol. It was recrystallized again from a mixture of 8 mL of acetonitrile and 5 mL of methanol. The pale product was dried in vacuum at 70 °C for 8 hours. Yield: 70.0 mg (93.2  $\mu$ mol, 8.8%).



**<sup>1</sup>H NMR** (500 MHz, CDCl<sub>3</sub>)  $\delta_{CDCl_3}$ : 7.35 (d,  $J$  = 8.6 Hz, 4H), 7.20 (d,  $J$  = 8.6 Hz, 4H), 7.18 (d,  $J$  = 8.3 Hz, 4H), 7.12 (d,  $J$  = 8.2 Hz, 4H), 6.38 (s, 2H), 4.09 (t,  $J$  = 6.7 Hz, 4H), 3.57 (s, 4H), 1.59 (dt,  $J$  = 14.5, 6.7 Hz, 4H), 1.38 – 1.30 (m, 22H), 0.90 (t,  $J$  = 7.4 Hz, 6H).

**<sup>13</sup>C NMR** (126 MHz, CDCl<sub>3</sub>)  $\delta_{CDCl_3}$ : 171.69, 148.45, 137.38, 135.37, 132.60, 131.74, 131.68, 128.95, 128.11, 125.89, 124.61, 94.70, 64.69, 41.14, 34.50, 31.39, 30.55, 19.03, 13.65.

**HR MS** (APCI<sup>+</sup>): calculated for C<sub>50</sub>H<sub>59</sub>N<sub>2</sub>O<sub>4</sub> [M+H]<sup>+</sup>: 751.4475; found 751.4470.

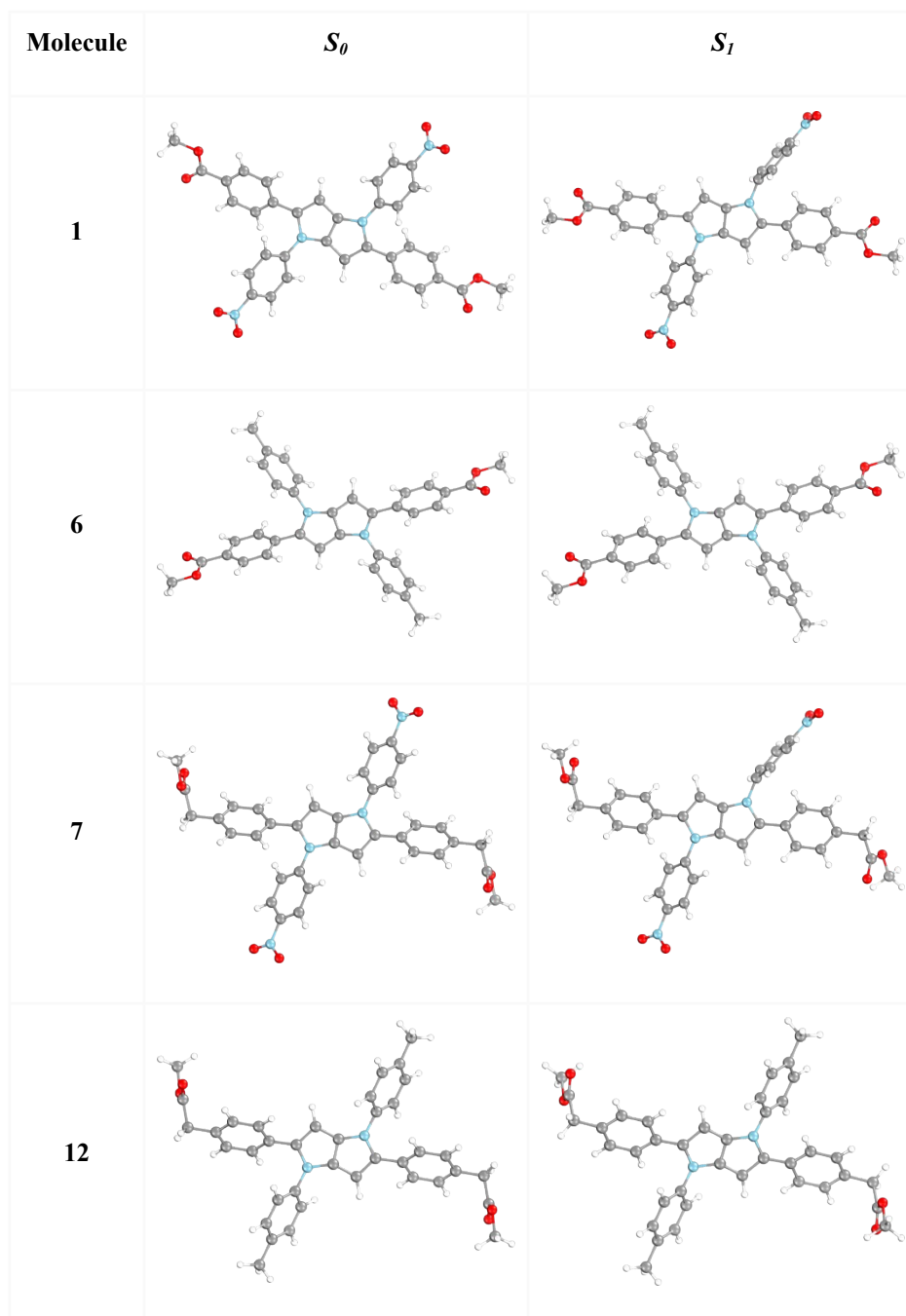
**Melting point:** 194.4 - 195.6 °C

### 3. Computational details

The truncated alkyl chains were employed to construct the molecular model structures of the **1-12** TAPP derivatives (Figure S1), as they were used only to ensure solubility in organic solvents, allowing reduced computational time. *Ab initio* calculations were performed for all model molecules using TURBOMOLE (version 7.8.1).<sup>4</sup> Geometry optimizations and vertical transition energies were obtained in vacuum using the resolution of identity (RI) approximation<sup>5</sup> and the correlation-consistent valence double-zeta basis set with polarization functions on all atoms (cc-pVDZ).<sup>6</sup> Equilibrium ground-state ( $S_0$ ) geometries were optimized at the second-order Møller-Plesset perturbation theory (MP2) level.<sup>7</sup>

Three lowest-energy vertical excited states were calculated using the second-order algebraic diagrammatic construction (ADC(2)) method.<sup>8-10</sup> The same level of theory was applied to optimize the structures of the first singlet excited state ( $S_1$ ) of all studied molecules.  $C_i$  symmetry was imposed to estimate the energy difference between the  $a_u$  and  $a_g$  states. This approach allows the evaluation of the barrier for the population of the  $a_g$  state, which is non-emissive by symmetry, leading to nonradiative decay. The conductor-like screening model (COSMO) was used with dimethyl sulfoxide as a solvent to include solvent effects for selected compounds.<sup>11</sup>

## 4. Theoretical Data

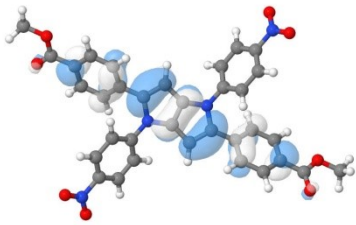
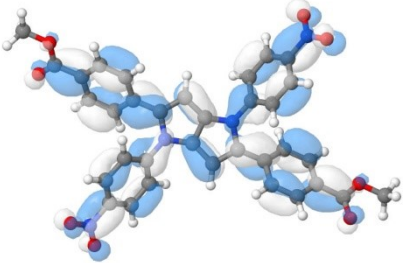
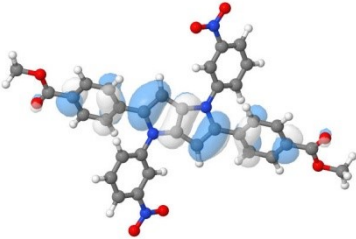
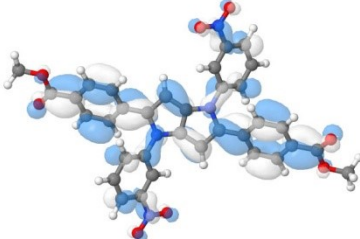
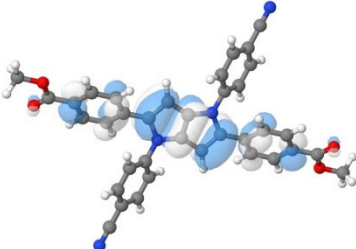
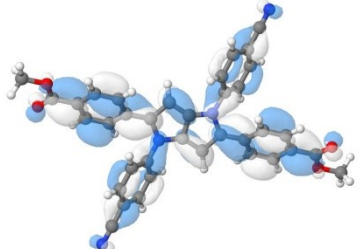
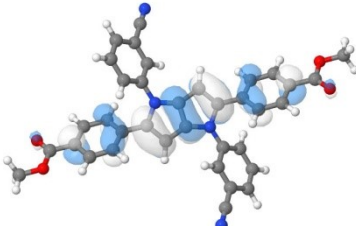
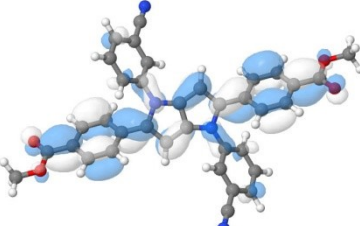
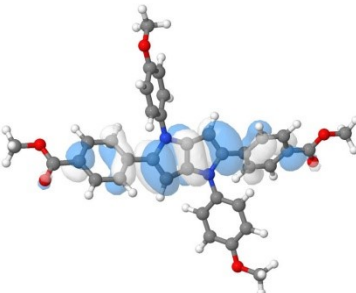
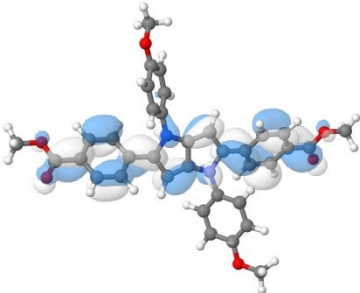
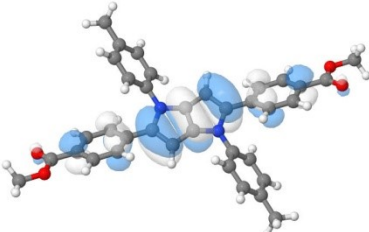
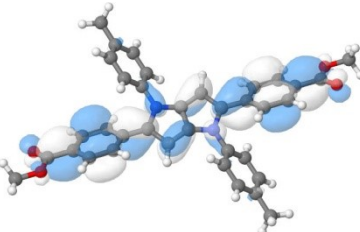


**Figure S1.** Optimized geometries of **1**, **6**, **7**, and **12** for the ground and the first excited singlet state in the gas phase were computed at the MP2/cc-pVDZ level of theory without symmetry constraints.

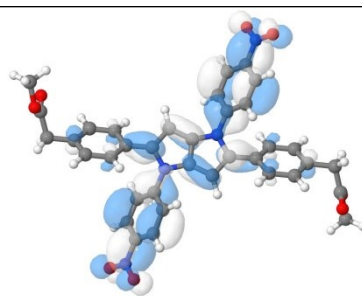
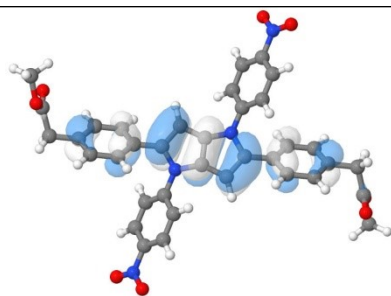
**Table S1a.** Vertical transition energy ( $\Delta E$ ), oscillator strength ( $f$ ), CT values representing the extent of charge transfer character between fragments in the molecule, quantifying the degree of electronic redistribution between donor and acceptor moieties, and leading electronic configurations of all compounds computed with the ADC(2)/cc-pVDZ method at the MP2/cc-pVDZ equilibrium geometry of the ground state. The values in parentheses represent the excitation energies calculated using the COSMO model with DMSO as solvent available in Turbomole for selected molecules (**1**, **3** and **8**).

Molecule	State	$\Delta E$ eV	$f$	CT	el. config.
<b>1</b>	$^1\pi\pi^*$	3.52 (3.43)	0.95	0.77	0.94(160a-161a)
	$^1\pi\pi^*$	3.73 (3.70)	0.00	0.04	0.42(143a-162a)
	$^1\pi\pi^*$	3.84 (3.72)	0.20	0.81	0.71(160a-162a)
<b>2</b>	$^1\pi\pi^*$	3.58	1.27	0.73	0.98(150a-151a)
	$^1\pi\pi^*$	3.96	0.00	0.18	0.95(150a-152a)
	$^1\pi\pi^*$	3.98	0.44	0.04	0.88(149a-151a)
<b>3</b>	$^1\pi\pi^*$	3.57 (3.49)	1.16	0.72	0.75(160a-163a)
	$^1\pi\pi^*$	3.72 (3.63)	0.00	0.34	0.58(142a-162a)
	$^1\pi\pi^*$	3.72 (3.90)	0.01	0.69	0.59(142a-161a)
<b>4</b>	$^1\pi\pi^*$	3.58	1.34	0.70	0.98(150a-151a)
	$^1\pi\pi^*$	4.03	0.27	0.69	0.89(149a-151a)
	$^1\pi\pi^*$	4.04	0.00	0.80	0.86(150a-154a)
<b>5</b>	$^1\pi\pi^*$	3.44	1.42	0.71	0.97(154a-155a)
	$^1\pi\pi^*$	3.74	0.15	0.79	0.92(153a-155a)
	$^1\pi\pi^*$	4.04	0.00	0.78	0.96(154a-156a)
<b>6</b>	$^1\pi\pi^*$	3.46	1.43	0.71	0.98(146a-147a)
	$^1\pi\pi^*$	3.87	0.17	0.73	0.92(145a-147a)
	$^1\pi\pi^*$	3.95	0.00	0.77	0.92(146a-148a)
<b>7</b>	$^1\pi\pi^*$	3.53	0.34	0.84	0.96(168a-169a)
	$^1\pi\pi^*$	3.63	0.00	0.94	0.95(168a-170a)
	$^1\pi\pi^*$	3.73	0.00	0.04	0.62(150a-170a)
<b>8</b>	$^1\pi\pi^*$	3.71 (3.68)	0.73	0.78	0.98(158a-159a)
	$^1\pi\pi^*$	3.90 (3.86)	0.00	0.92	0.96(158a-160a)
	$^1\pi\pi^*$	4.05 (4.00)	0.53	0.67	0.90(157a-159a)
<b>9</b>	$^1\pi\pi^*$	3.56	0.11	0.95	0.96(168a-169a)
	$^1\pi\pi^*$	3.58	0.00	0.99	0.97(168a-170a)
	$^1\pi\pi^*$	3.72	0.01	0.04	0.61(150a-169a)
<b>10</b>	$^1\pi\pi^*$	3.79	0.87	0.73	0.93(158a-159a)
	$^1\pi\pi^*$	3.96	0.06	0.97	0.95(158a-160a)
	$^1\pi\pi^*$	4.03	0.20	0.94	0.92(158a-161a)
<b>11</b>	$^1\pi\pi^*$	3.80	1.27	0.67	0.97(162a-163a)
	$^1\pi\pi^*$	4.10	0.30	0.69	0.92(161a-163a)
	$^1\pi\pi^*$	4.40	0.00	0.77	0.81(162a-164a)
<b>12</b>	$^1\pi\pi^*$	3.78	1.32	0.61	0.98(154a-155a)
	$^1\pi\pi^*$	4.29	0.00	0.75	0.88(154a-156a)
	$^1\pi\pi^*$	4.43	0.00	0.73	0.63(154a-158a)

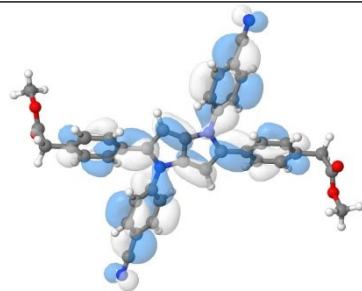
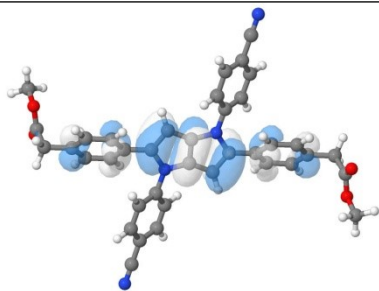
**Table S1b.** Natural Transition Orbitals (NTOs) of the lowest-lying transitions computed without symmetry constraints at MP2/ADC(2)/cc-pVDZ level of theory for each compound.

Molecule	<i>Occupied</i>	<i>Virtual</i>
1		
2		
3		
4		
5		
6		

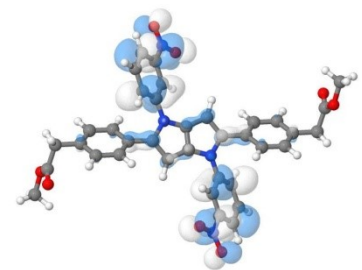
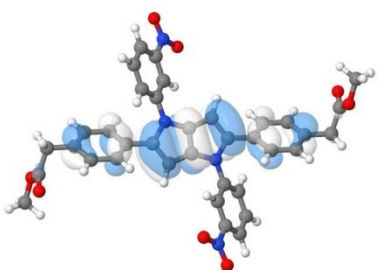
7



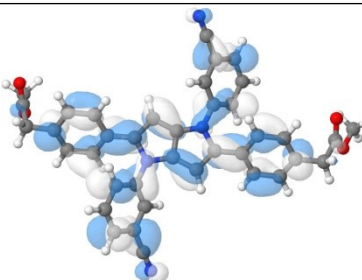
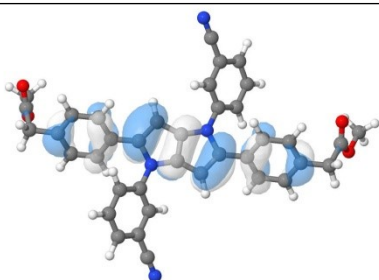
8



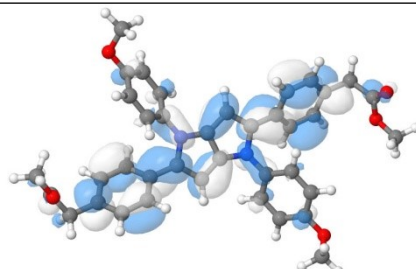
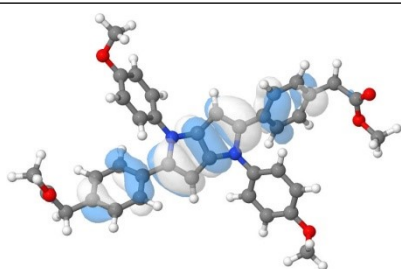
9



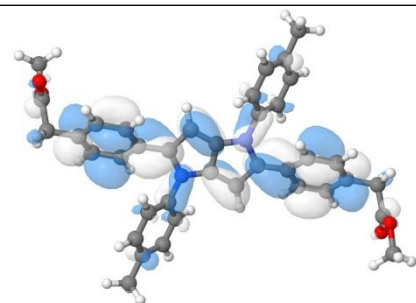
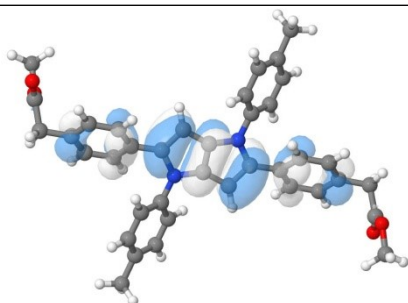
10



11



12



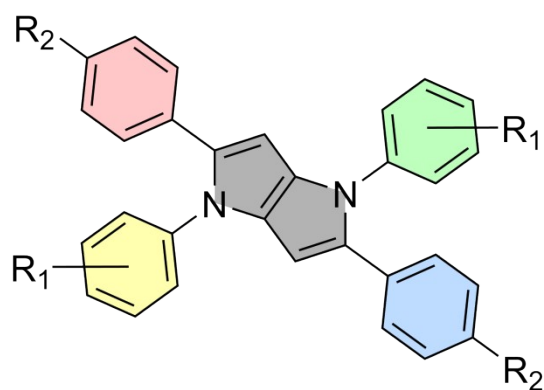


**Figure S2.** Schematic representation of the molecular partitioning into five fragments for the calculation of charge transfer (CT) values using the TheoDORE software.

**Table S2.** Vertical transition energy ( $\Delta E$ ), oscillator strength ( $f$ ), and CT values representing the extent of electronic density rearrangement between fragments in the molecule, quantifying the degree of electronic redistribution between donor and acceptor moieties, computed with ADC(2)/cc-pVDZ method at the respective equilibrium geometry of the  $S_1$  state obtained without symmetry constraints.

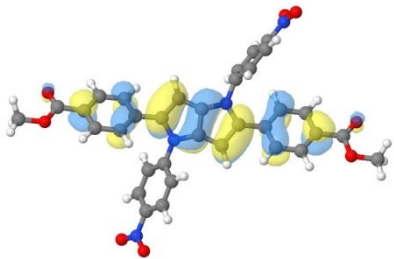
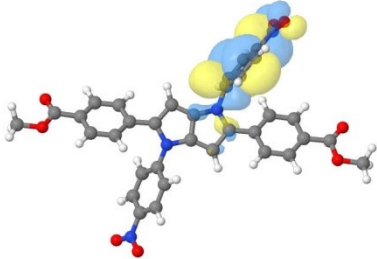
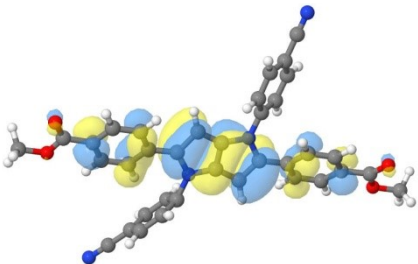
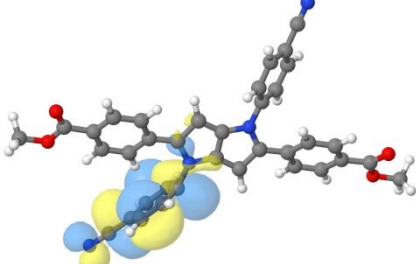
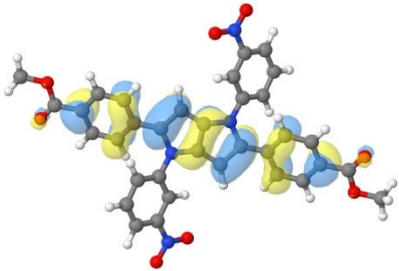
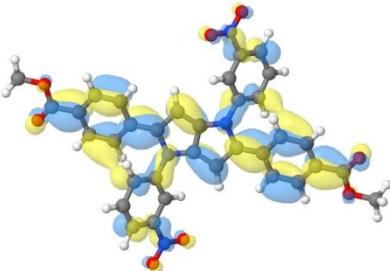
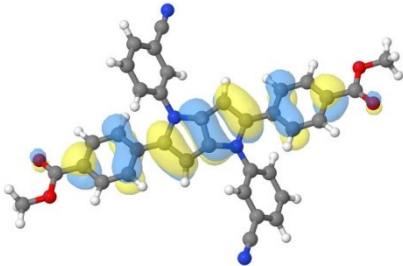
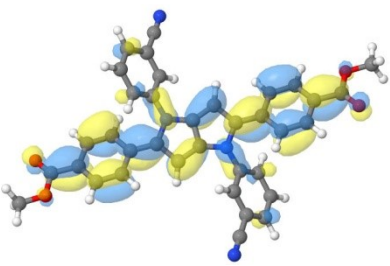
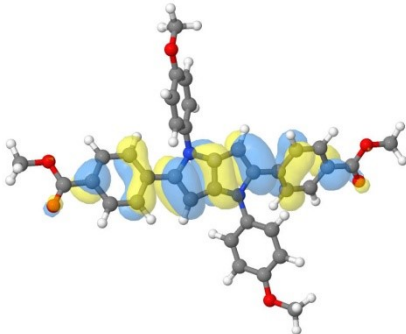
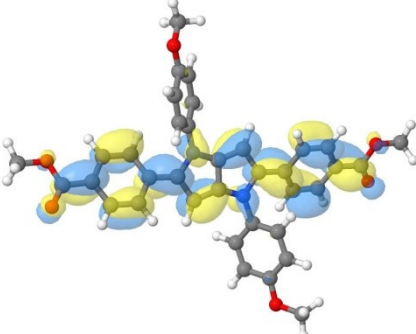
Molecule	$\Delta E/\text{eV}$	$f$	$\mu(S_1)/\text{Debye}$	CT
1	2.44	0.01	23.21	0.97
2	2.43	0.01	15.31	0.87
3	2.99	1.54	0.03	0.71
4	3.01	1.72	0.03	0.69
5	2.96	1.77	3.96	0.64
6	2.97	1.83	0.01	0.63
7	2.17	0.01	20.44	0.78
8	2.14	0.01	16.36	0.96
9	2.19	0.00	24.22	0.76
10	2.84	0.09	14.88	0.72
11	3.17	1.68	3.20	0.63
12	3.15	1.67	0.02	0.77

**Table S3.** Vertical transition energy ( $\Delta E$ ), oscillator strength ( $f$ ) and leading electronic configurations of all compounds were computed with the ADC(2)/cc-pVDZ method at the MP2/cc-pVDZ equilibrium geometry of the ground state of **1-12** corresponding to the  $C_i$  symmetry.

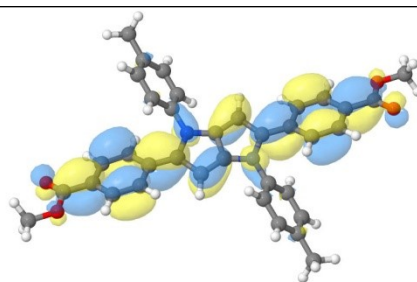
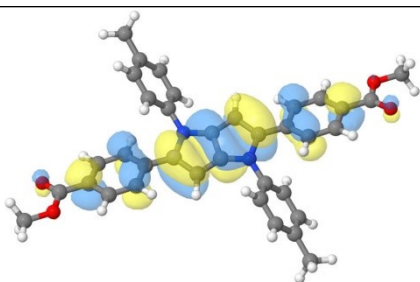
Molecule	State	$\Delta E/\text{eV}$	$f$	el. config.
1	$1a_u$	3.53	0.96	$0.94(80a_u-81a_g)$
2	$1a_u$	4.02	1.14	$0.97(75a_u-76a_g)$
3	$1a_u$	3.56	1.16	$0.76(80a_u-82a_g)$
4	$1a_u$	3.58	1.34	$0.98(75a_u-76a_g)$
5	$1a_u$	3.45	1.44	$0.98(77a_u-78a_g)$
6	$1a_u$	3.46	1.43	$0.98(73a_u-74a_g)$
7	$1a_u$	3.54	0.34	$0.96(84a_u-85a_u)$
8	$1a_u$	3.71	0.73	$0.98(79a_u-80a_g)$
9	$1a_u$	3.56	0.11	$0.96(84a_u-85a_g)$
10	$1a_u$	3.79	0.92	$0.93(79a_u-80a_g)$
11	$1a_u$	3.81	1.31	$0.98(81a_u-82a_g)$
12	$1a_u$	3.78	1.31	$0.98(77a_u-78a_g)$



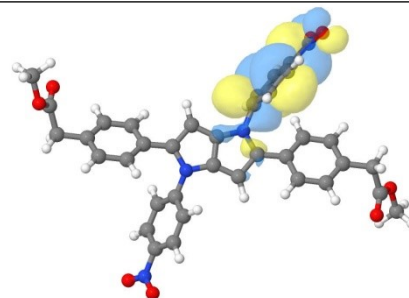
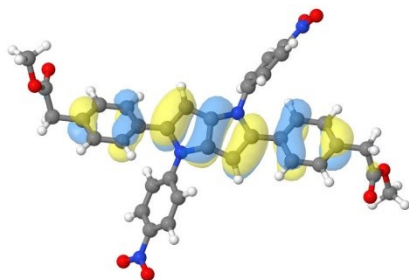
**Table S4.** Natural Transition Orbitals (NTOs) of the lowest-lying transitions computed at ADC(2)/cc-pVDZ level of theory without symmetry constraints.

Molecule	<i>Occupied</i>	<i>Virtual</i>
1		
2		
3		
4		
5		

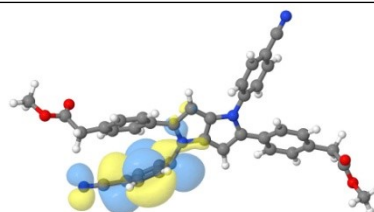
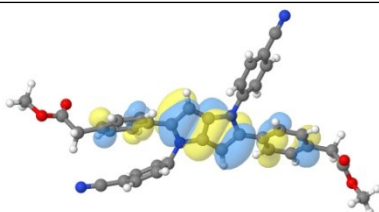
6



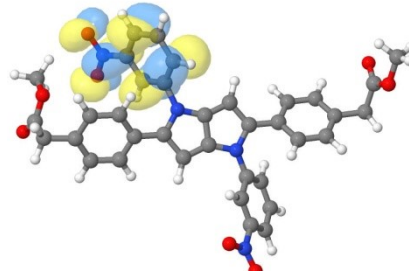
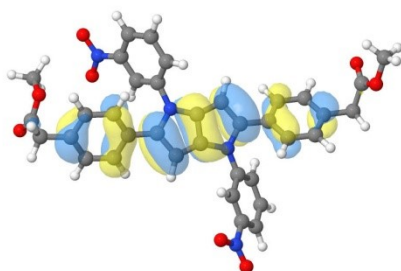
7



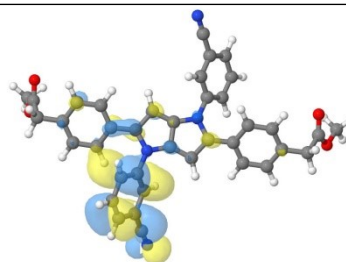
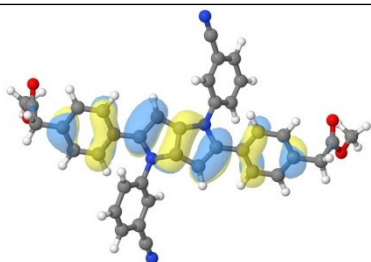
8



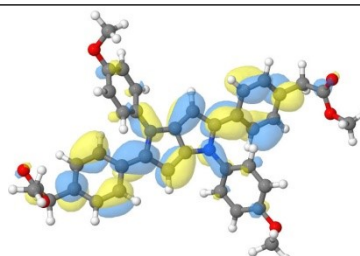
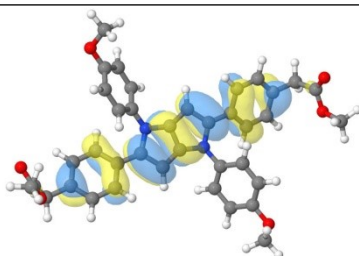
9



10



11



12

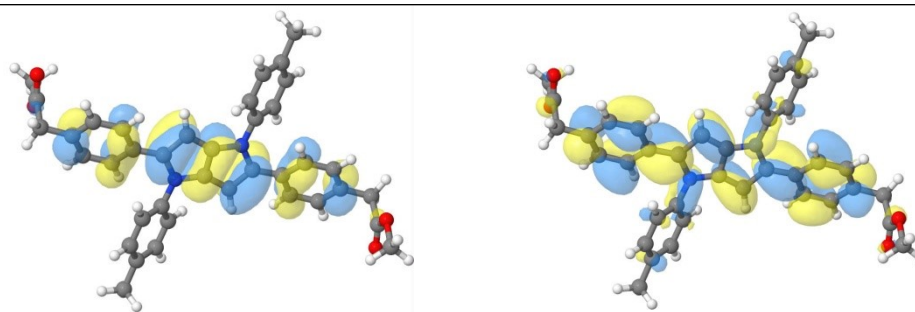
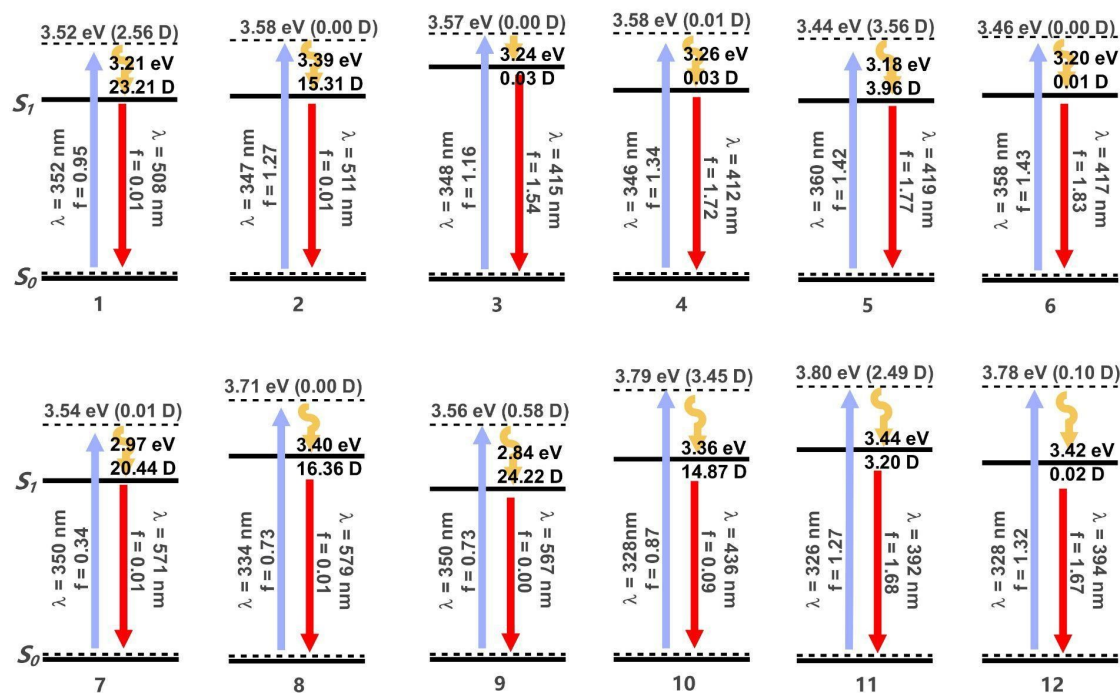
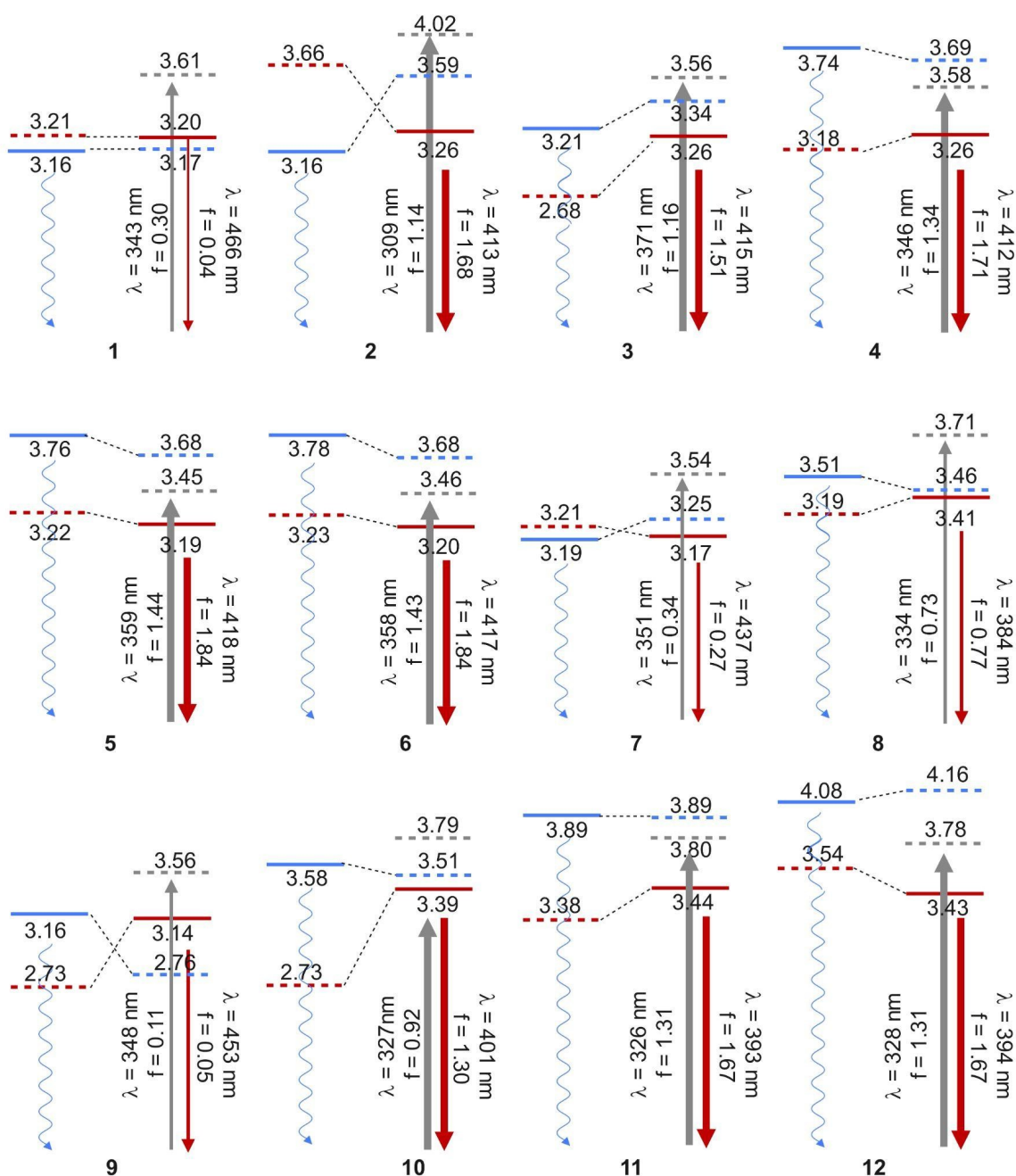


**Table S5.** Vertical transition energy ( $\Delta E$ ), oscillator strength ( $f$ ), and dipole moments ( $\mu$ ) of the ground and excited states, computed with ADC(2)/cc-pVDZ method at the respective equilibrium geometry of the  $S_i$  state obtained by imposing  $C_i$  symmetry.

Molecule	$\Delta E/\text{eV}$	$f$
1	2.97	1.35
2	3.00	1.68
3	2.99	1.51
4	3.01	1.71
5	2.97	1.84
6	2.97	1.84
7	2.84	0.27
8	3.23	0.77
9	2.74	0.05
10	3.10	1.30
11	3.16	1.67
12	3.15	1.67



**Scheme S1.** Jablonski energy diagram for all TAPP derivatives computed at ADC(2)/cc-pVDZ level of theory without symmetry. Solid lines represent the vertical excitation/emission energies of a given state computed at the respective ground/excited state minimum. The dashed black line represents vertical energy of the ground state computed at the optimized geometry of the respective compound. Numbers denote relevant energies in eV, transition dipole moments in parenthesis in Debye, and dimensionless oscillator strengths for each absorbing/emissive state.



**Scheme S2.** Energy diagram for all compounds computed at the ADC(2)/cc-pVDZ level of theory. Horizontal lines represent the vertical (dashed) and adiabatic (solid) energies of  $a_g$  and  $a_u$  states (marked in blue and red, respectively). Gray dashed lines and arrows correspond to the vertical excited states computed at the ground state of each derivative. Numbers denote relevant energies in eV. Wavy and straight arrows represent internal conversion and radiative decay, respectively. The width of the latter indicates the intensity of their fluorescence.

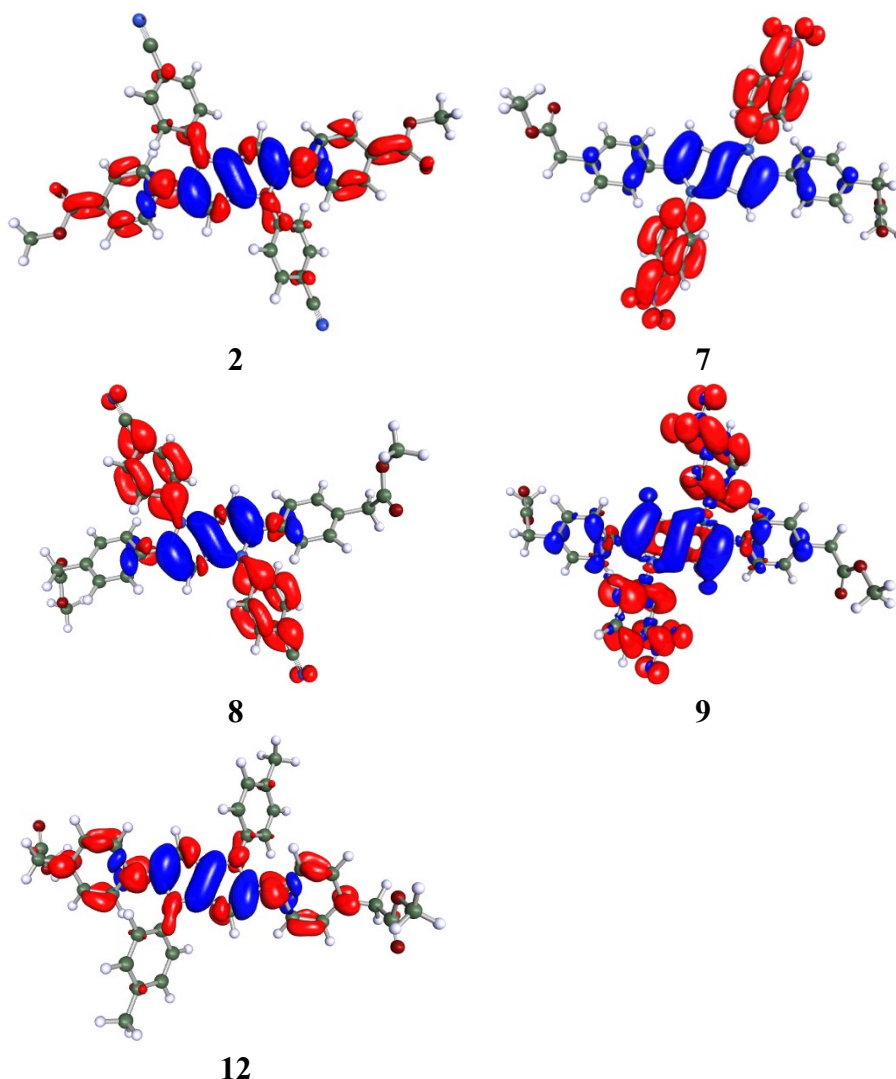


**Figure S3.**  $S_1$ - $S_0$  electron density difference computed for bright  $1a_u$  states for compounds **2**, **7**, **8**, **9**, and **12** obtained at the ADC(2)/cc-pVDZ level of theory (cut-off = 0.001). Red (blue) indicates electron acceptor (donor) regions.

### Excited state dipole moment calculation using McRae plot

Excited state dipole moments are calculated using McRae plot, formed according to equation (S1), where  $\Delta\bar{\nu}$  is the Stokes shift in  $\text{m}^{-1}$ ,  $\Delta\mu$  is the dipole moment change upon excitation in  $\text{C}\cdot\text{m}$ ,  $h$  is the Planck constant in  $\text{J}\cdot\text{s}$ ,  $c$  is the velocity of light in  $\text{m}\cdot\text{s}^{-1}$ ,  $a$  is the Onsager cavity radius in  $\text{m}$ ,  $\epsilon_0$  is the vacuum permittivity in  $\text{F}\cdot\text{m}^{-1}$  and  $F$  is a function of solvent properties.<sup>12</sup>

$$\Delta\bar{\nu} = \text{const} + \frac{\Delta\mu^2}{2\pi\epsilon_0 h c a^3} F \quad (\text{S1})$$

$F$  is defined according to equation (S2), where  $\epsilon$  is the relative permittivity of the solvent and  $n$  is the refractive index.

$$F = \frac{\epsilon - 1}{\epsilon + 2} - \frac{n^2 - 1}{n^2 + 2} \quad (\text{S2})$$

The radius  $a$  is defined as in equation (S3), where  $M$  is the molecular mass in  $\text{g}\cdot\text{mol}^{-1}$ ,  $\delta$  is the molecular density in  $\text{g}\cdot\text{m}^{-3}$  and  $N$  is the Avogadro number in  $\text{mol}^{-1}$ .<sup>13</sup>

$$a = \left( \frac{3M}{4\pi\delta N} \right)^{\frac{1}{3}} \quad (\text{S3})$$

Molecular volume needed to calculate  $\delta$  is obtained using <https://molinspiration.com/>.

Dipole moment in the ground state in all cases is equal to 0. Table S5 shows the results of the calculations –  $\mu_e$  is the dipole moment in the excited state.. Compounds **1**, **3**, **7** and **9** are omitted because they do not fit the model.

**Table S6.** Excited state dipole moments calculated with McRae plots.

Dye	$a/\text{m}$	Slope/ $\text{m}^{-1}$	$\mu_e/\text{D}$
<b>2</b>	$5.44 \cdot 10^{-10}$	$1.78 \cdot 10^5$	5.34
<b>4</b>	$5.44 \cdot 10^{-10}$	$1.62 \cdot 10^5$	5.09
<b>5</b>	$5.49 \cdot 10^{-10}$	$2.45 \cdot 10^5$	6.34
<b>6</b>	$5.70 \cdot 10^{-10}$	$2.40 \cdot 10^5$	6.63
<b>8</b>	$5.35 \cdot 10^{-10}$	$7.37 \cdot 10^5$	10.6
<b>10</b>	$5.35 \cdot 10^{-10}$	$6.84 \cdot 10^5$	10.2
<b>11</b>	$5.40 \cdot 10^{-10}$	$9.66 \cdot 10^4$	3.89
<b>12</b>	$5.61 \cdot 10^{-10}$	$9.05 \cdot 10^4$	3.99



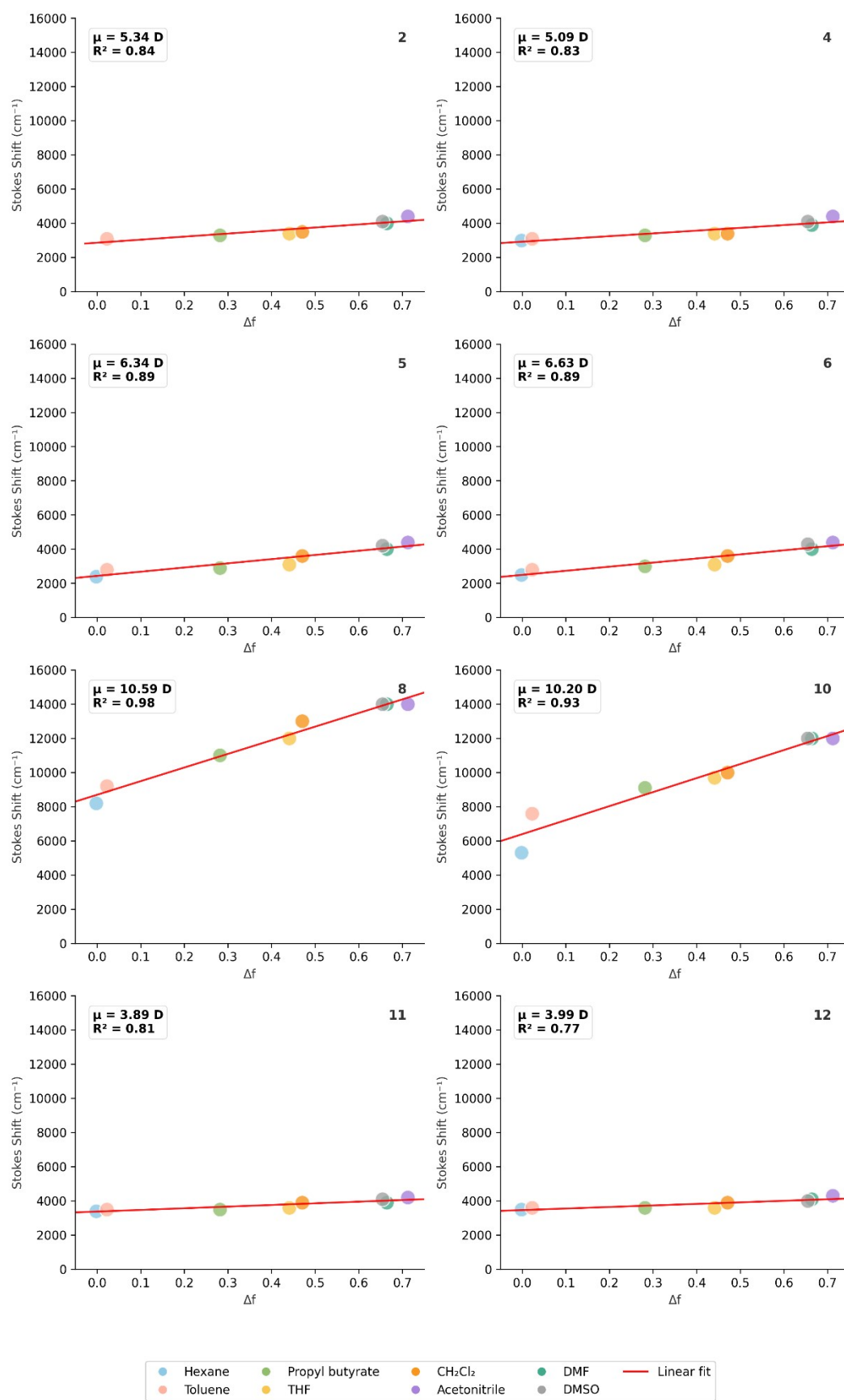
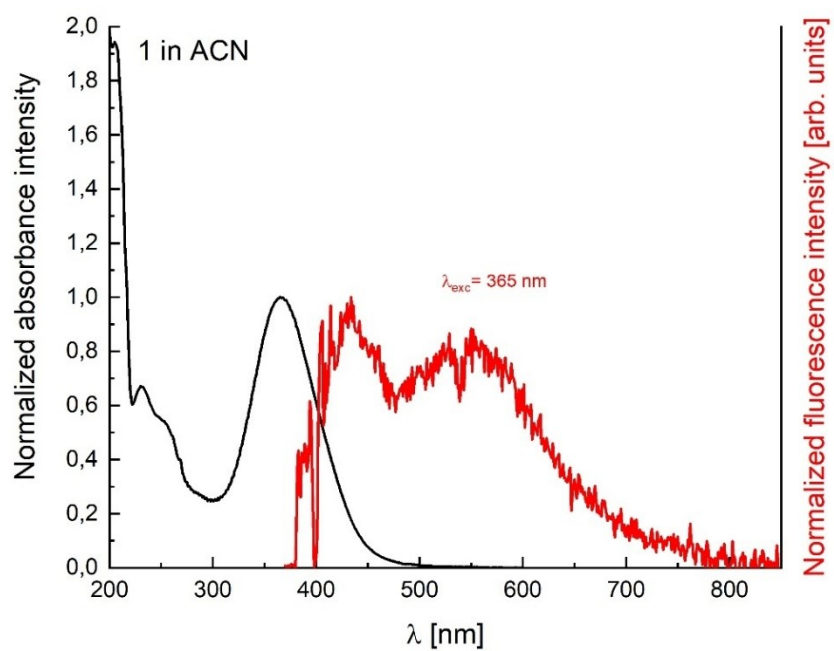


Figure S4. Mcrae plots of compounds 2, 4, 5, 6, 8, 10, 11 and 12.



## 5. UV/Vis spectra



**Figure S4.** Absorption and emission spectra of TAPP 1 in acetonitrile.

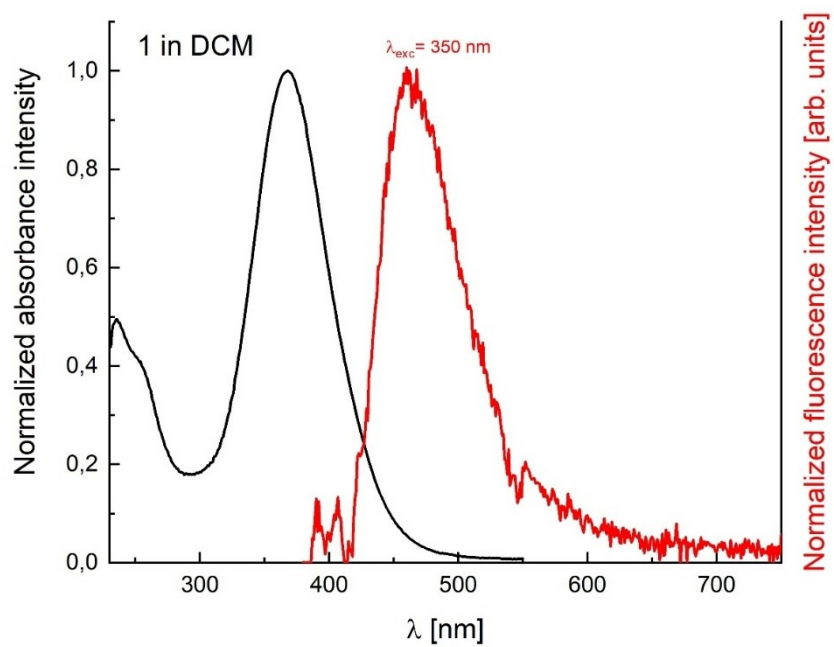


**Figure S5.** Absorption and emission spectra of TAPP 1 in DCM.

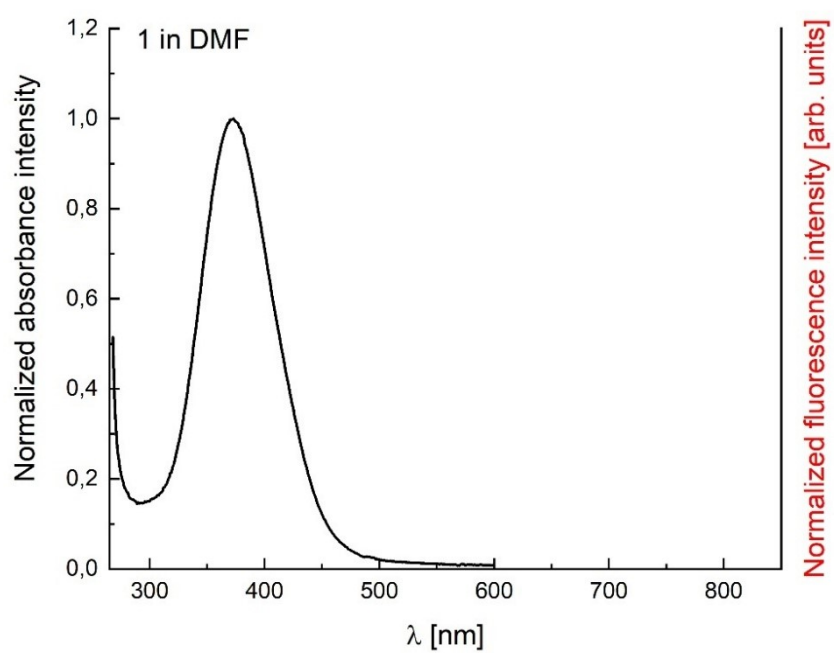


**Figure S6.** Absorption and emission spectra of TAPP **1** in DMF.

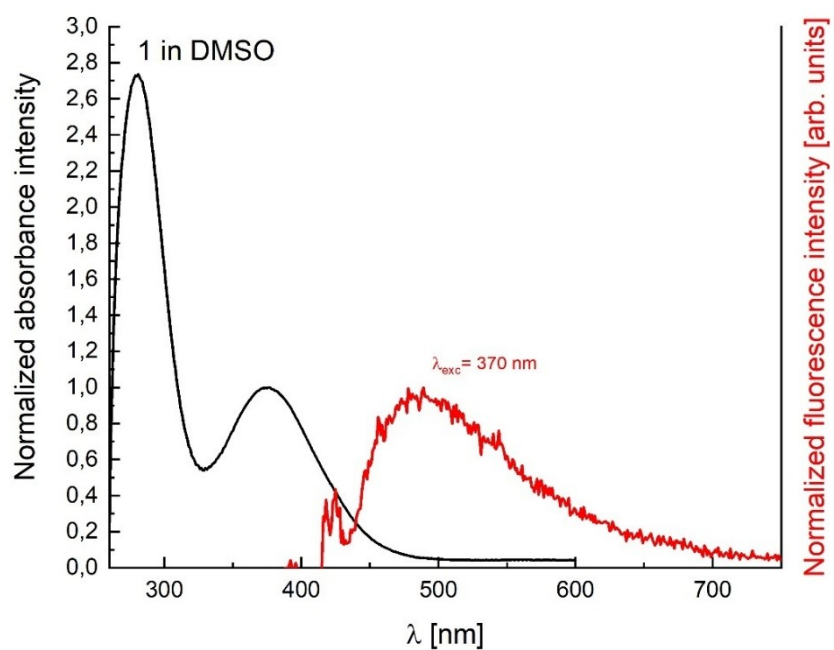


**Figure S7.** Absorption and emission spectra of TAPP **1** in DMSO.

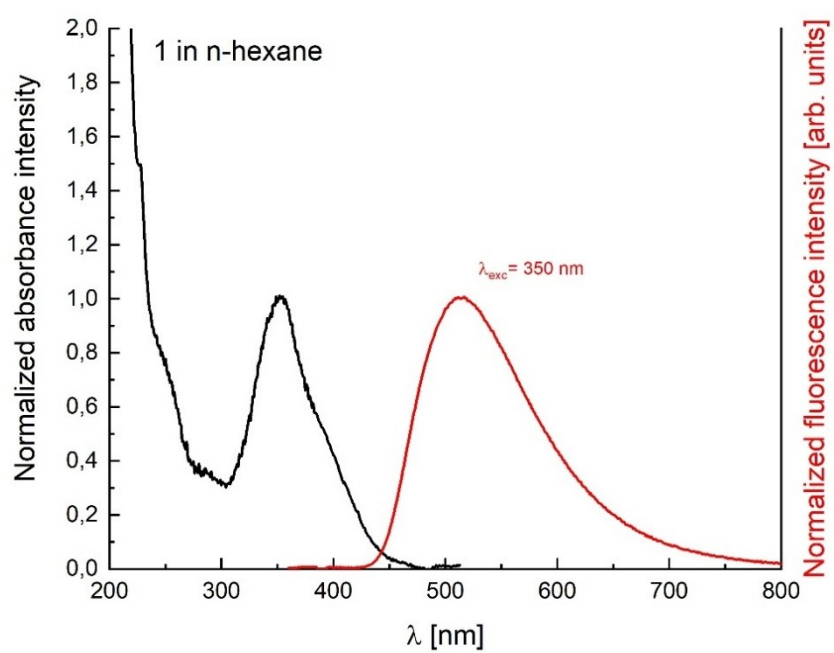


**Figure S8.** Absorption and emission spectra of TAPP 1 in hexane.

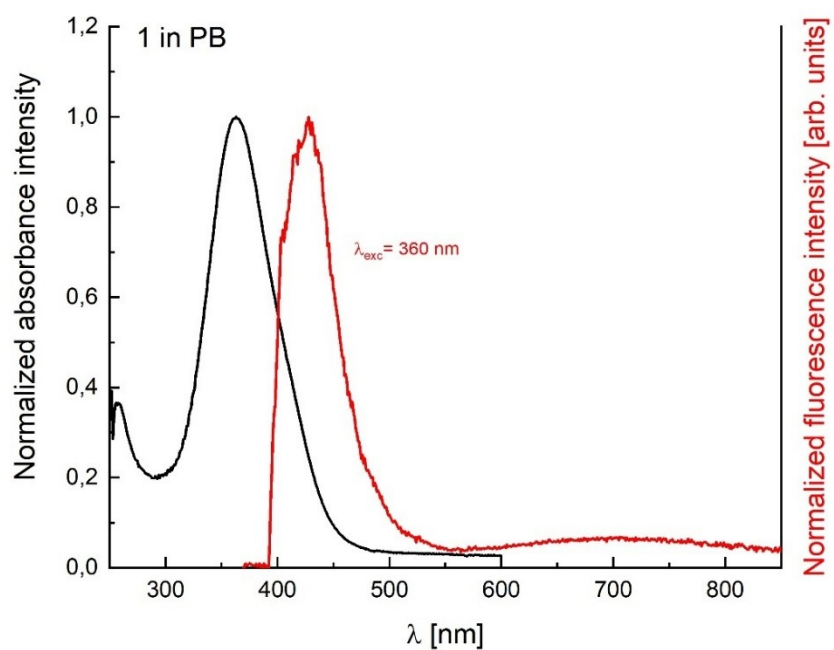


**Figure S9.** Absorption and emission spectra of TAPP 1 in propyl butyrate.

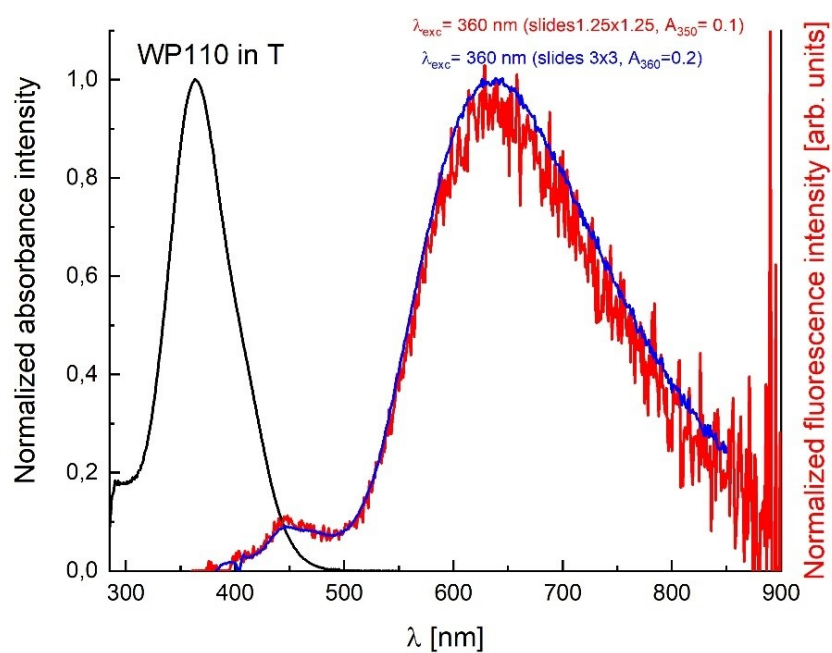


**Figure S10.** Absorption and emission spectra of TAPP **1** in toluene.

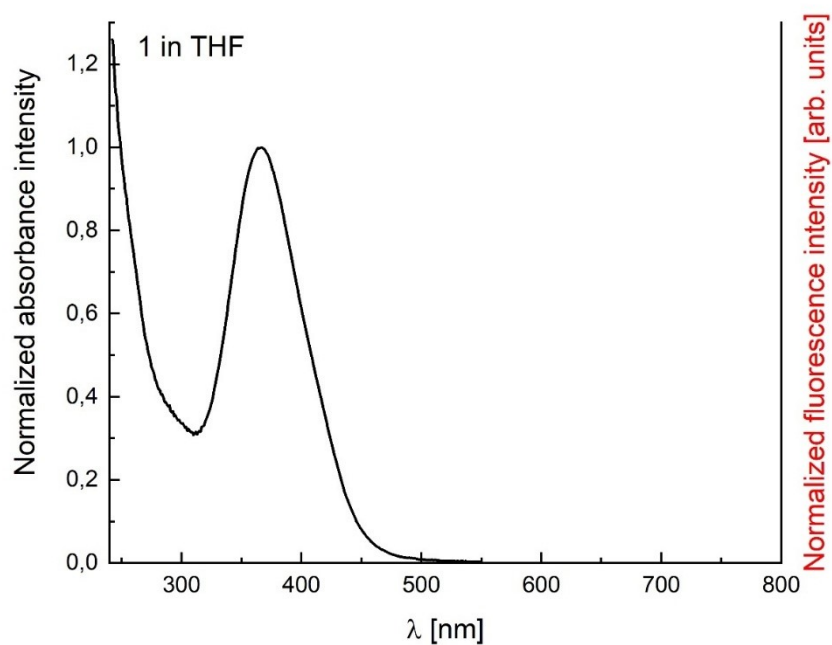


**Figure S11.** Absorption and emission spectra of TAPP **1** in THF.

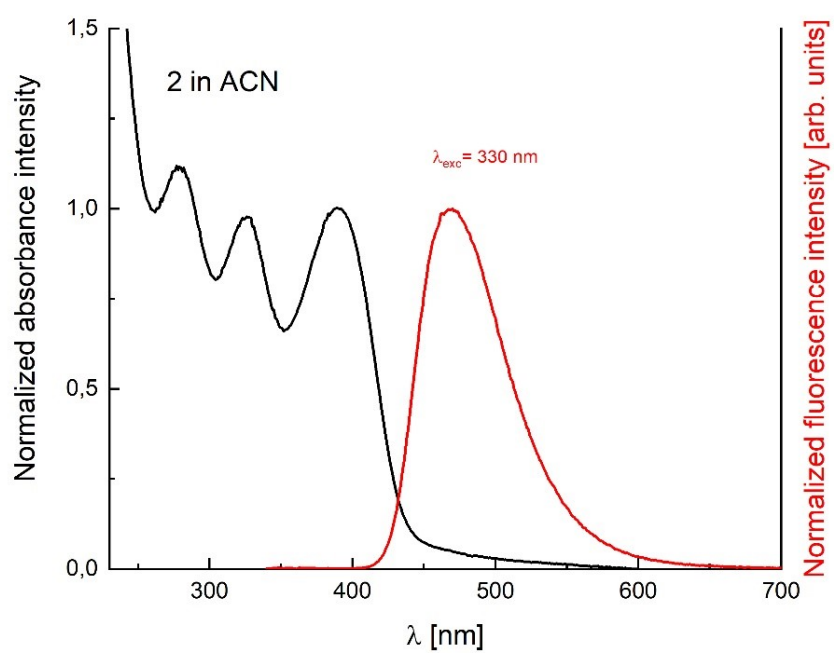


**Figure S12.** Absorption and emission spectra of TAPP 2 in acetonitrile.

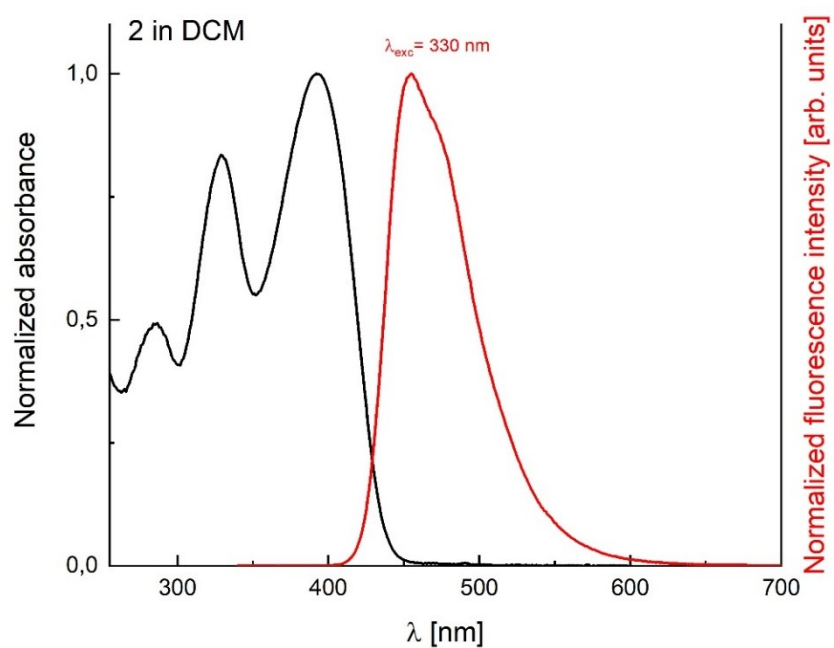


**Figure S13.** Absorption and emission spectra of TAPP 2 in DCM.

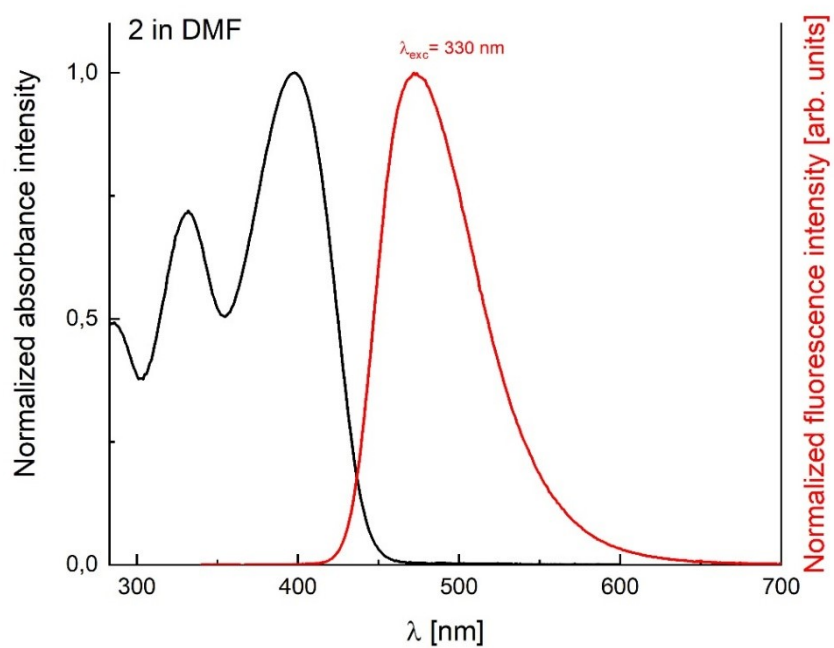


**Figure S14.** Absorption and emission spectra of TAPP 2 in DMF.

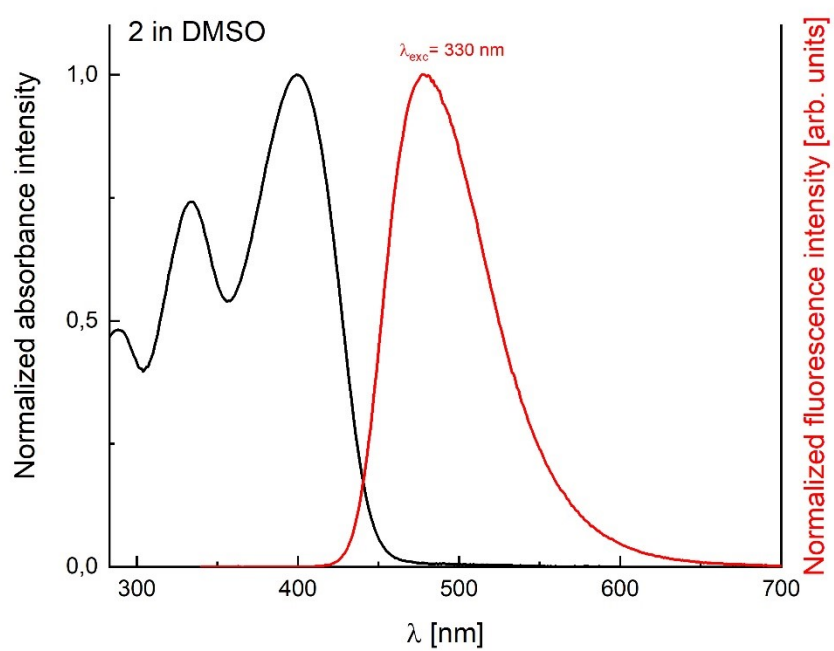


**Figure S15.** Absorption and emission spectra of TAPP 2 in DMSO.

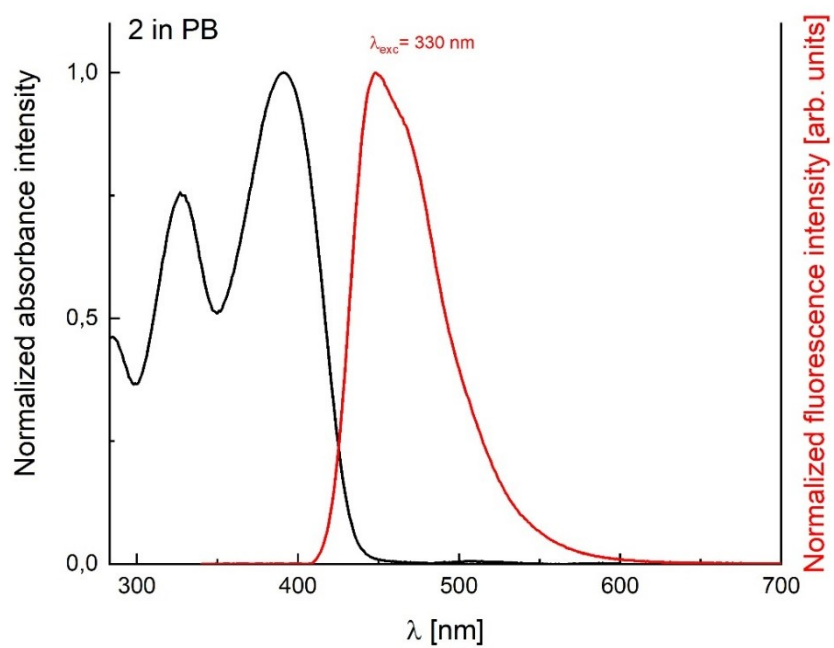


**Figure S16.** Absorption and emission spectra of TAPP 2 in propyl butyrate.

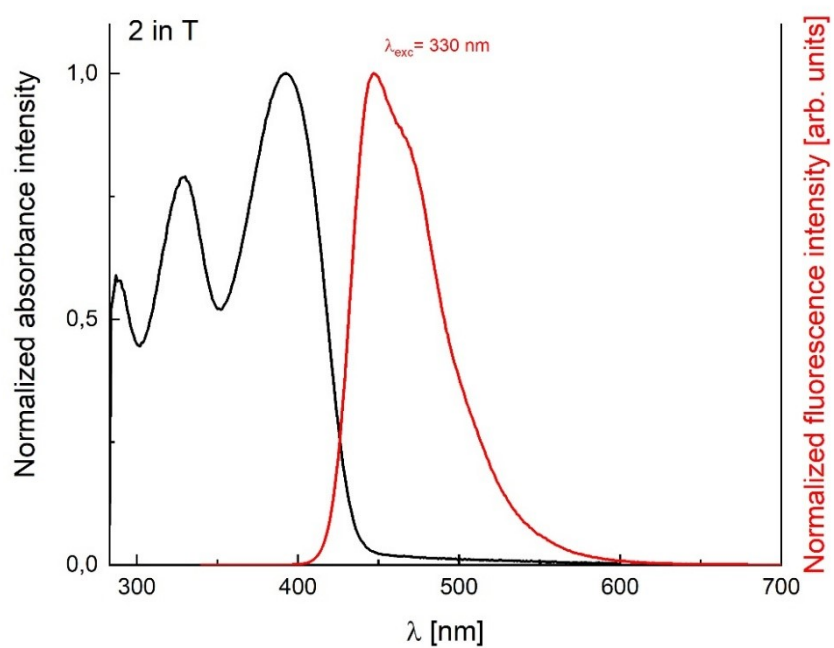


**Figure S17.** Absorption and emission spectra of TAPP 2 in toluene.

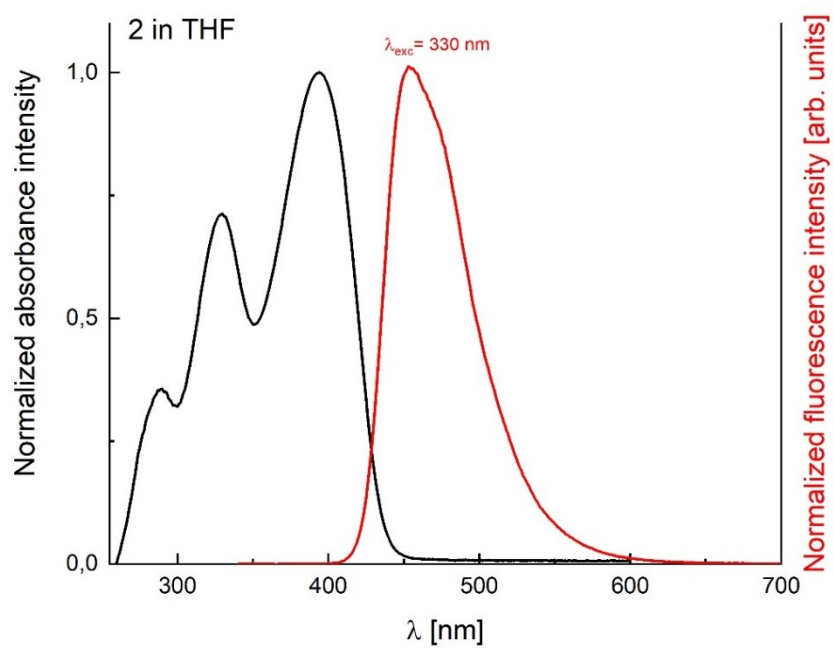


**Figure S18.** Absorption and emission spectra of TAPP 2 in THF.

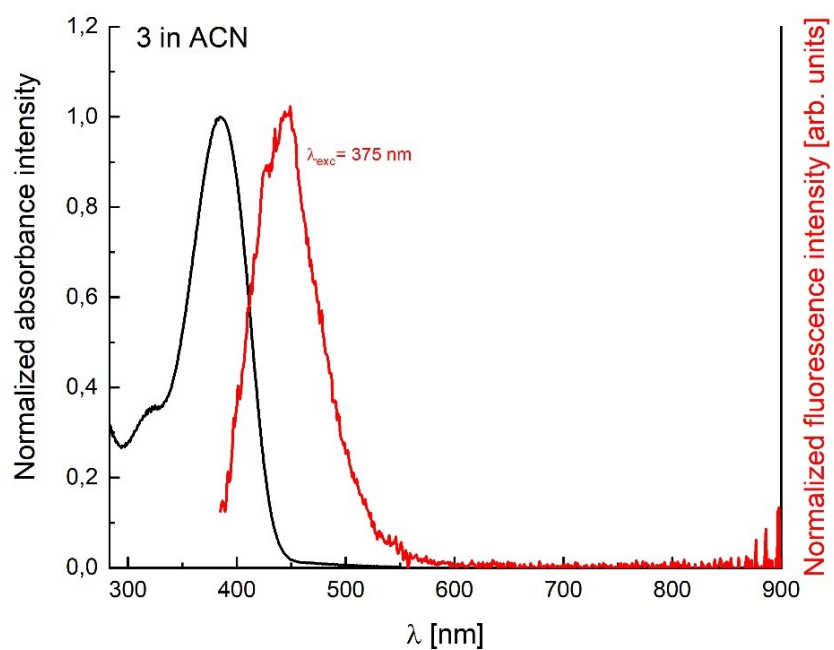


**Figure S19.** Absorption and emission spectra of TAPP 3 in acetonitrile.



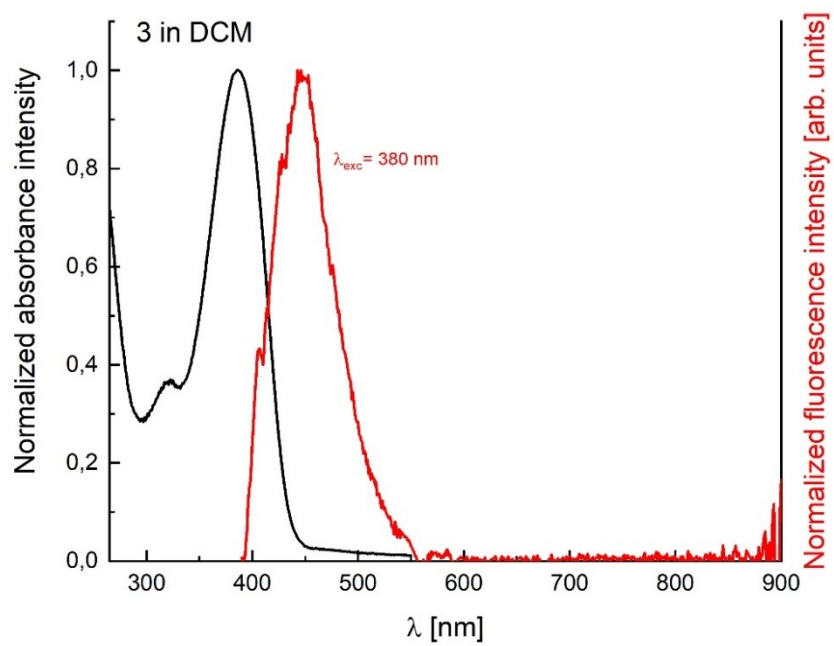


**Figure S20.** Absorption and emission spectra of TAPP 3 in DCM.

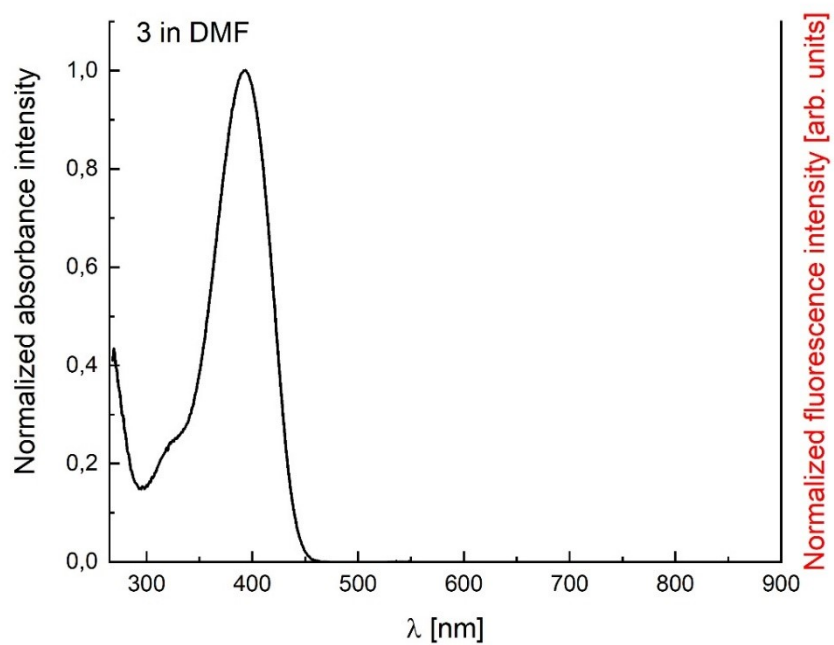


**Figure S21.** Absorption and emission spectra of TAPP 3 in DMF.

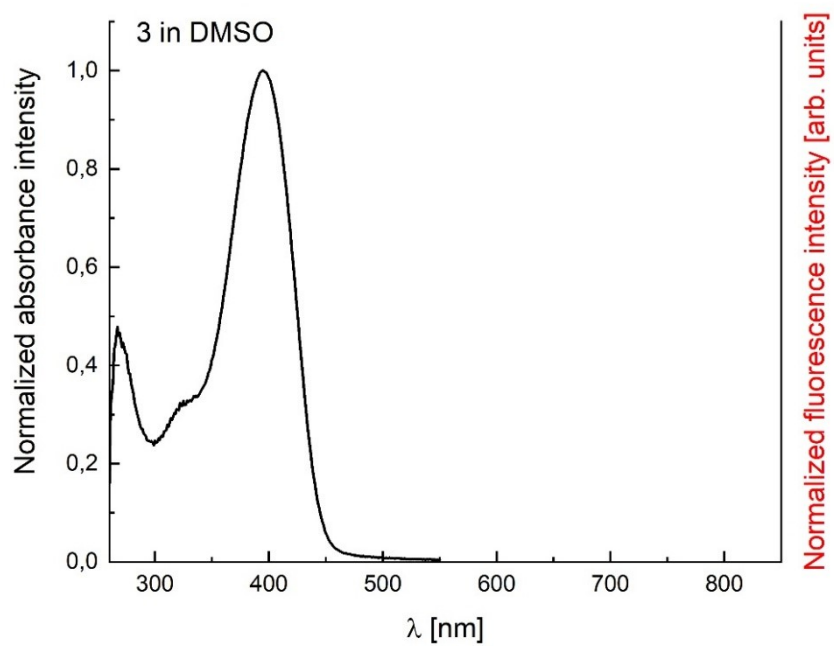


**Figure S22.** Absorption and emission spectra of TAPP 3 in DMSO.

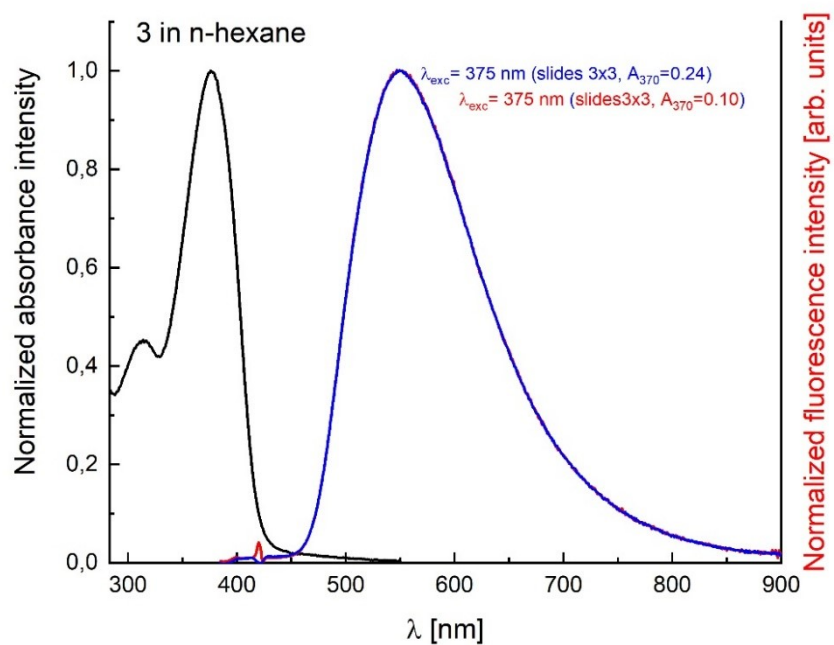


**Figure S23.** Absorption and emission spectra of TAPP 3 in hexane.

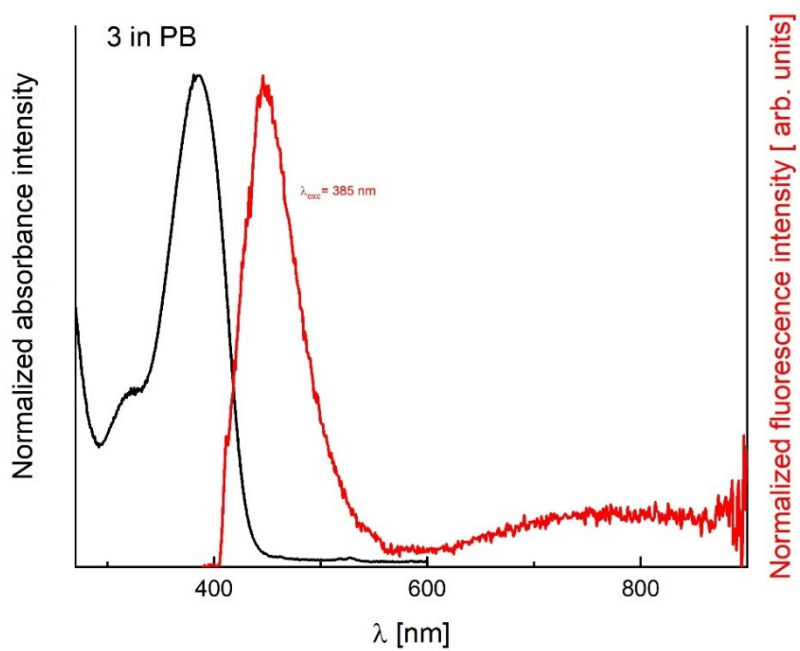


**Figure S24.** Absorption and emission spectra of TAPP **3** in propyl butyrate.

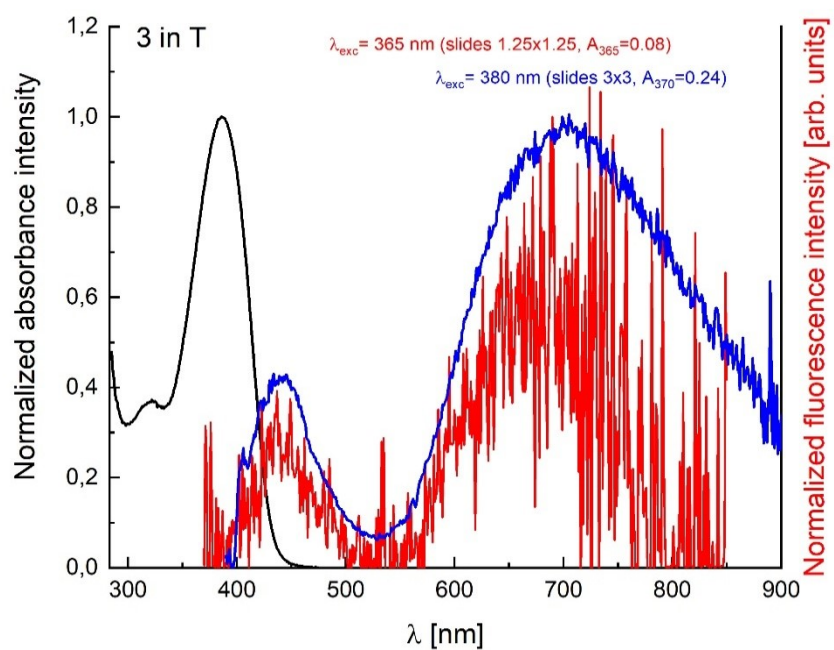


**Figure S25.** Absorption and emission spectra of TAPP **3** in toluene.

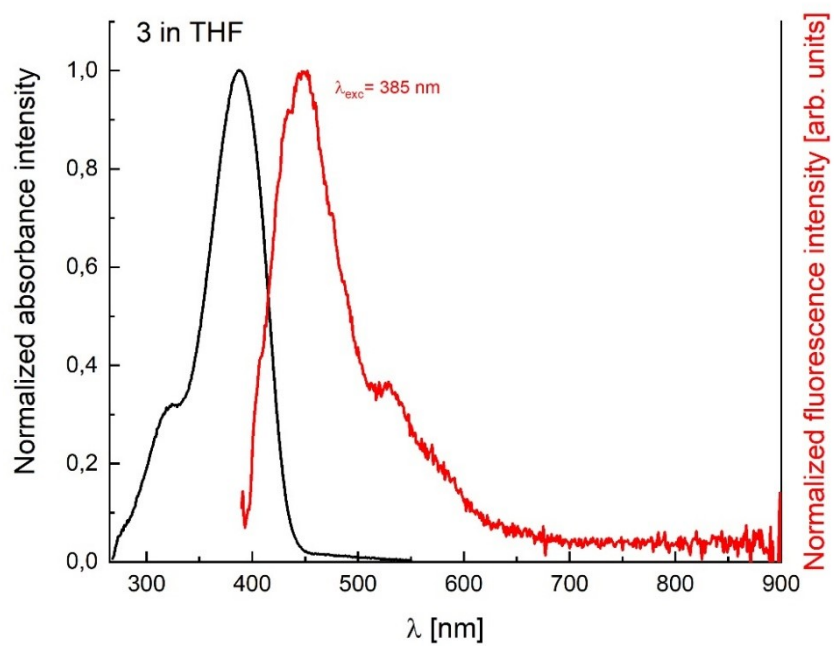


**Figure S26.** Absorption and emission spectra of TAPP 3 in THF.

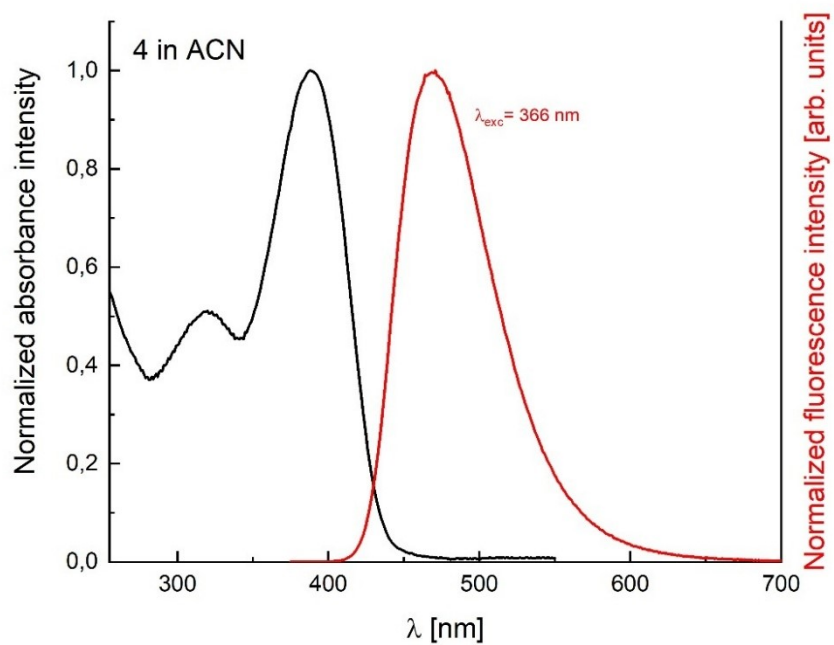


**Figure S27.** Absorption and emission spectra of TAPP 4 in acetonitrile.

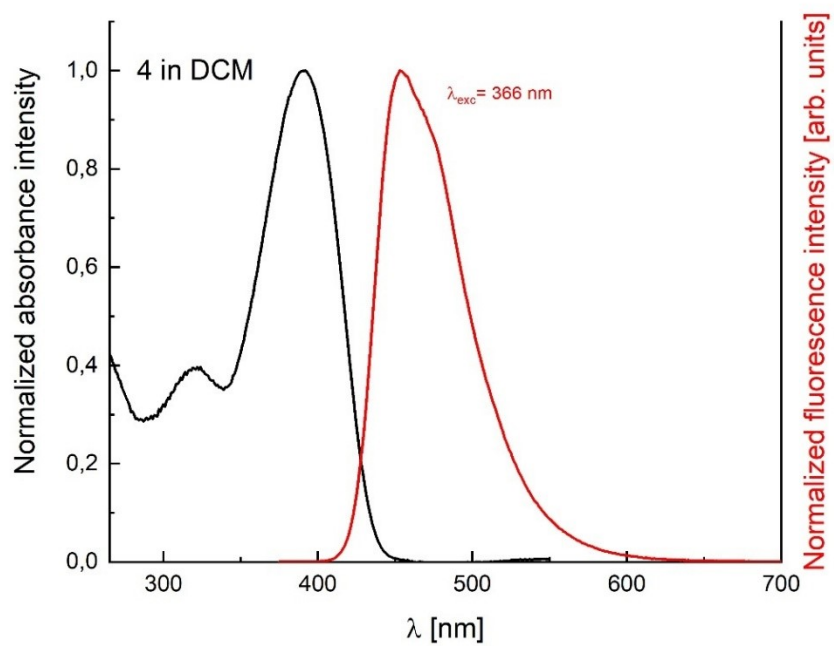


**Figure S28.** Absorption and emission spectra of TAPP 4 in DCM.

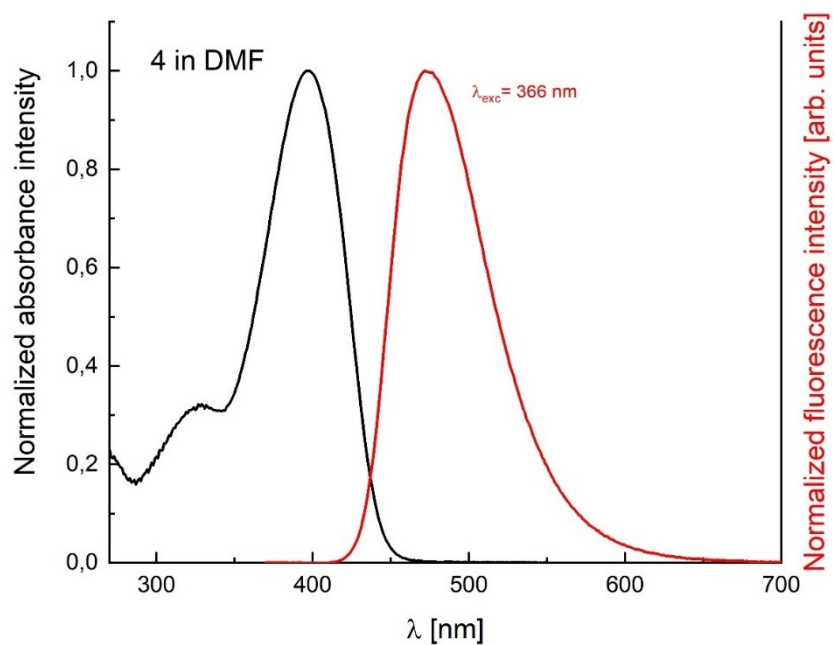


**Figure S29.** Absorption and emission spectra of TAPP 4 in DMF.

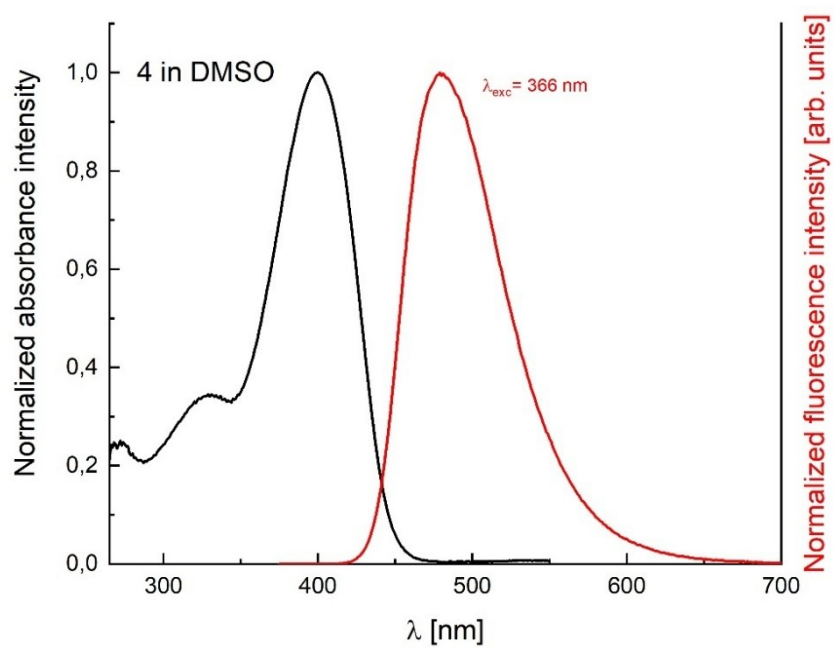


**Figure S30.** Absorption and emission spectra of TAPP 4 in DMSO.

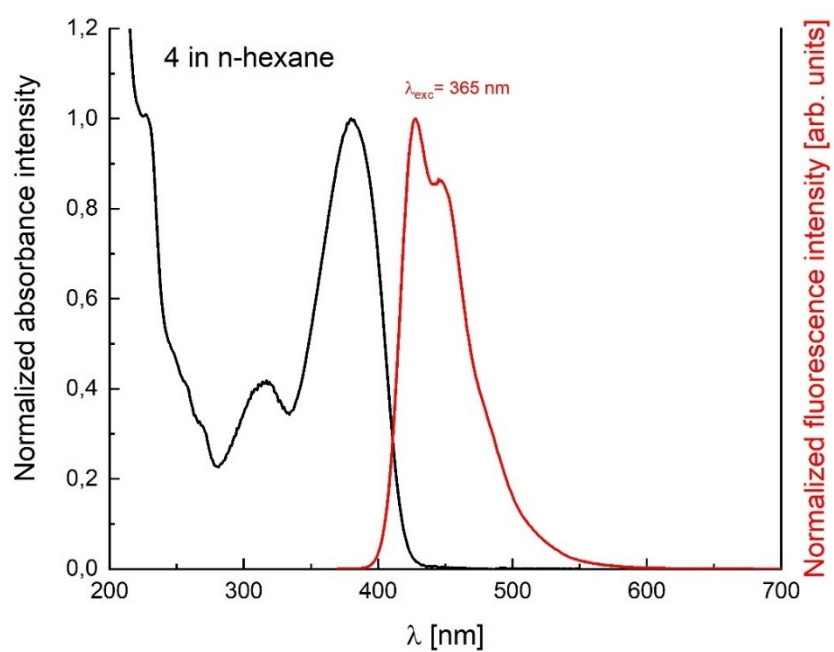


**Figure S31.** Absorption and emission spectra of TAPP 4 in hexane.

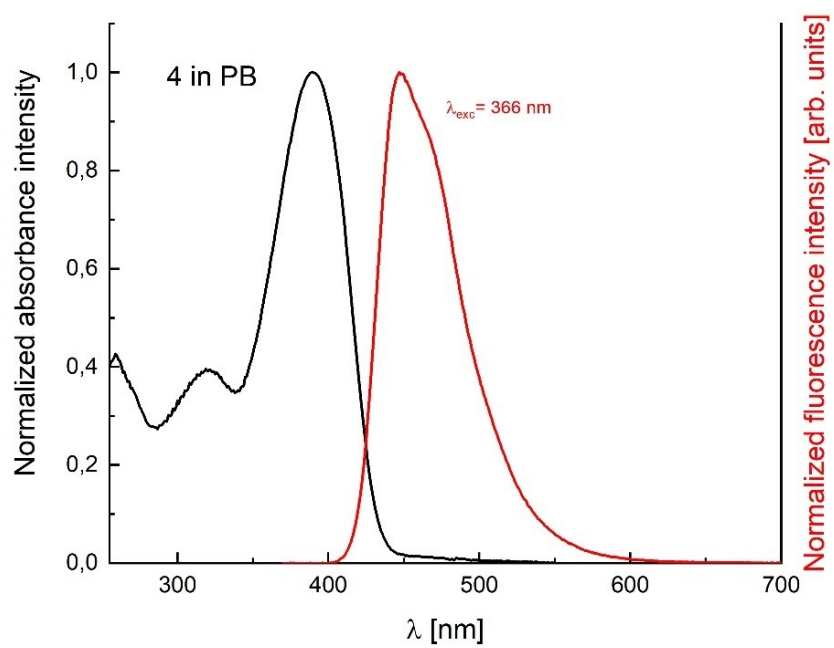


**Figure S32.** Absorption and emission spectra of TAPP 4 in propyl butyrate.

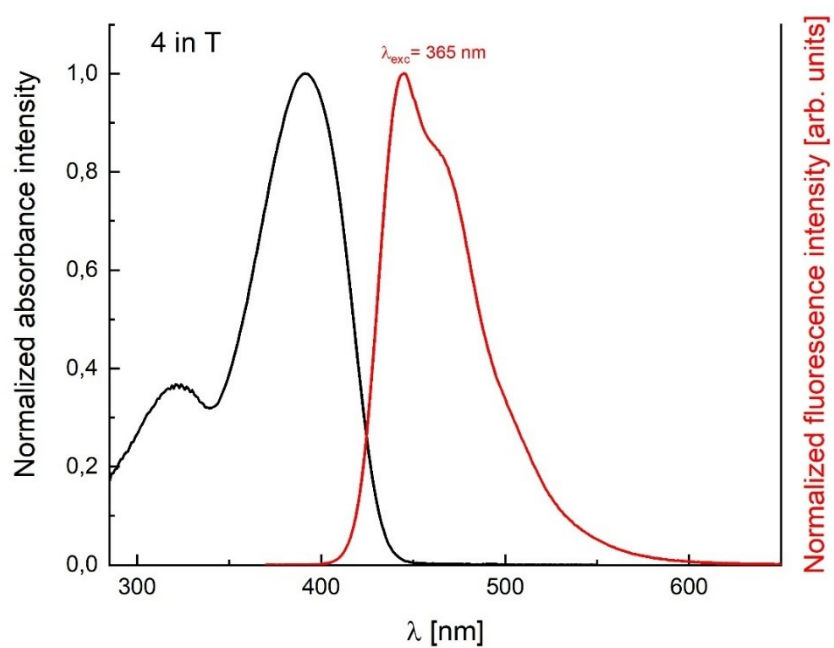


**Figure S33.** Absorption and emission spectra of TAPP 4 in toluene.

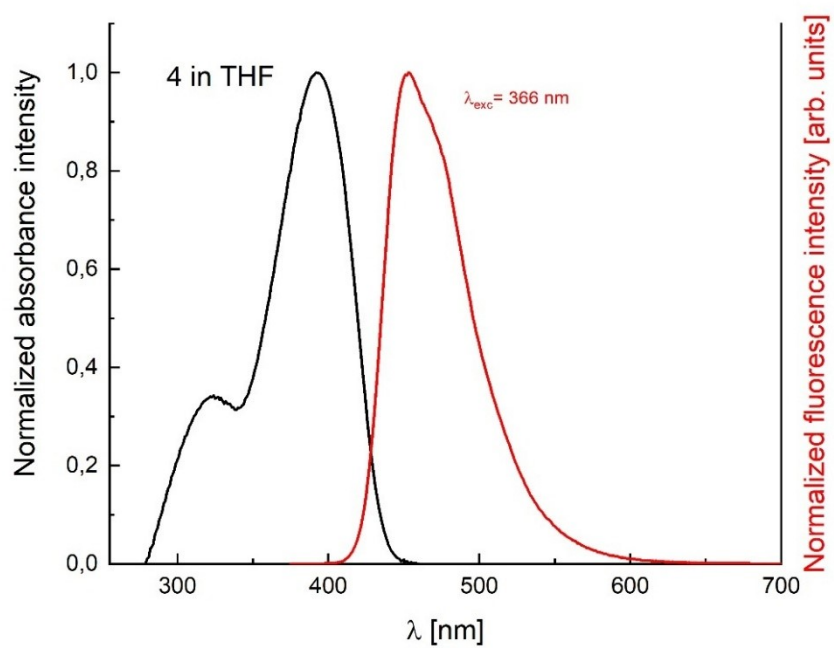


**Figure S34.** Absorption and emission spectra of TAPP **4** in THF.

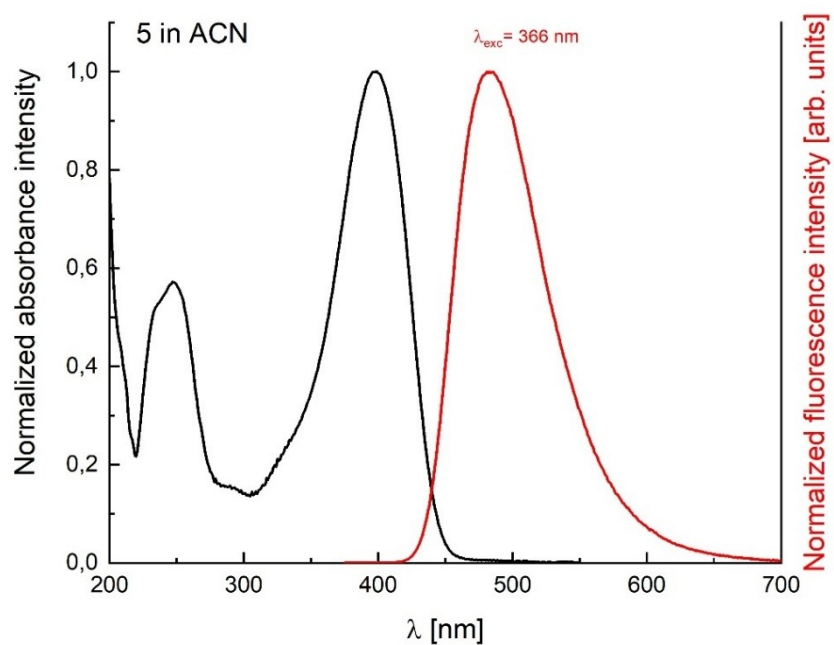


**Figure S35.** Absorption and emission spectra of TAPP **5** in acetonitrile.



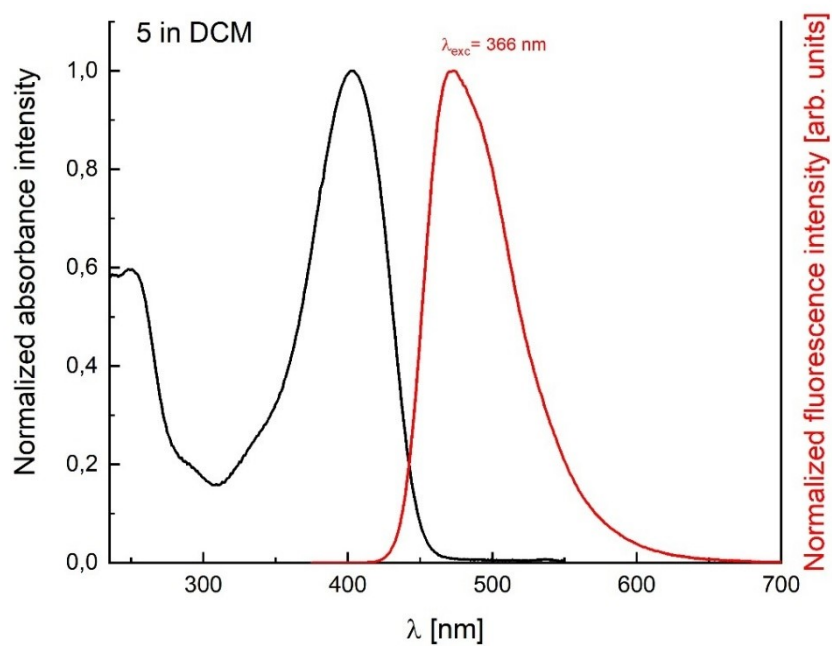


**Figure S36.** Absorption and emission spectra of TAPP 5 in DCM.

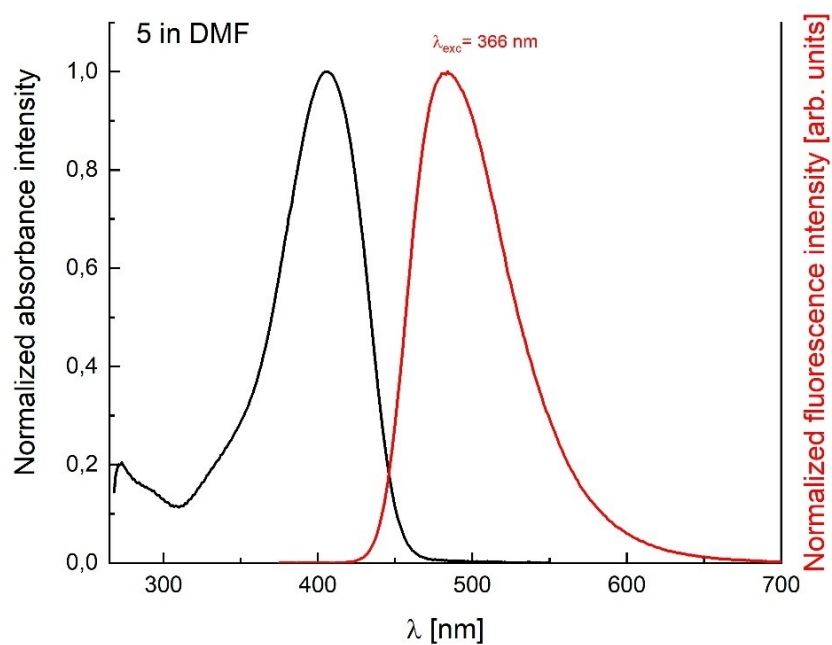


**Figure S37.** Absorption and emission spectra of TAPP 5 in DMF.

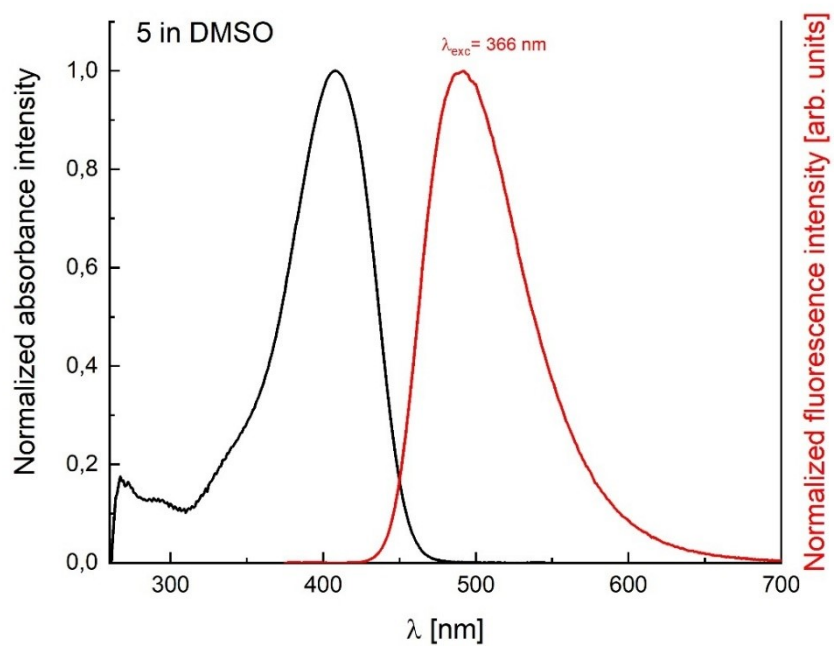


**Figure S38.** Absorption and emission spectra of TAPP 5 in DMSO.

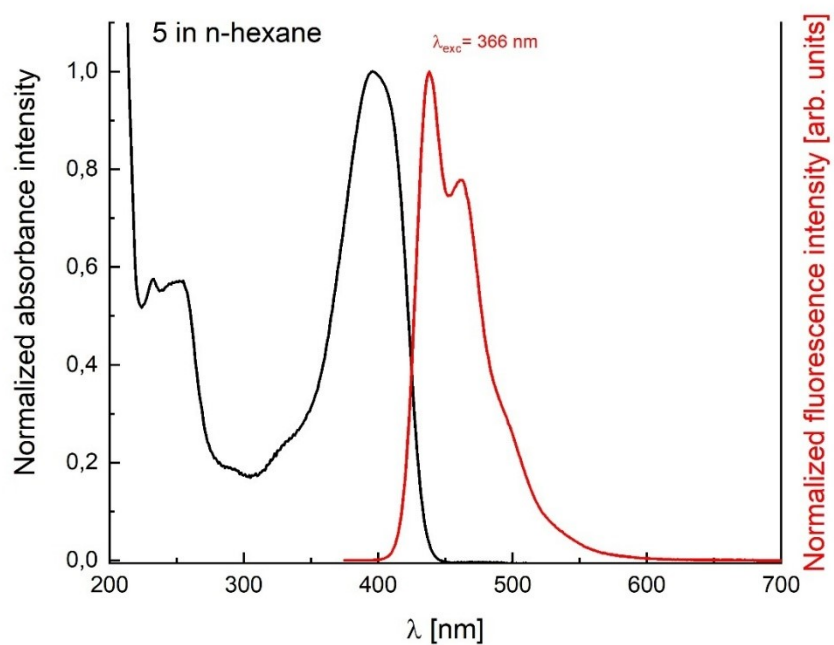


**Figure S39.** Absorption and emission spectra of TAPP 5 in hexane.

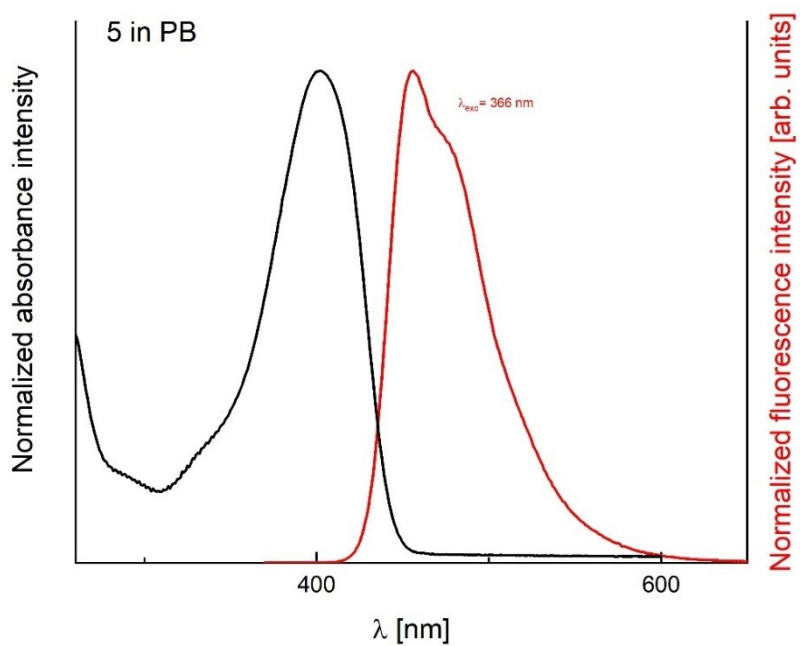


**Figure S40.** Absorption and emission spectra of TAPP **5** in propyl butyrate.

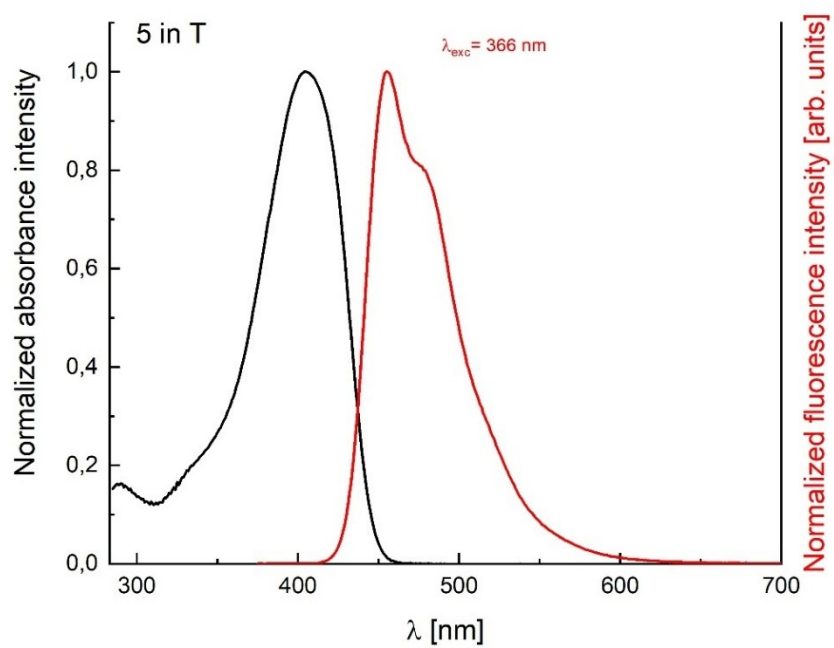


**Figure S41.** Absorption and emission spectra of TAPP **5** in toluene.

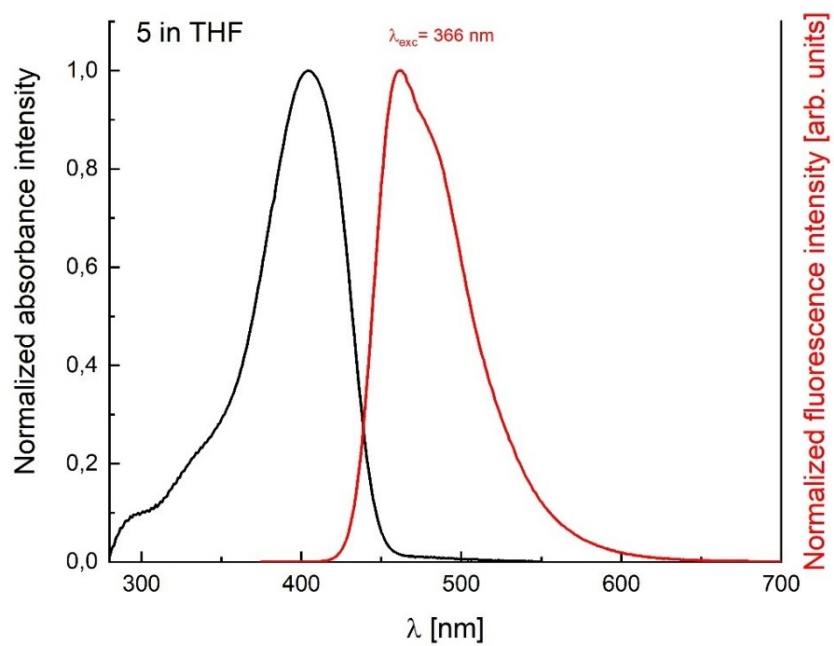


**Figure S42.** Absorption and emission spectra of TAPP **5** in THF.

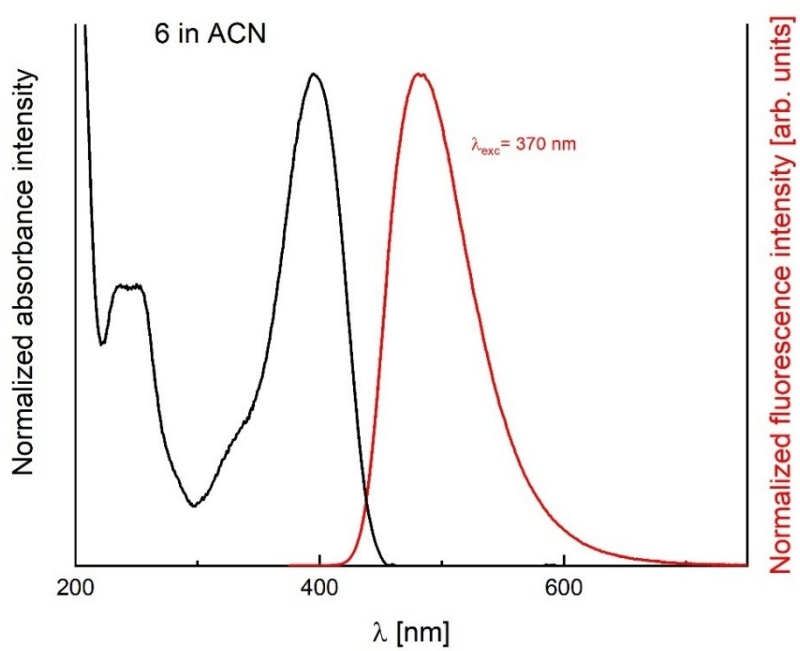


**Figure S43.** Absorption and emission spectra of TAPP **6** in acetonitrile.

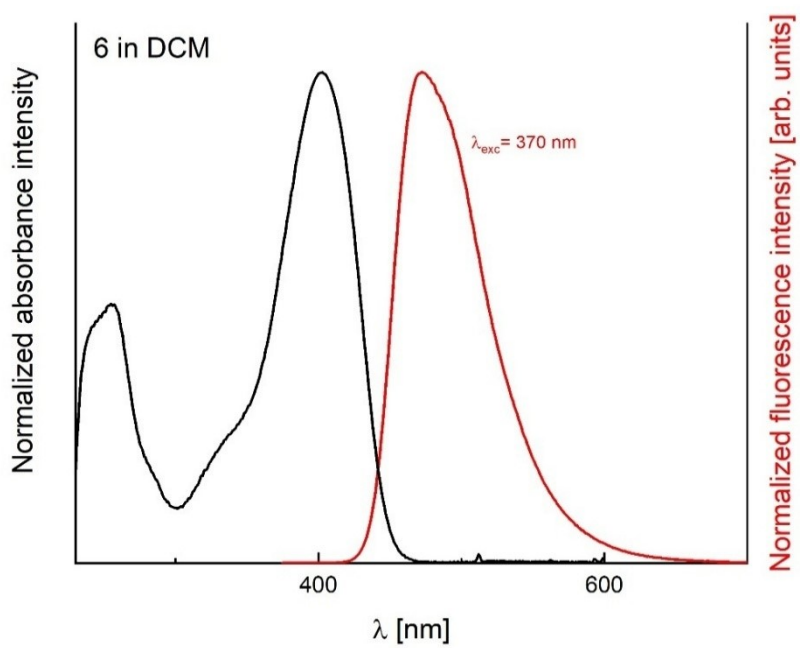


**Figure S44.** Absorption and emission spectra of TAPP **6** in DCM.

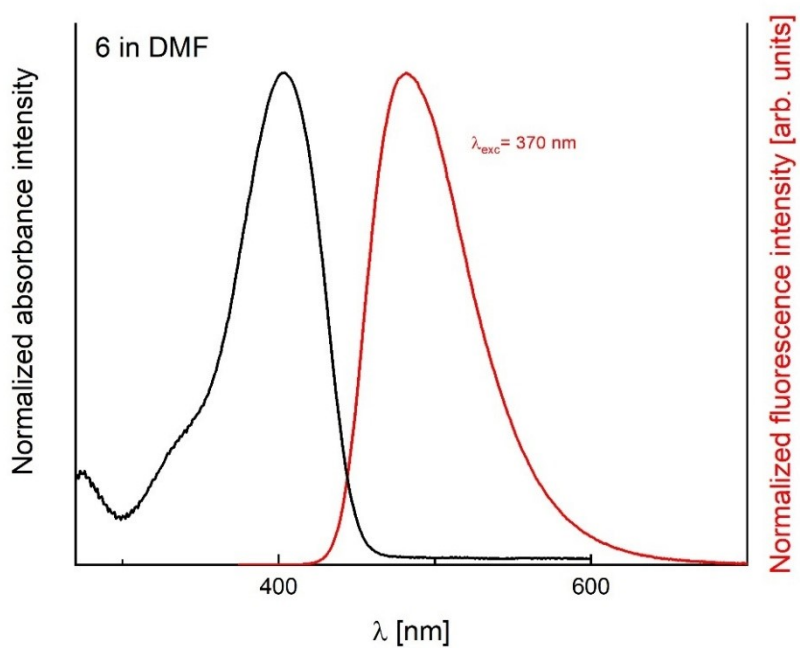


**Figure S45.** Absorption and emission spectra of TAPP **6** in DMF.

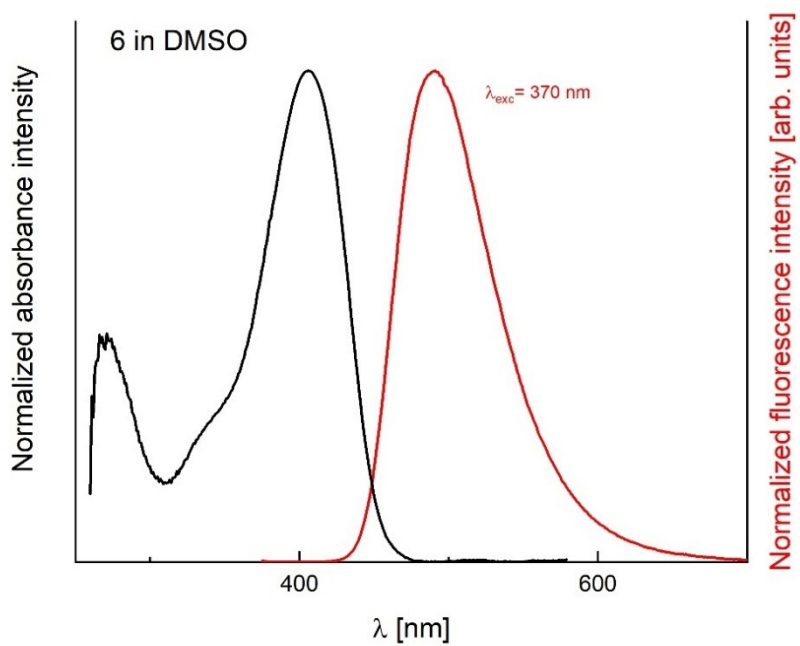


**Figure S46.** Absorption and emission spectra of TAPP **6** in DMSO.

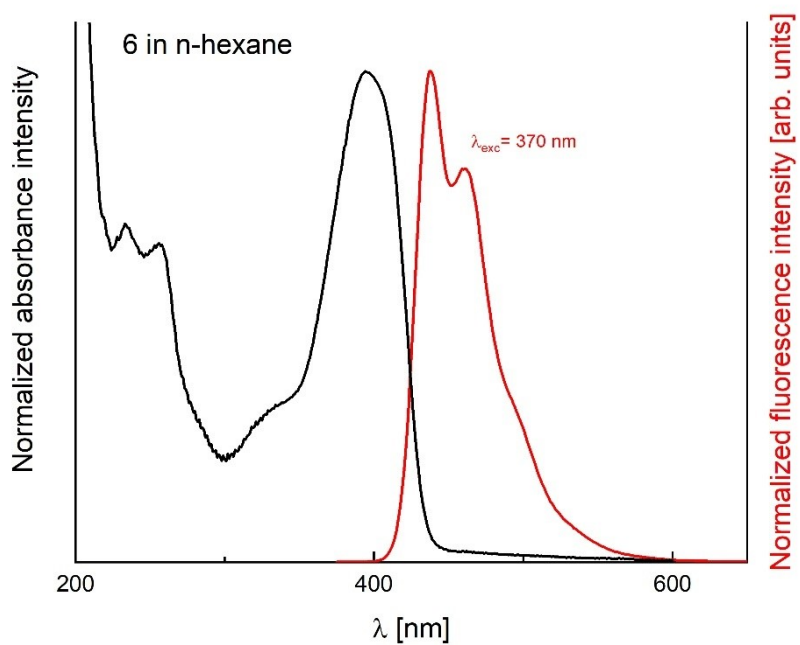


**Figure S47.** Absorption and emission spectra of TAPP **6** in hexane.

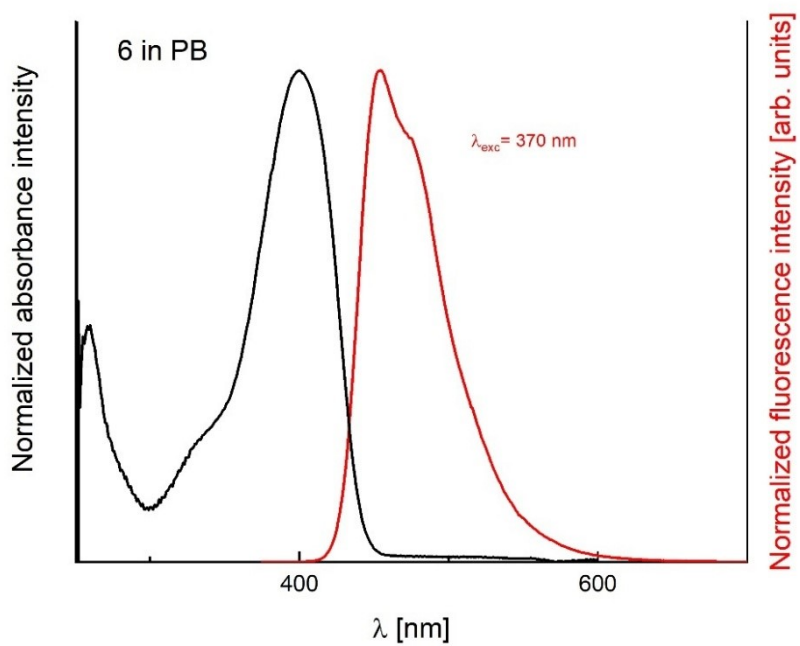


**Figure S48.** Absorption and emission spectra of TAPP **6** in propyl butyrate.

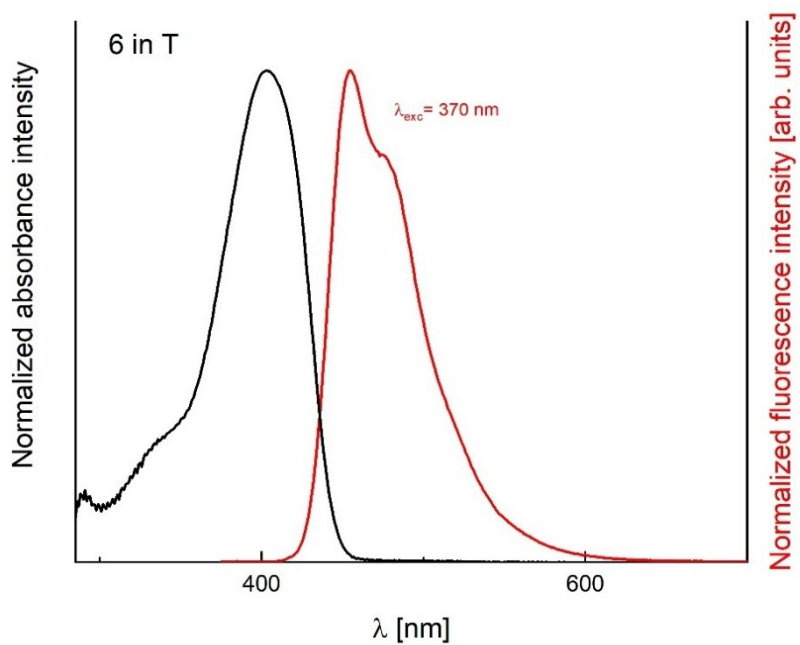


**Figure S49.** Absorption and emission spectra of TAPP **6** in toluene.

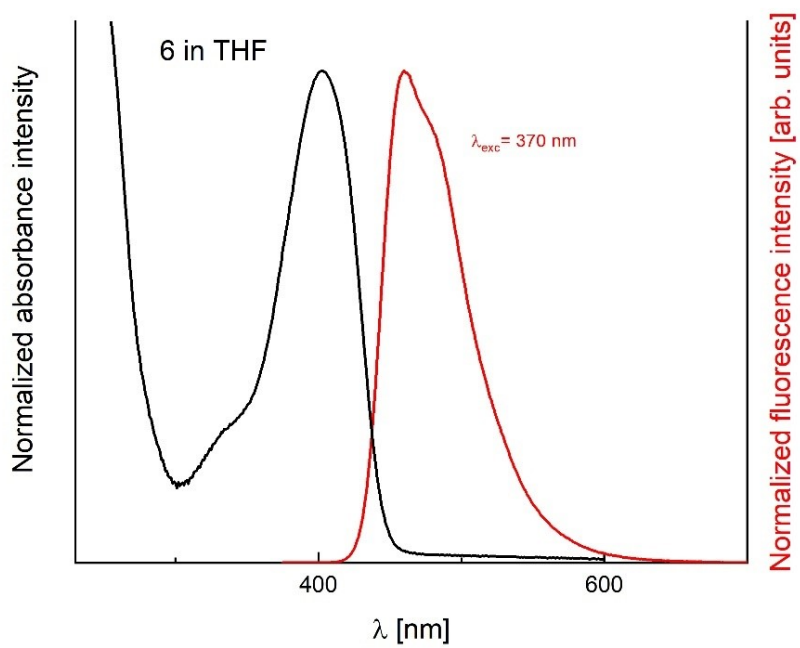


**Figure S50.** Absorption and emission spectra of TAPP **6** in THF.

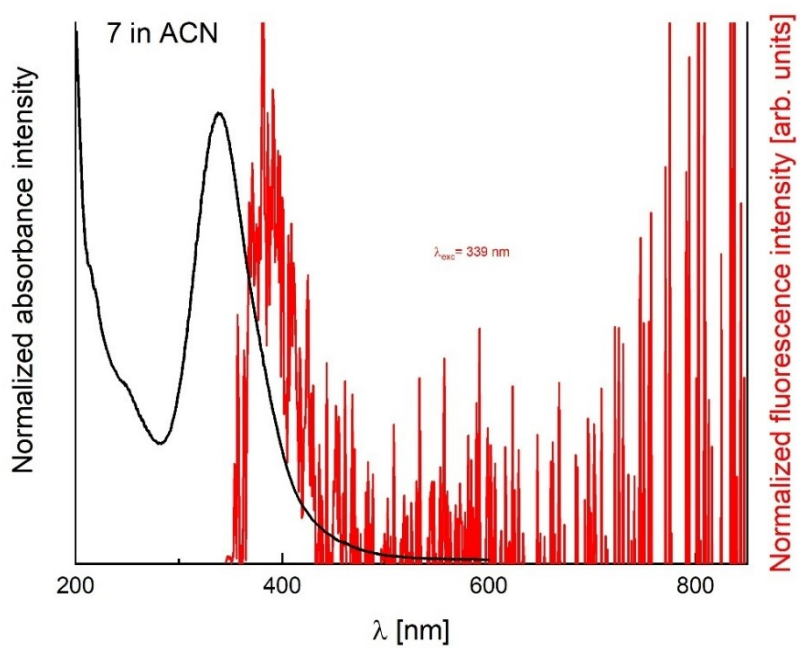


**Figure S51.** Absorption and emission spectra of TAPP **7** in acetonitrile.



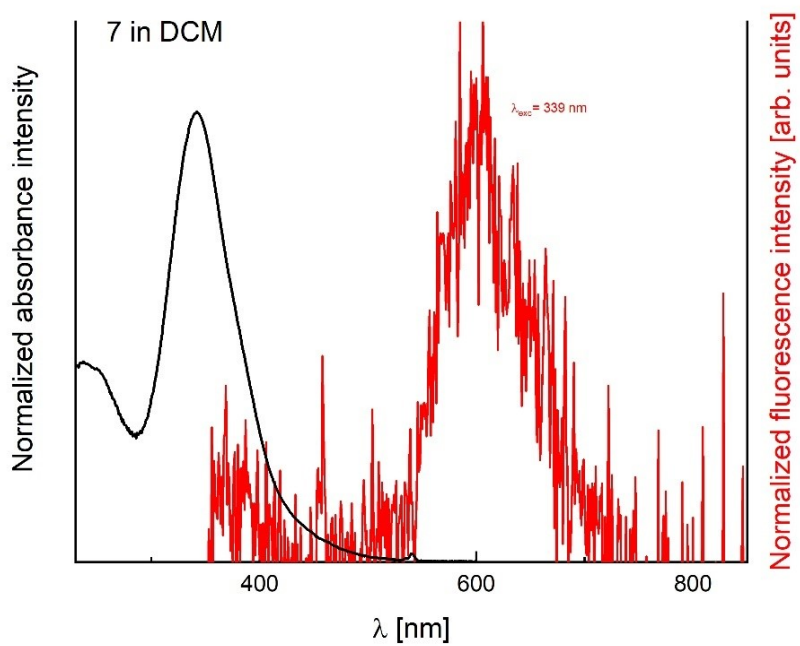


**Figure S52.** Absorption and emission spectra of TAPP 7 in DCM.

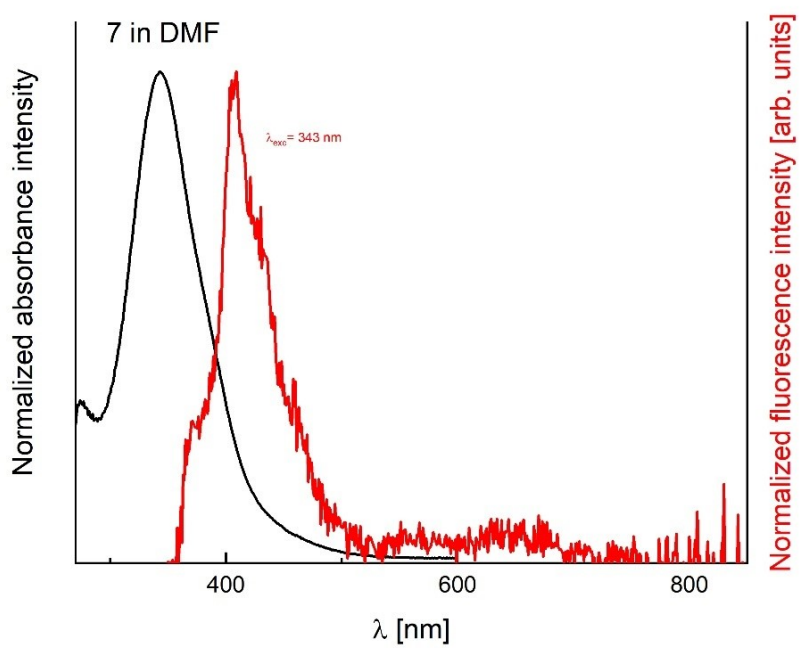


**Figure S53.** Absorption and emission spectra of TAPP 7 in DMF.

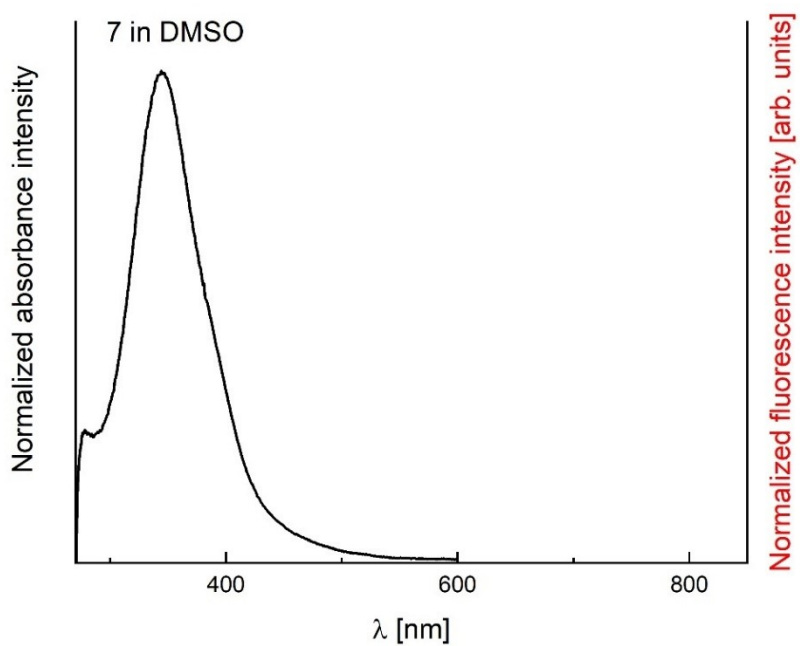


**Figure S54.** Absorption and emission spectra of TAPP 7 in DMSO.

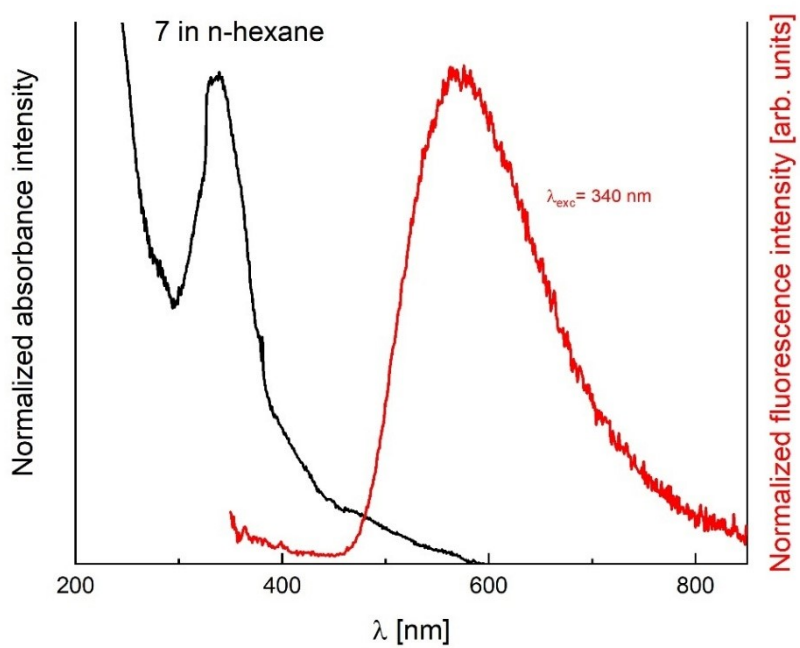


**Figure S55.** Absorption and emission spectra of TAPP 7 in hexane.

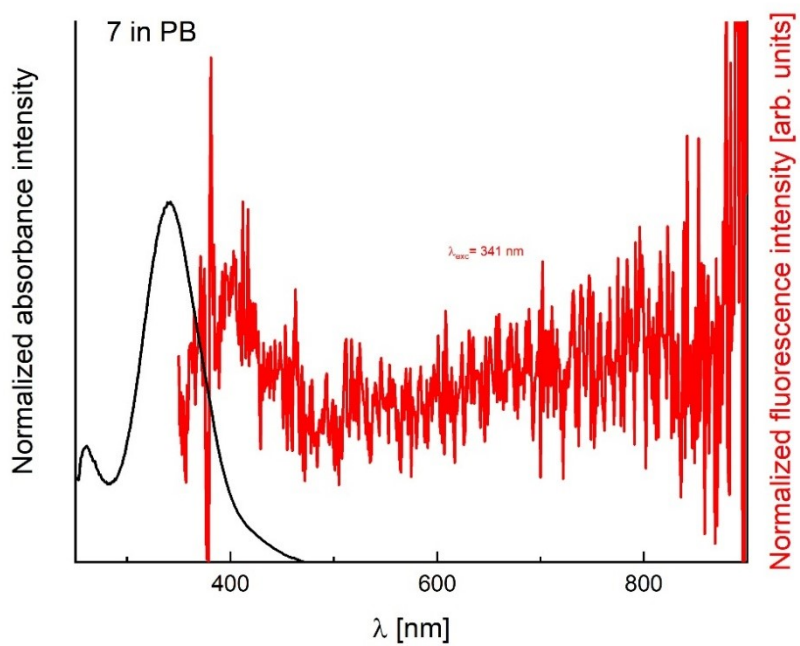


**Figure S56.** Absorption and emission spectra of TAPP 7 in propyl butyrate.

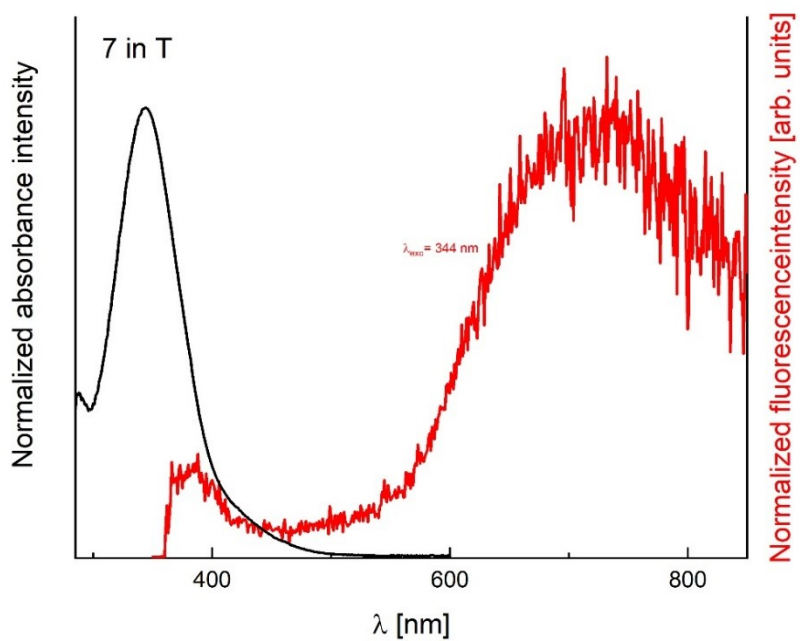


**Figure S57.** Absorption and emission spectra of TAPP 7 in toluene.

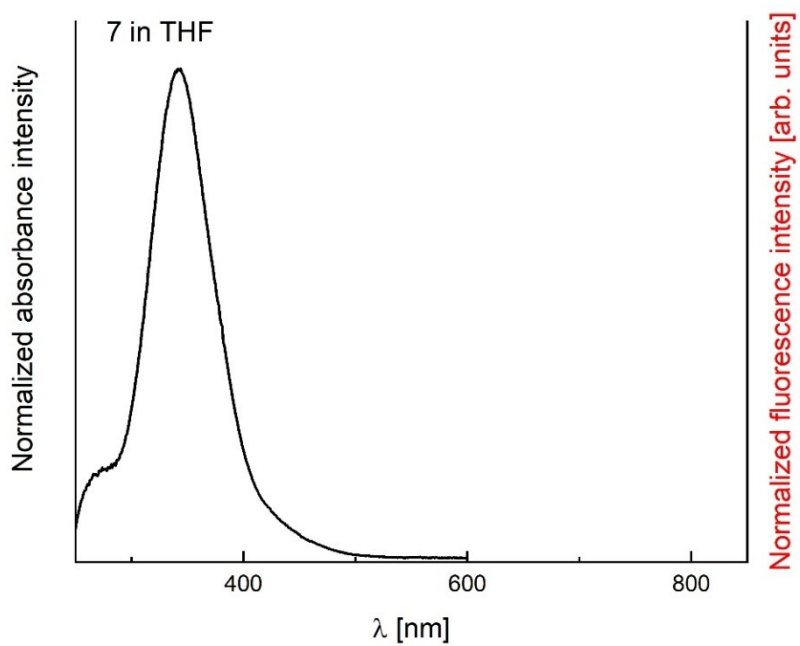


**Figure S58.** Absorption and emission spectra of TAPP 7 in THF.

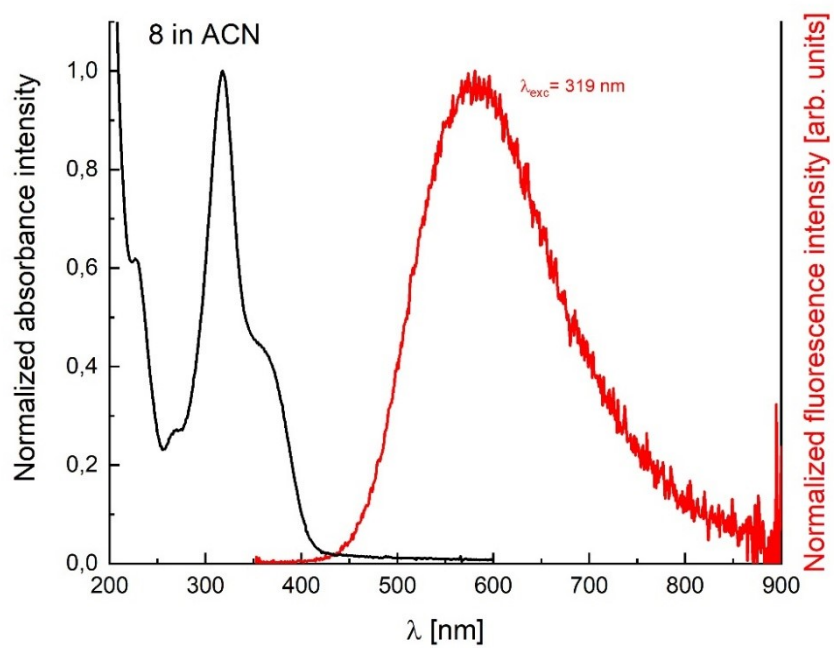


**Figure S59.** Absorption and emission spectra of TAPP 8 in acetonitrile.

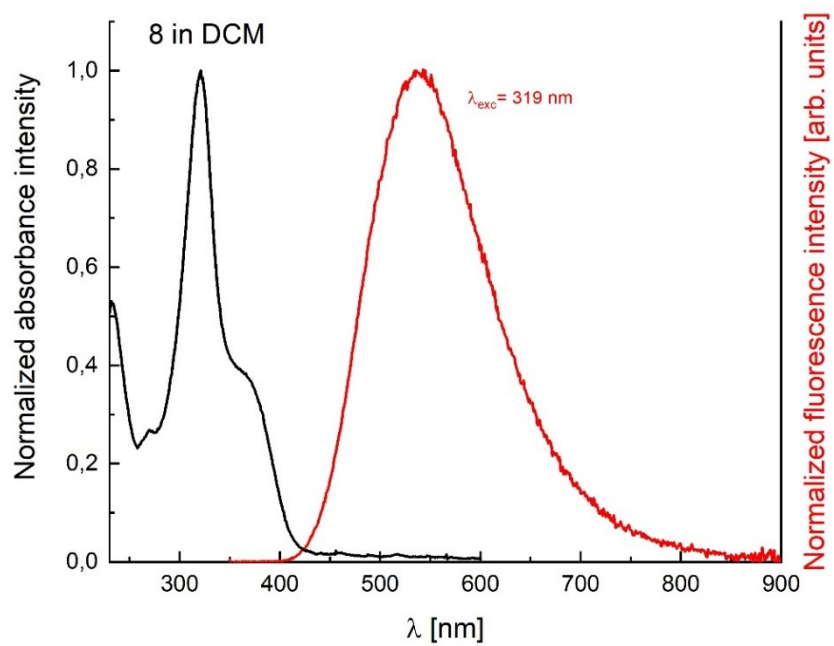


**Figure S60.** Absorption and emission spectra of TAPP 8 in DCM.

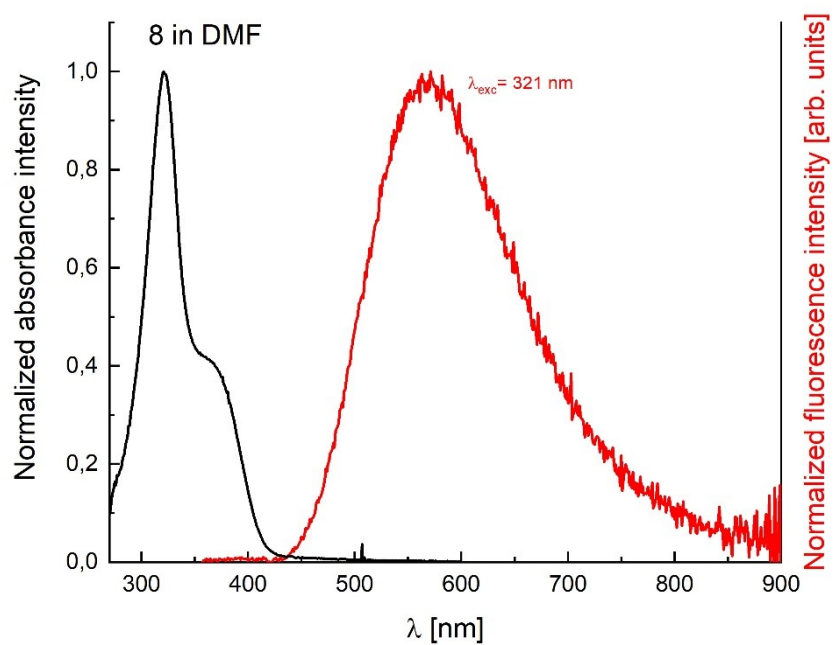


**Figure S61.** Absorption and emission spectra of TAPP 8 in DMF.

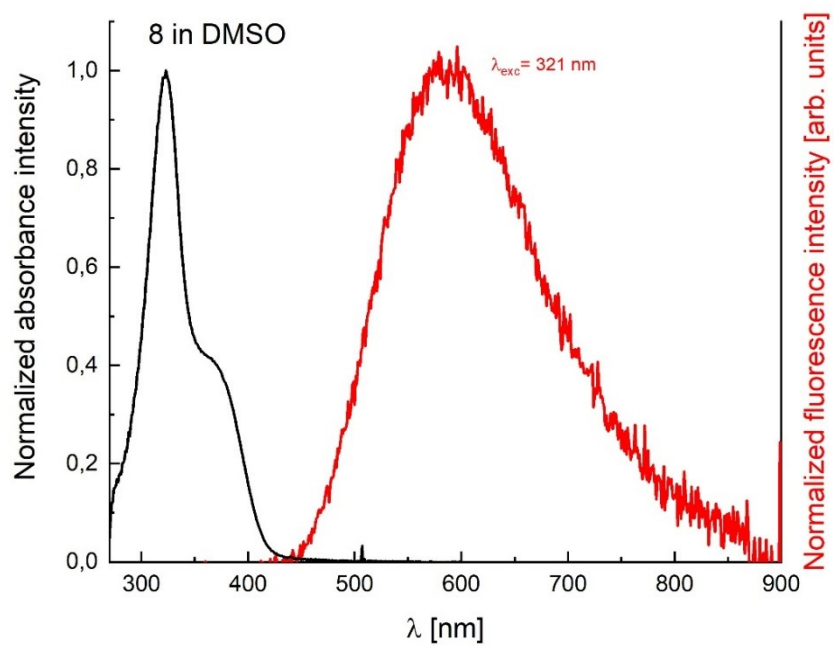


**Figure S62.** Absorption and emission spectra of TAPP **8** in DMSO.

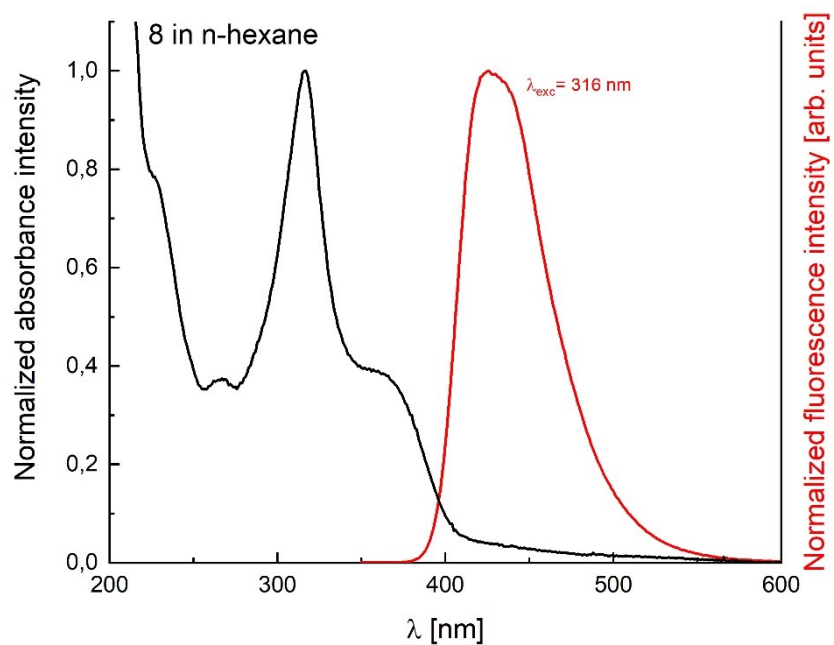


**Figure S63.** Absorption and emission spectra of TAPP **8** in hexane.

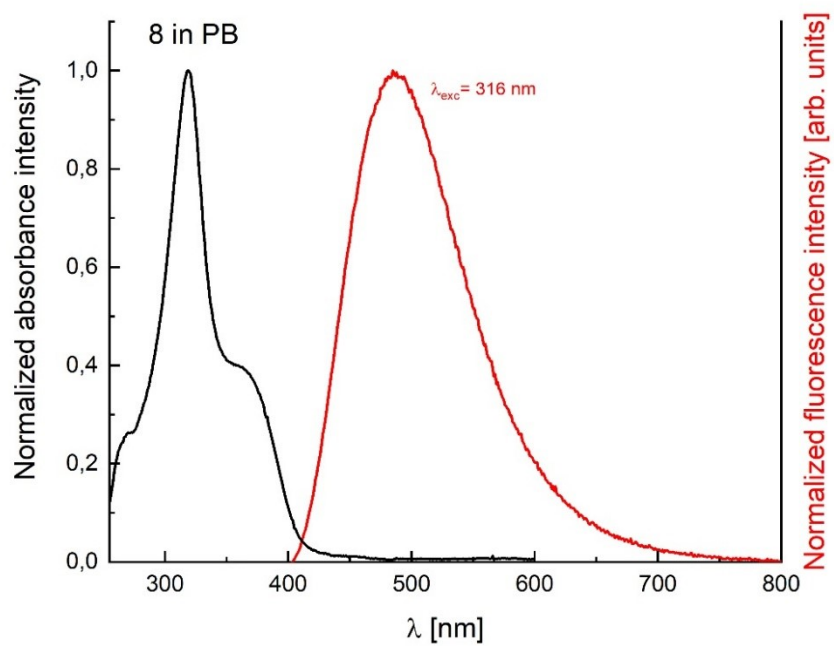


**Figure S64.** Absorption and emission spectra of TAPP **8** in propyl butyrate.

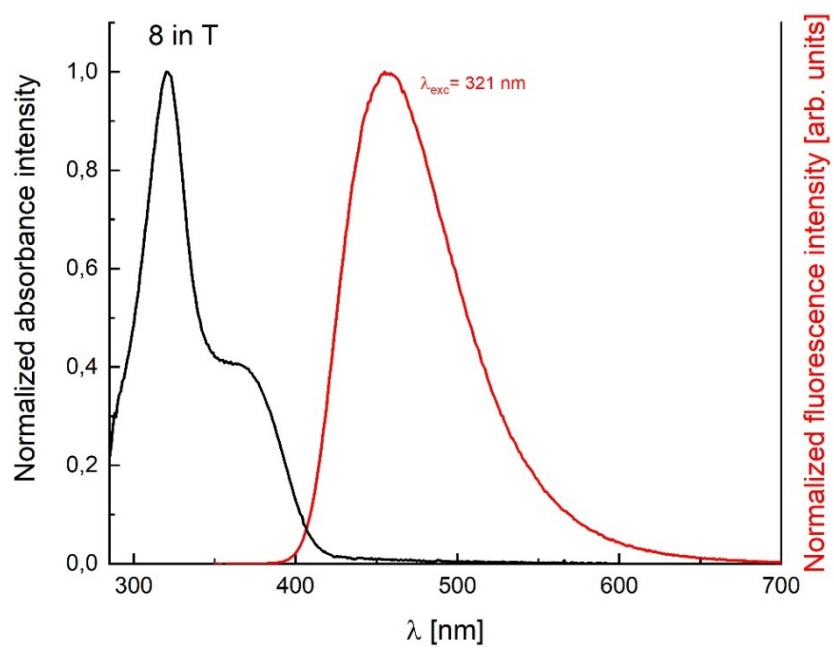


**Figure S65.** Absorption and emission spectra of TAPP **8** in toluene.

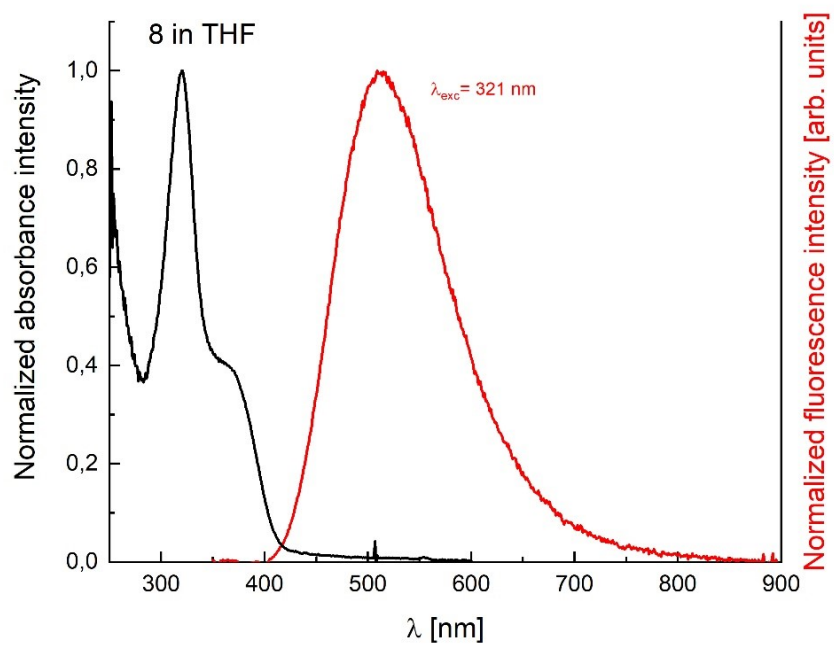


**Figure S66.** Absorption and emission spectra of TAPP **8** in THF.

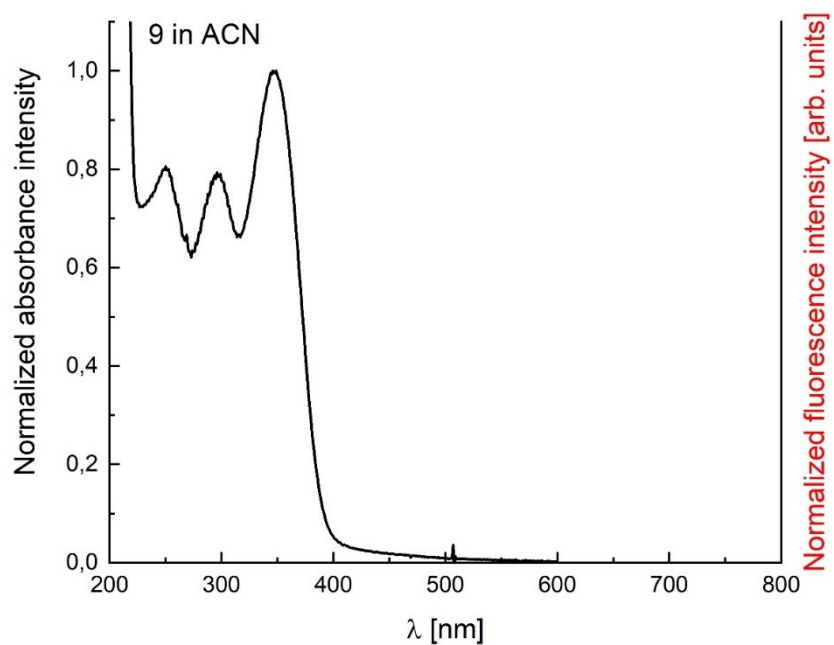


**Figure S67.** Absorption and emission spectra of TAPP **9** in acetonitrile.



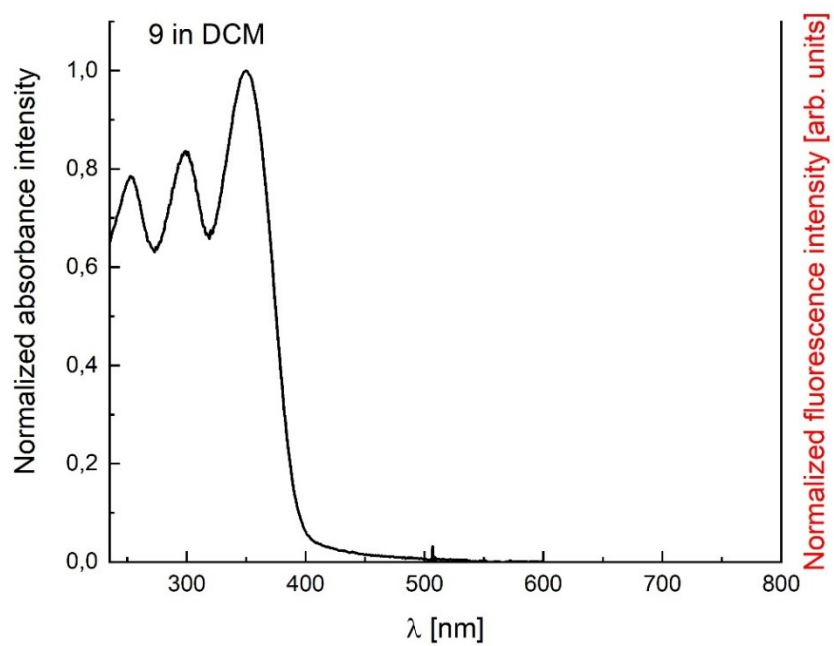


**Figure S68.** Absorption and emission spectra of TAPP 9 in DCM.

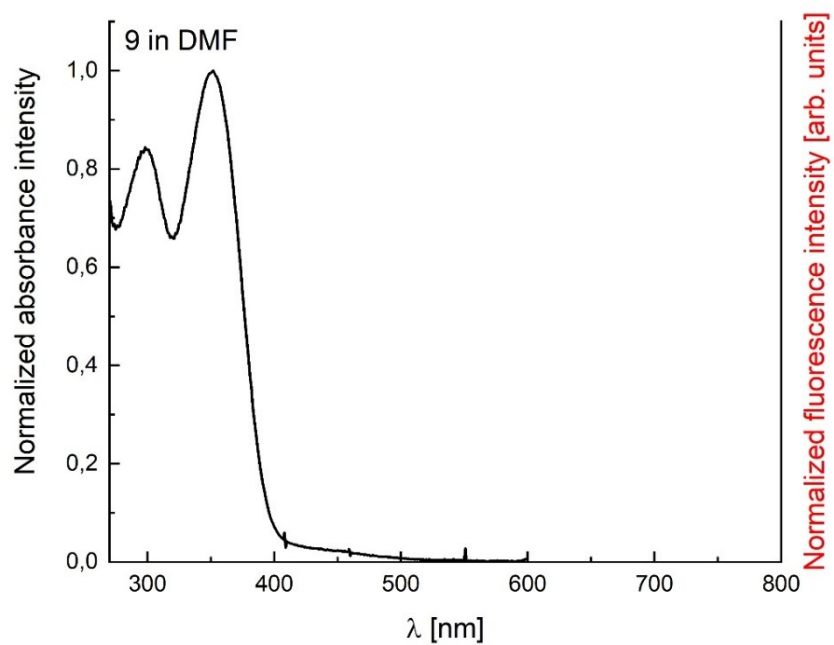


**Figure S69.** Absorption and emission spectra of TAPP 9 in DMF.

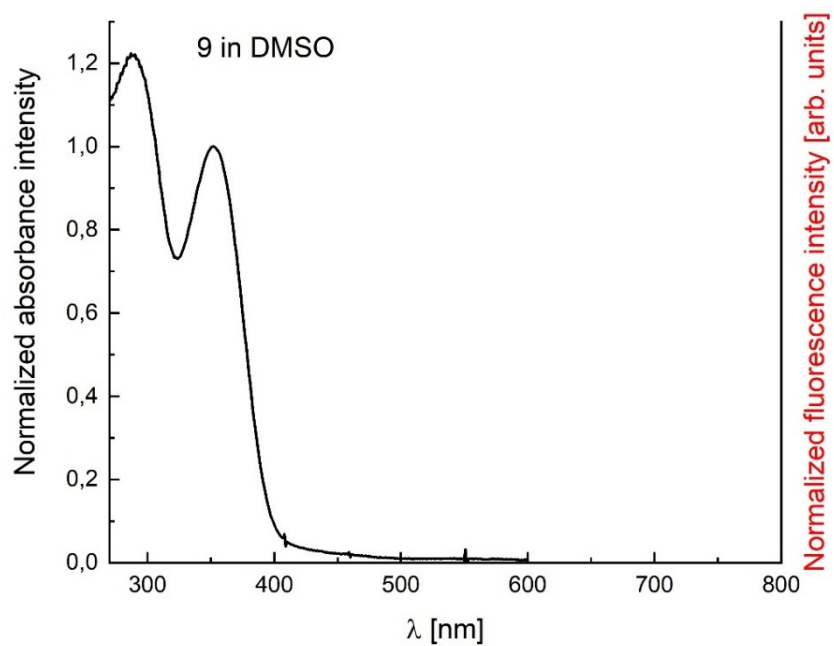


**Figure S70.** Absorption and emission spectra of TAPP **9** in DMSO.

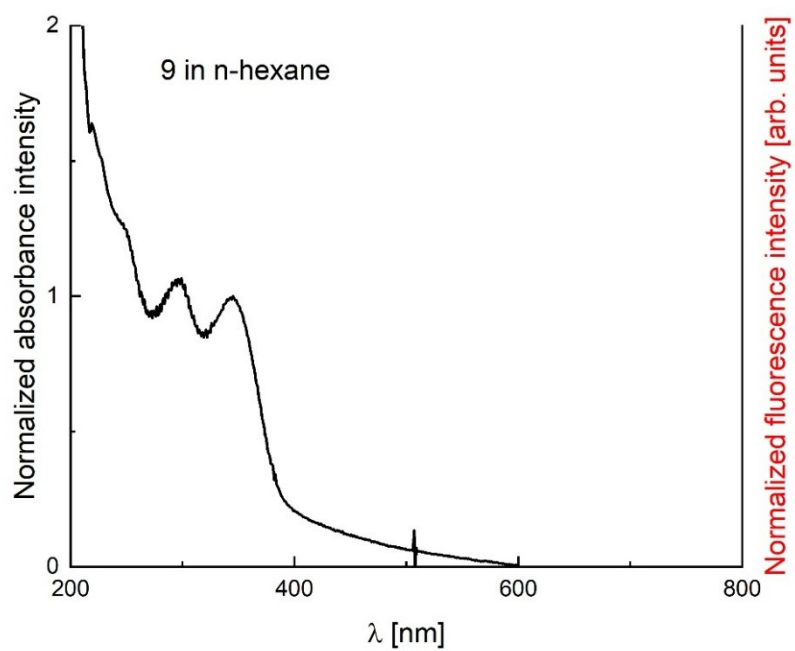


**Figure S71.** Absorption and emission spectra of TAPP **9** in hexane.

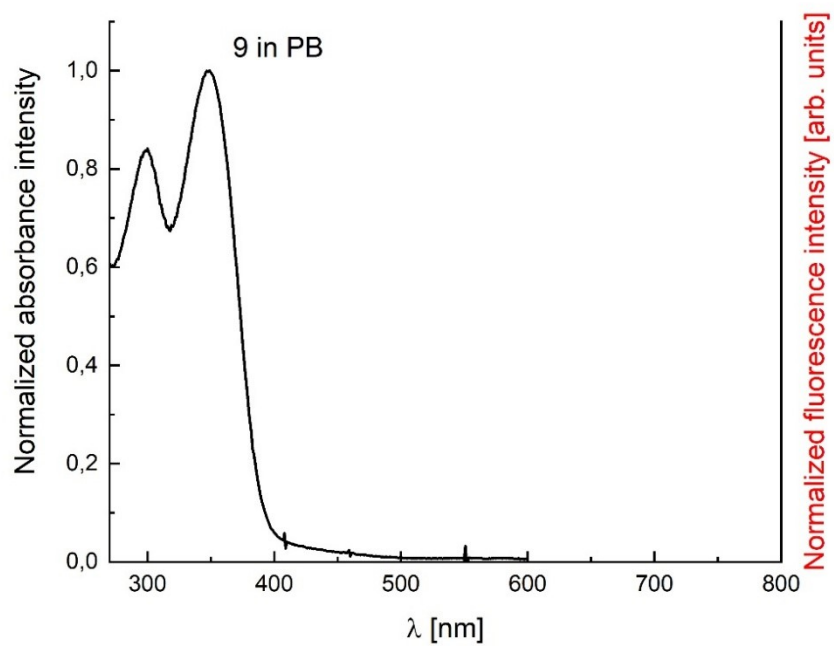


**Figure S72.** Absorption and emission spectra of TAPP 9 in propyl butyrate.

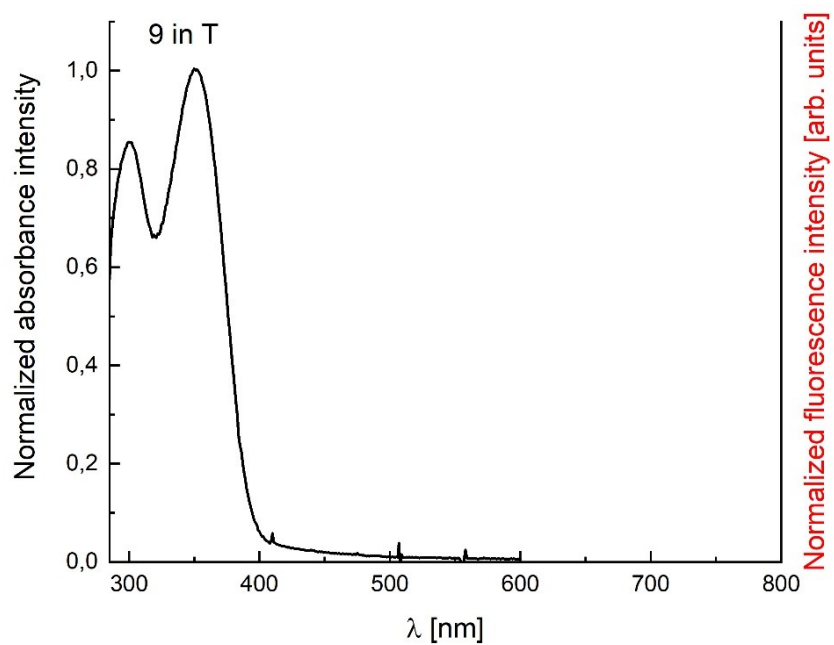


**Figure S73.** Absorption and emission spectra of TAPP 9 in toluene.

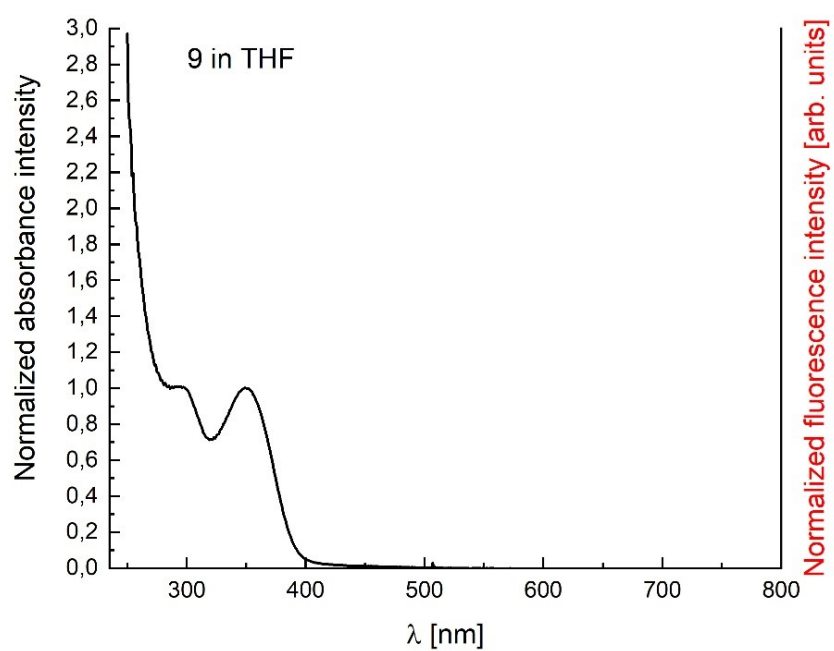


**Figure S74.** Absorption and emission spectra of TAPP **9** in THF.

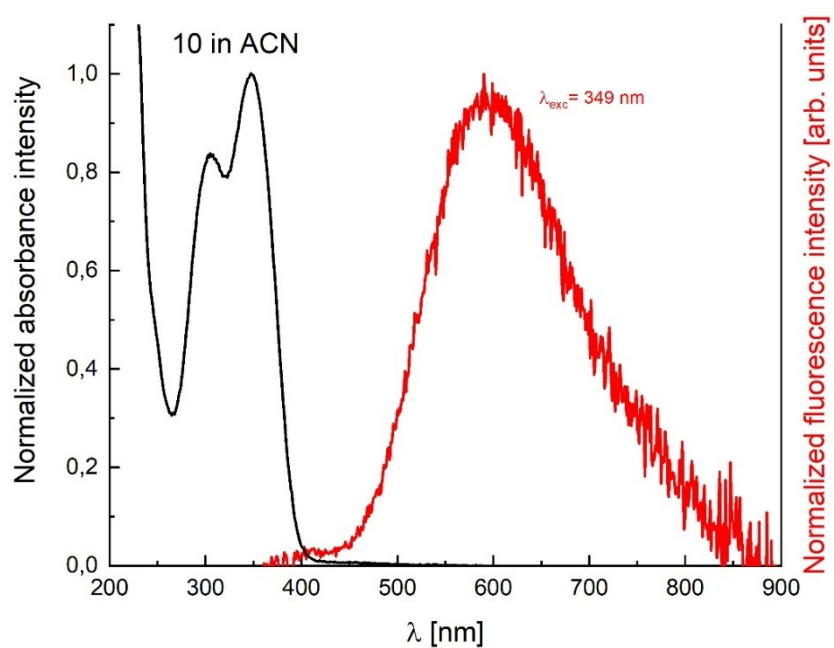


**Figure S75.** Absorption and emission spectra of TAPP **10** in acetonitrile.

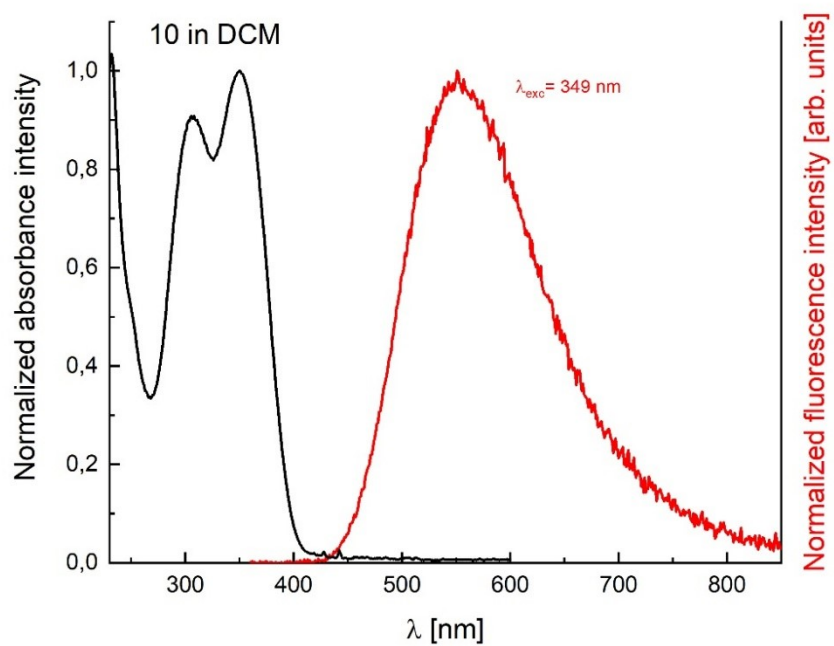


**Figure S76.** Absorption and emission spectra of TAPP **10** in DCM.

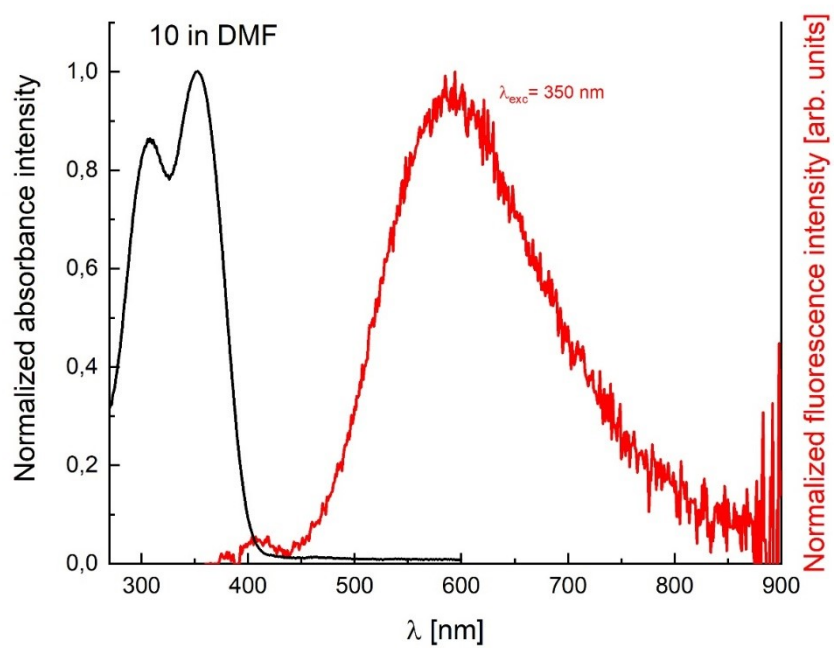


**Figure S77.** Absorption and emission spectra of TAPP **10** in DMF.

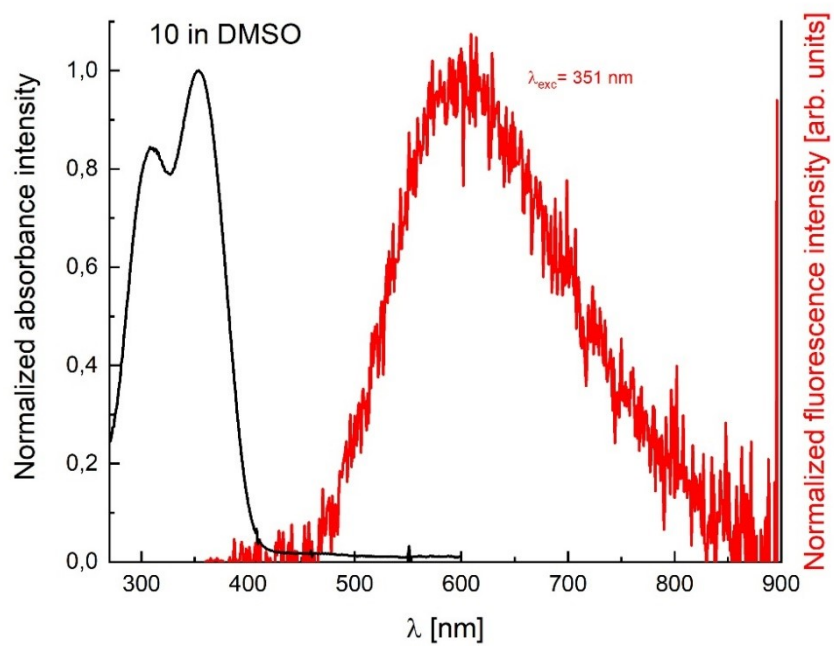


**Figure S78.** Absorption and emission spectra of TAPP **10** in DMSO.

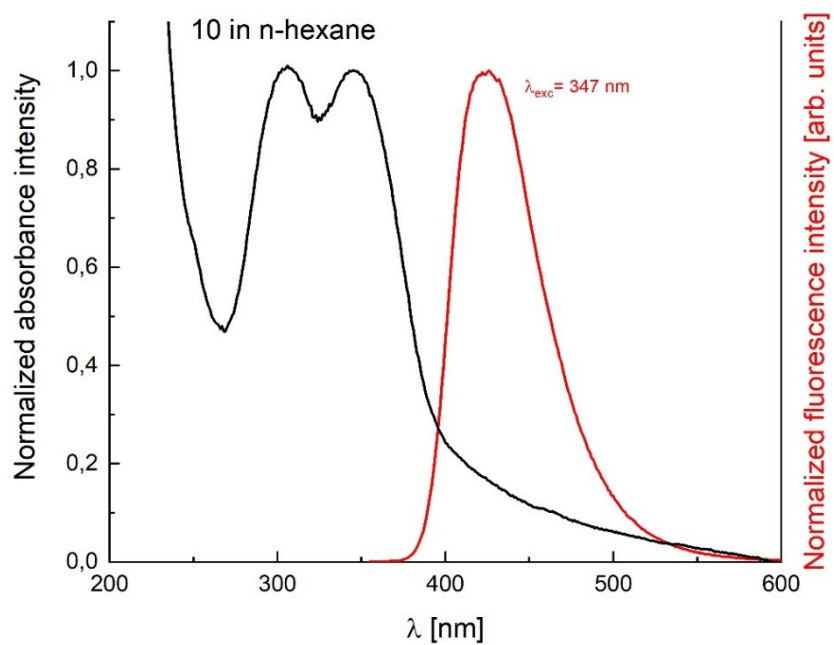


**Figure S79.** Absorption and emission spectra of TAPP **10** in hexane.

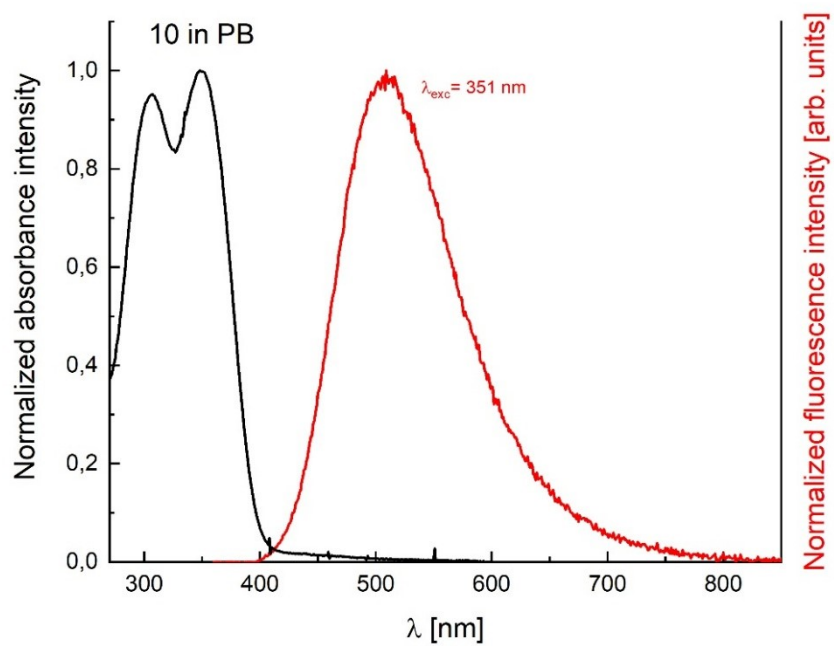


**Figure S80.** Absorption and emission spectra of TAPP **10** in propyl butyrate.

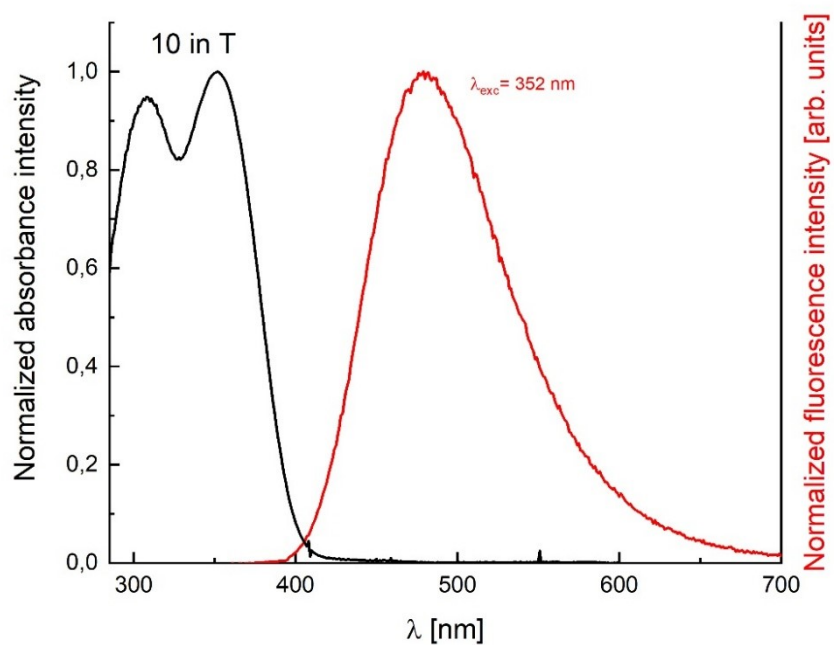


**Figure S81.** Absorption and emission spectra of TAPP **10** in toluene.

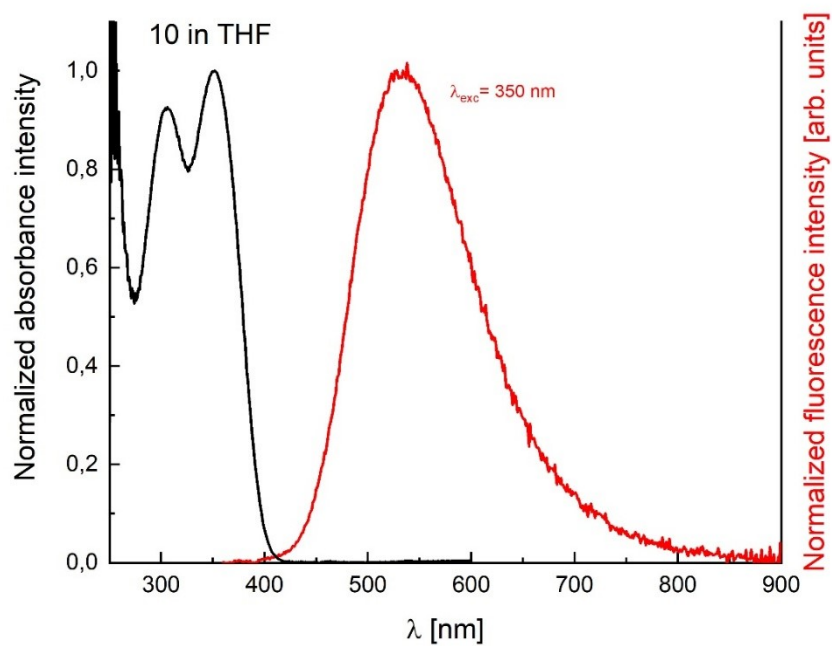


**Figure S82.** Absorption and emission spectra of TAPP **10** in THF.

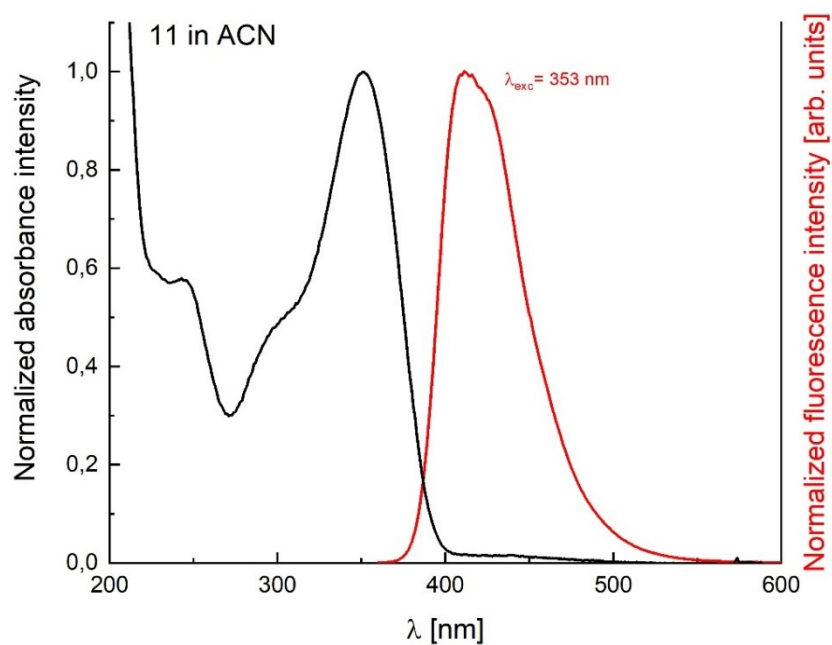


**Figure S83.** Absorption and emission spectra of TAPP **11** in acetonitrile.



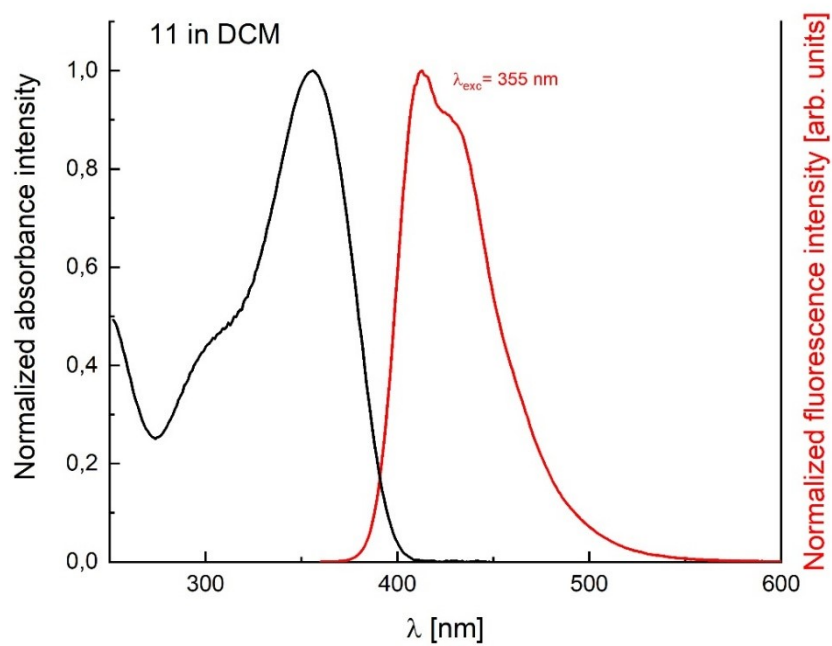


**Figure S84.** Absorption and emission spectra of TAPP 11 in DCM.

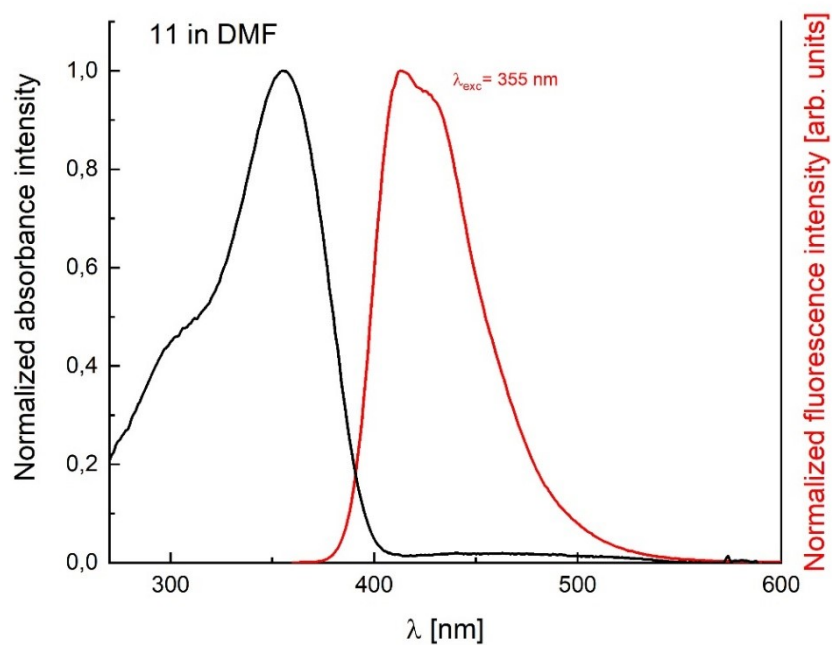


**Figure S85.** Absorption and emission spectra of TAPP 11 in DMF.

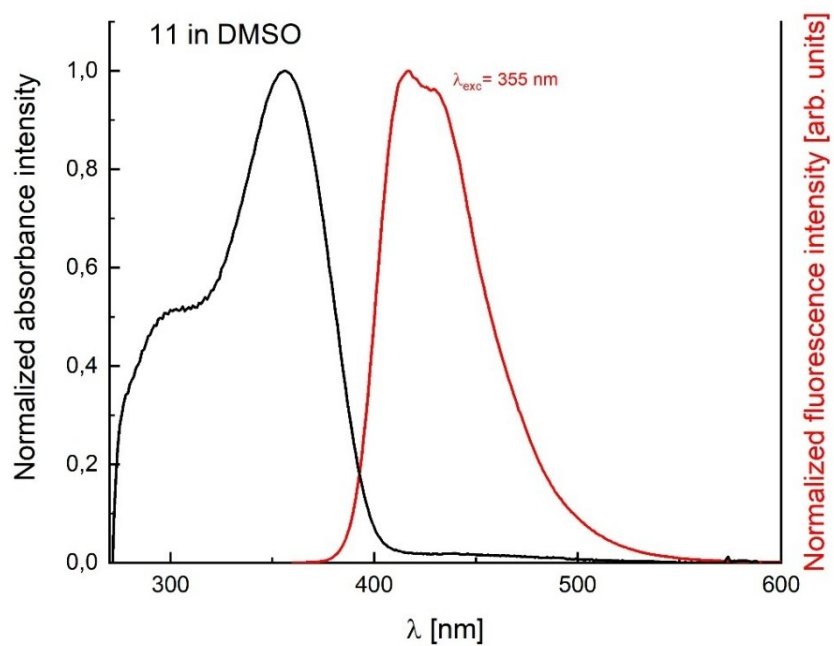


**Figure S86.** Absorption and emission spectra of TAPP **11** in DMSO.

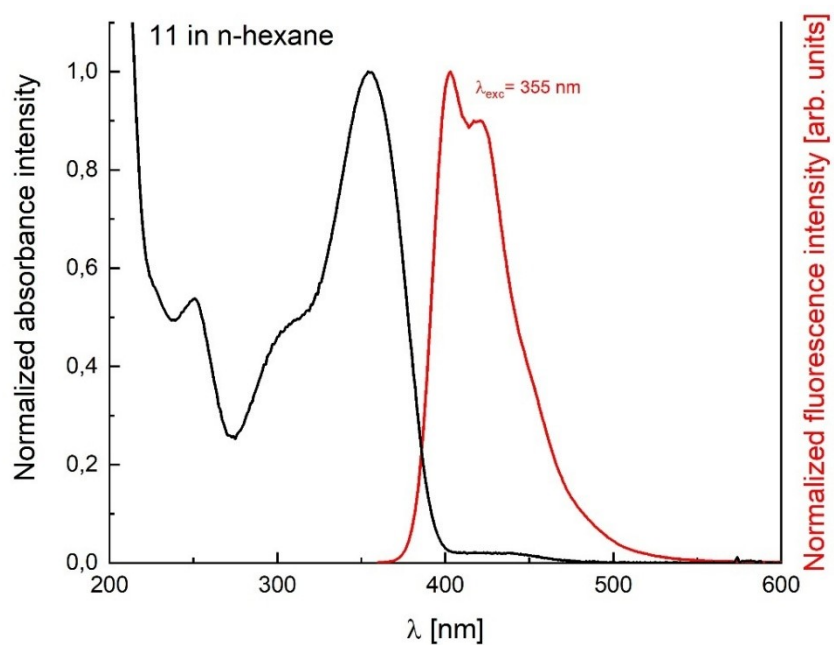


**Figure S87.** Absorption and emission spectra of TAPP **11** in hexane.

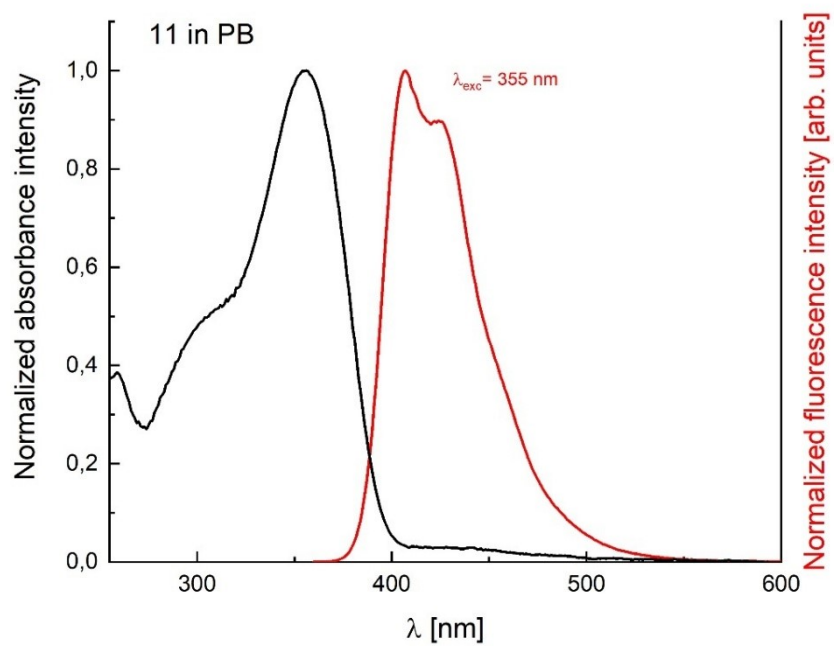


**Figure S88.** Absorption and emission spectra of TAPP **11** in propyl butyrate.

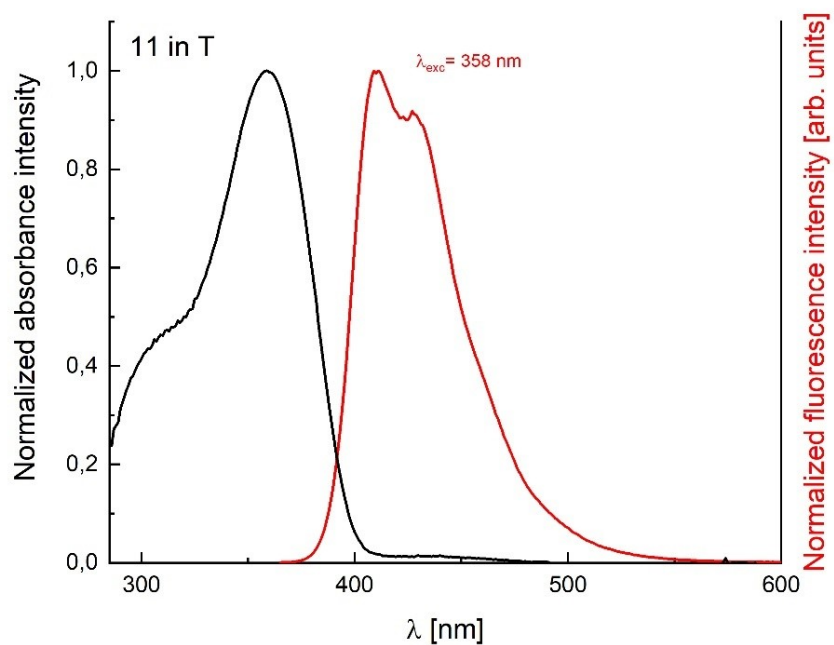


**Figure S89.** Absorption and emission spectra of TAPP **11** in toluene.

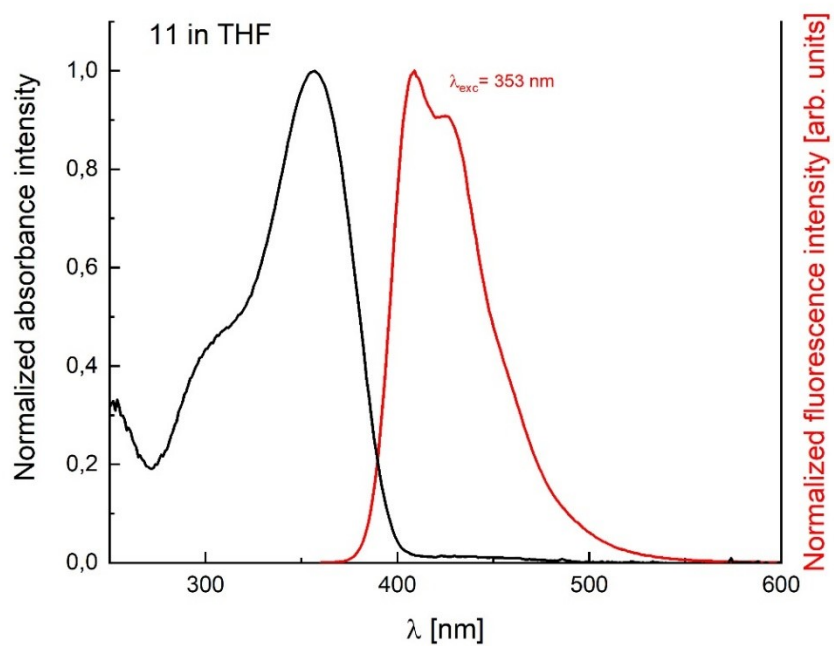


**Figure S90.** Absorption and emission spectra of TAPP **11** in THF.

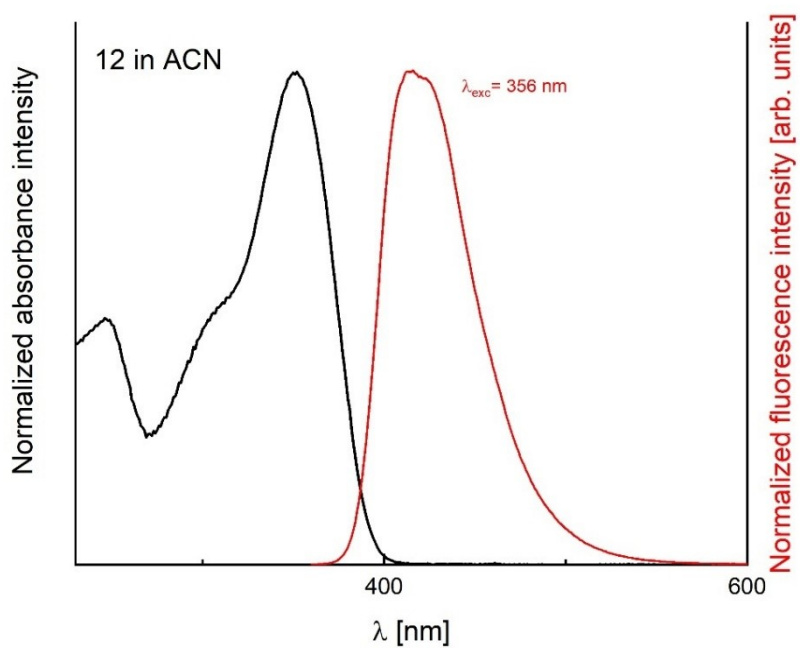


**Figure S91.** Absorption and emission spectra of TAPP **12** in acetonitrile.

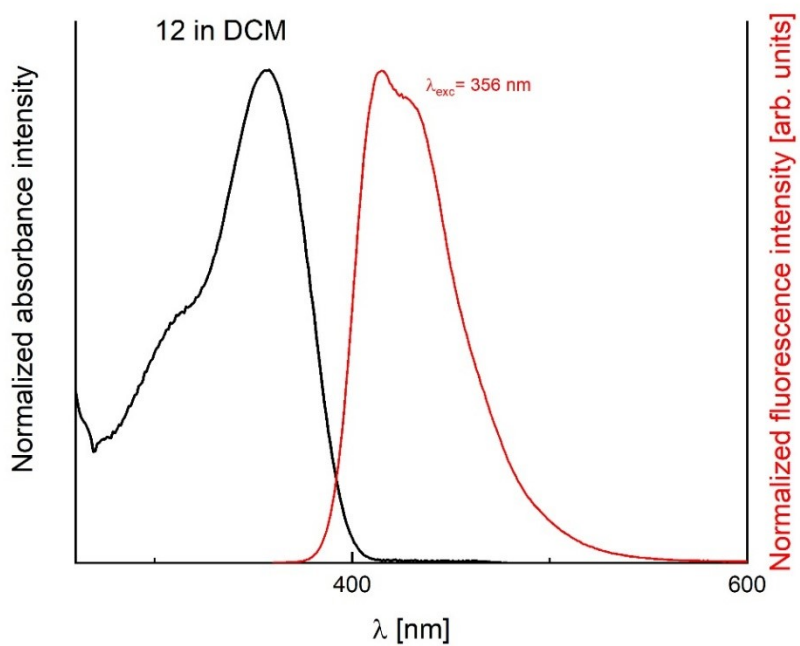


**Figure S92.** Absorption and emission spectra of TAPP **12** in DCM.

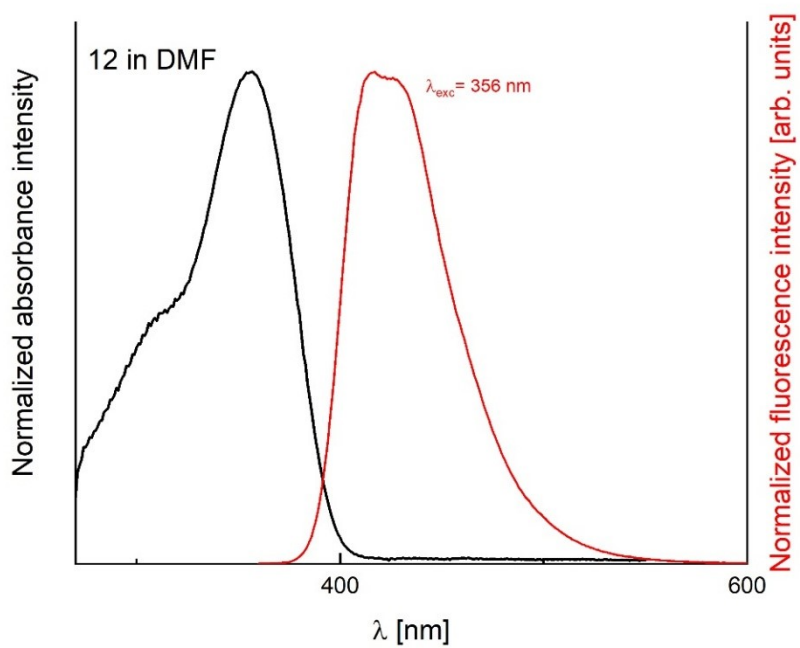


**Figure S93.** Absorption and emission spectra of TAPP **12** in DMF.

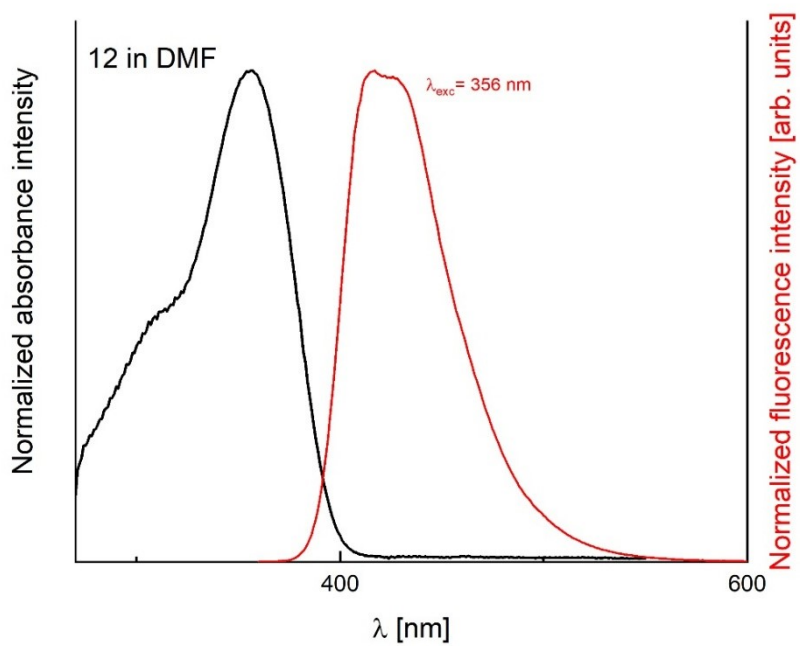


**Figure S94.** Absorption and emission spectra of TAPP **12** in DMSO.

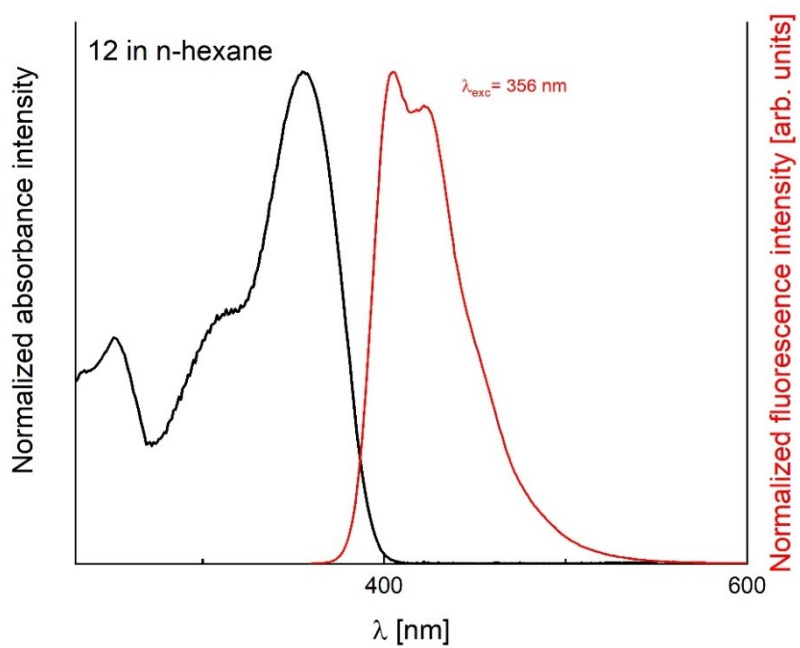


**Figure S95.** Absorption and emission spectra of TAPP **12** in hexane.

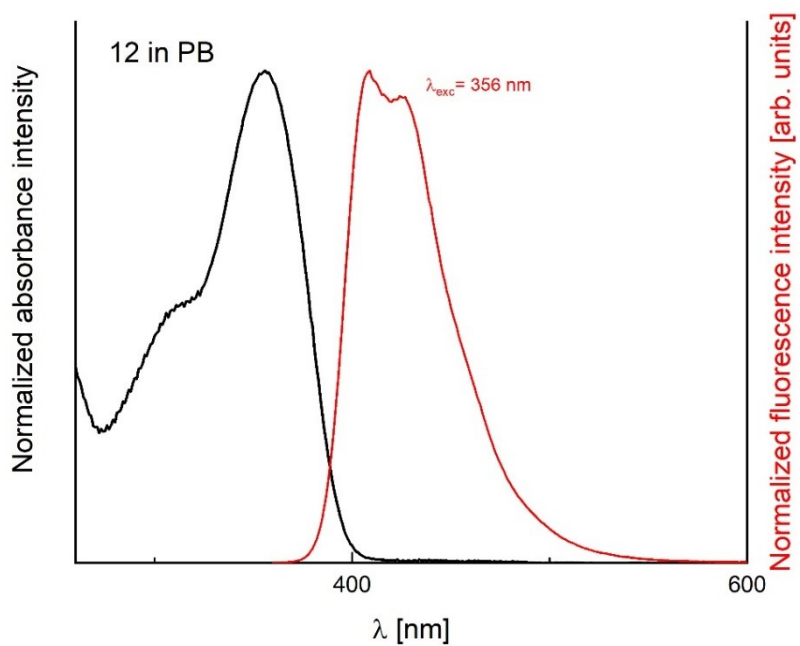


**Figure S96.** Absorption and emission spectra of TAPP **12** in propyl butyrate.

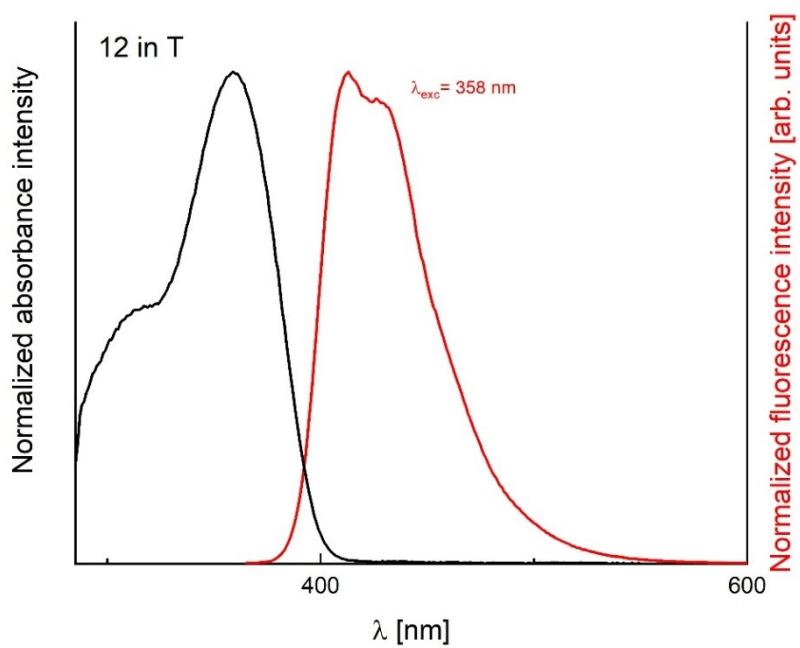


**Figure S97.** Absorption and emission spectra of TAPP **12** in toluene.

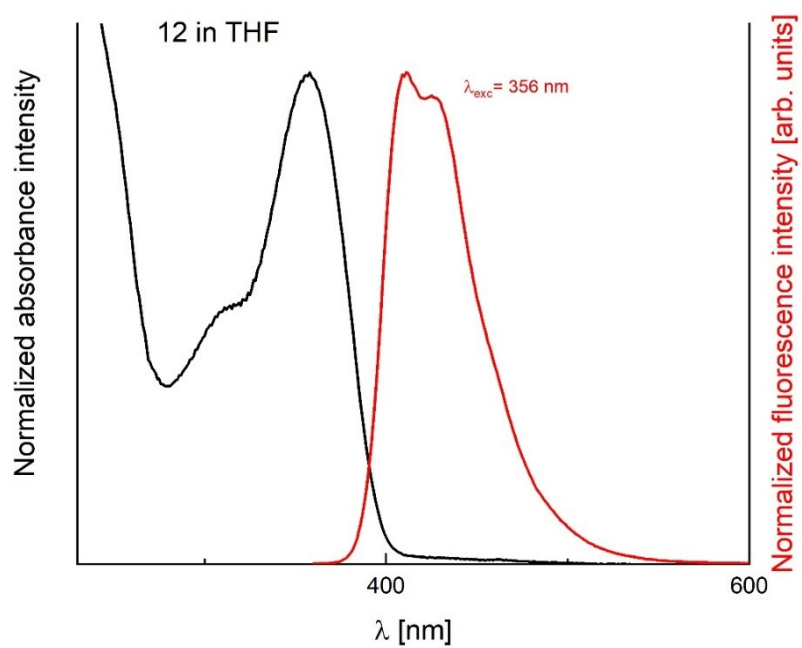


**Figure S98.** Absorption and emission spectra of TAPP **12** in THF.



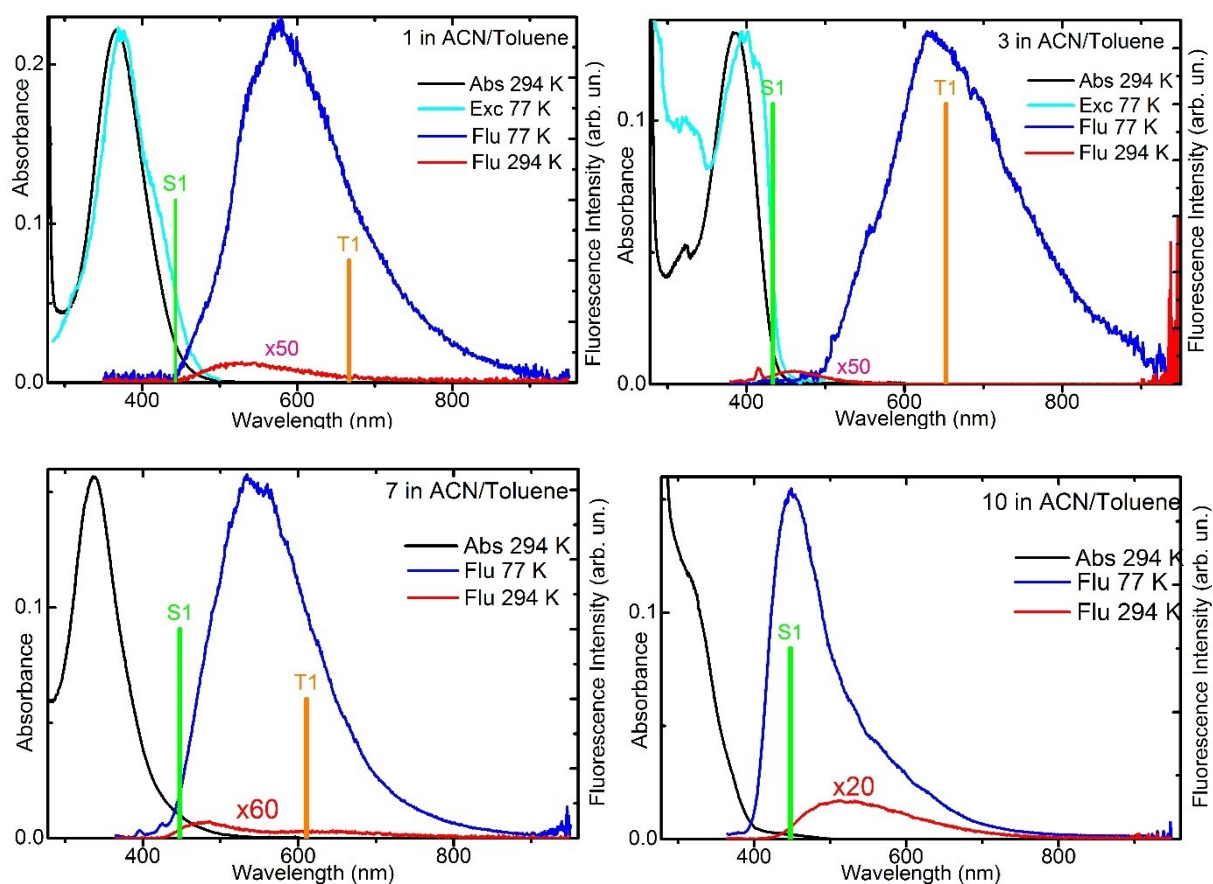
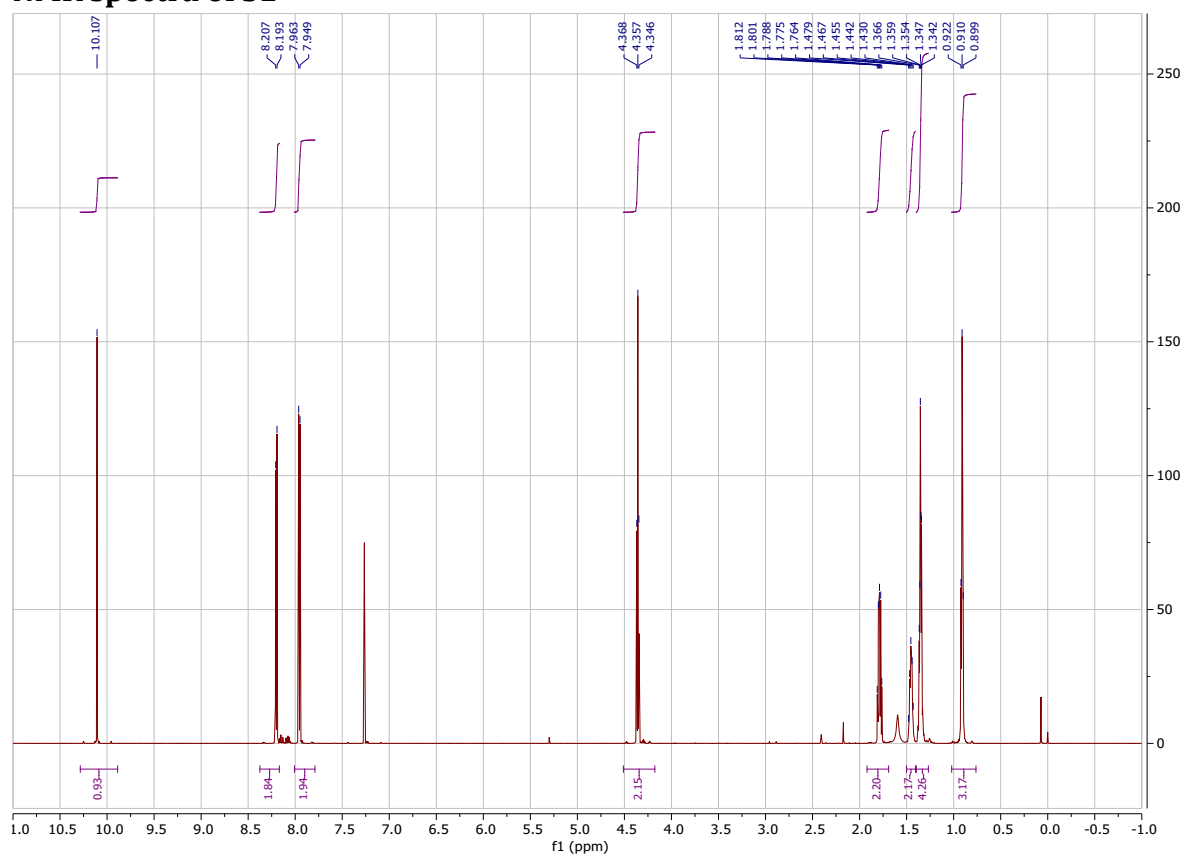


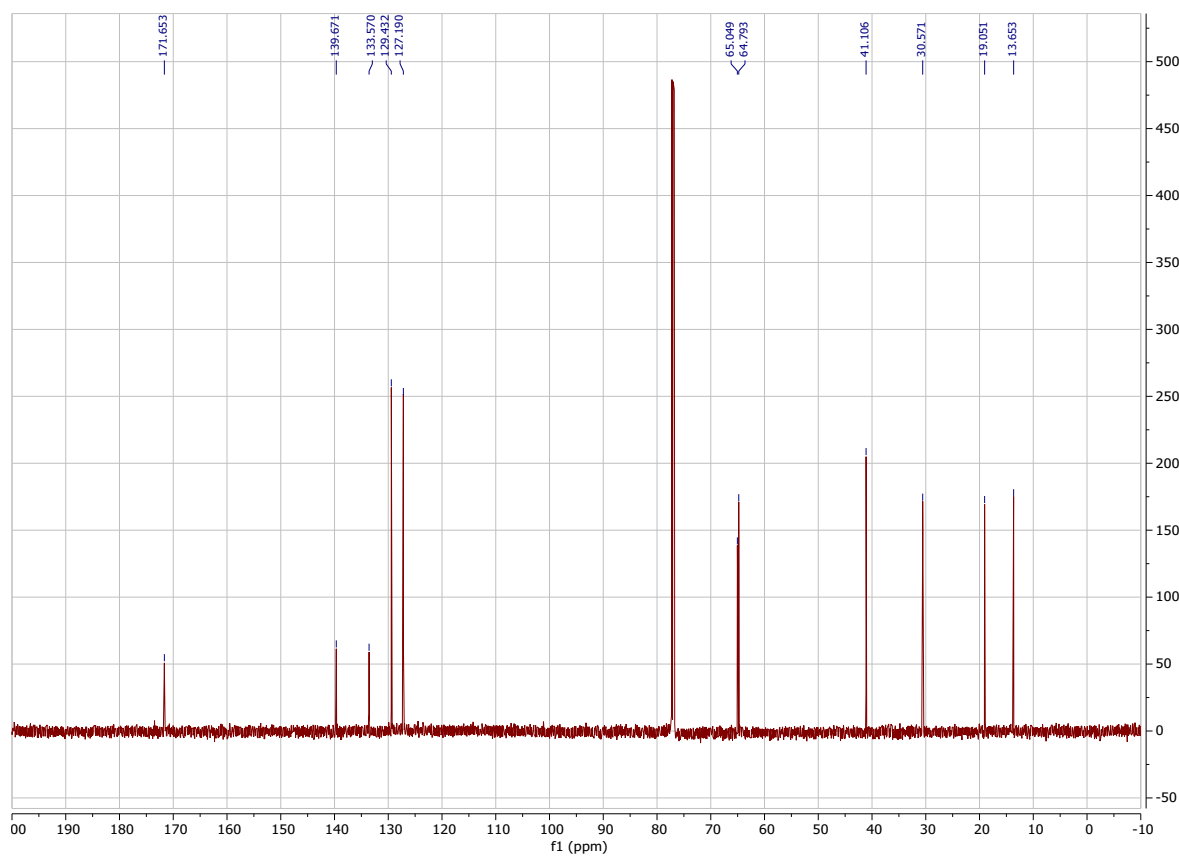
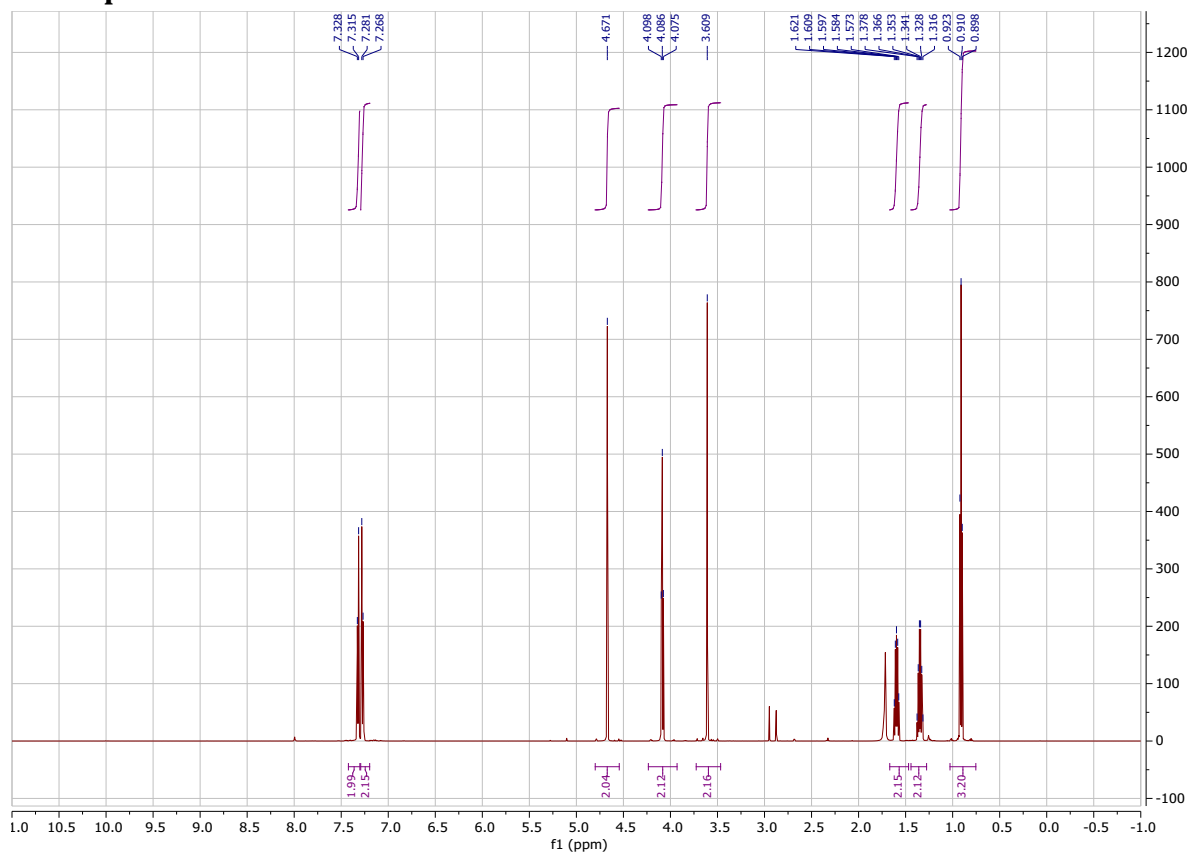
**Figure S99.** Optical spectra of **1**, **3**, **7** and **10** in CAN – toluene (10:1) mixture at room temperature and 77K: absorption at RT (black), fluorescence excitation at 77 K (magenta) and fluorescence at 77 K (blue line). Vertical bars represent transition energy calculated (with ADC(2) method and decreased with “standard“ value of 0.4 eV) for lowest singlet and triplet respectively (green bar for S<sub>1</sub> and orange bar for T<sub>1</sub>).

## 6. NMR spectra

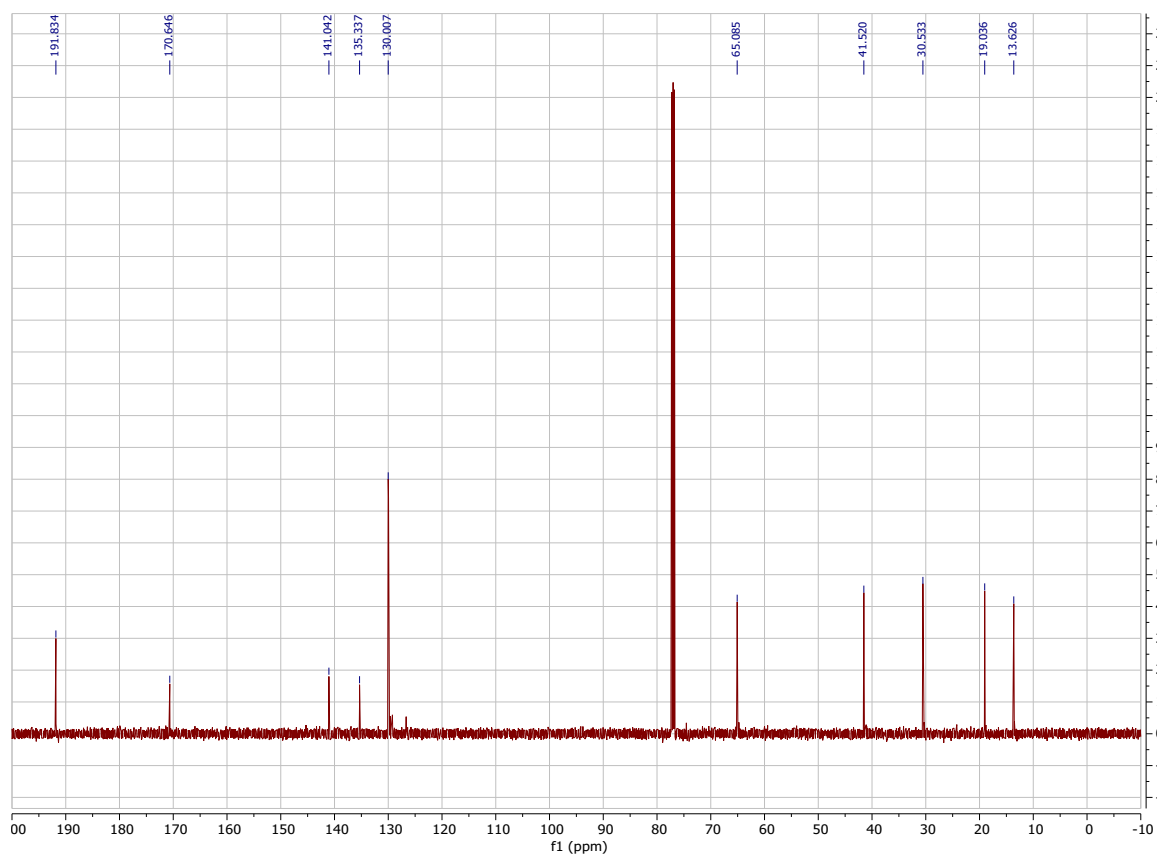
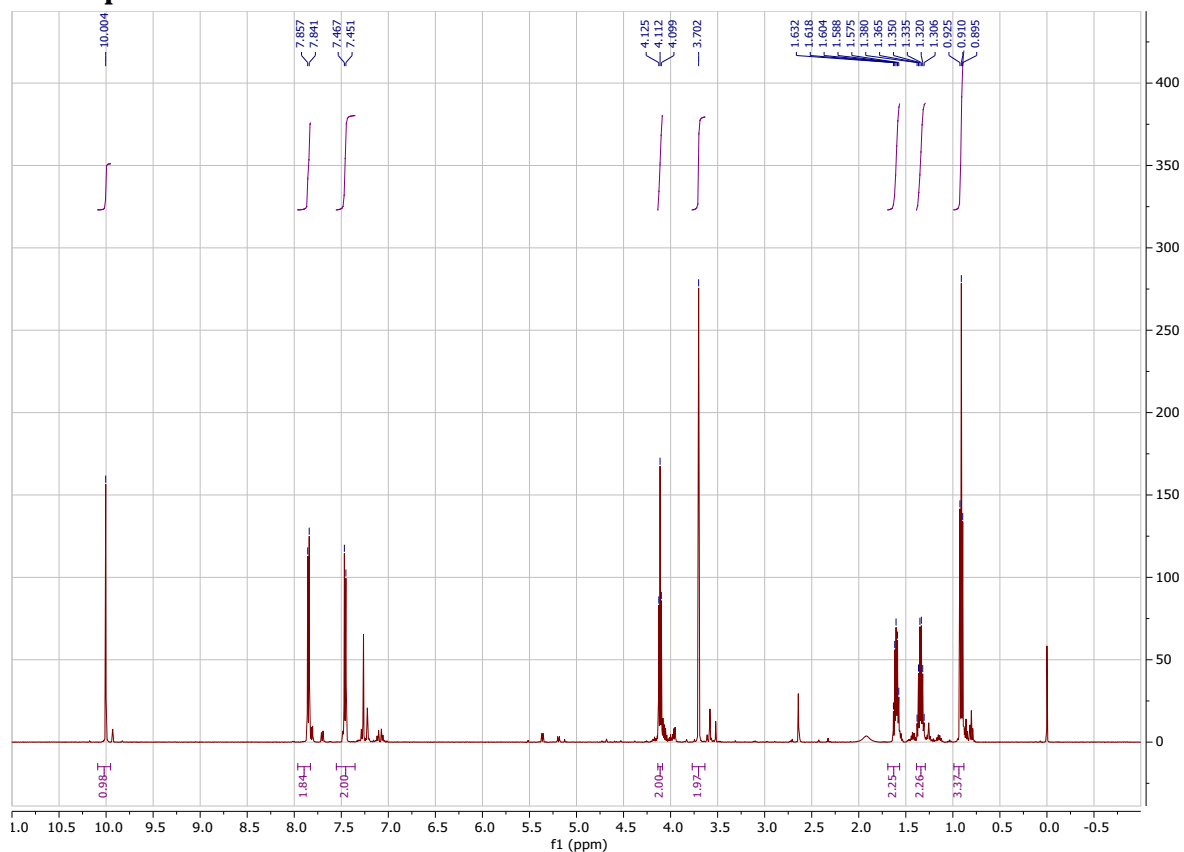
### NMR spectra of S1



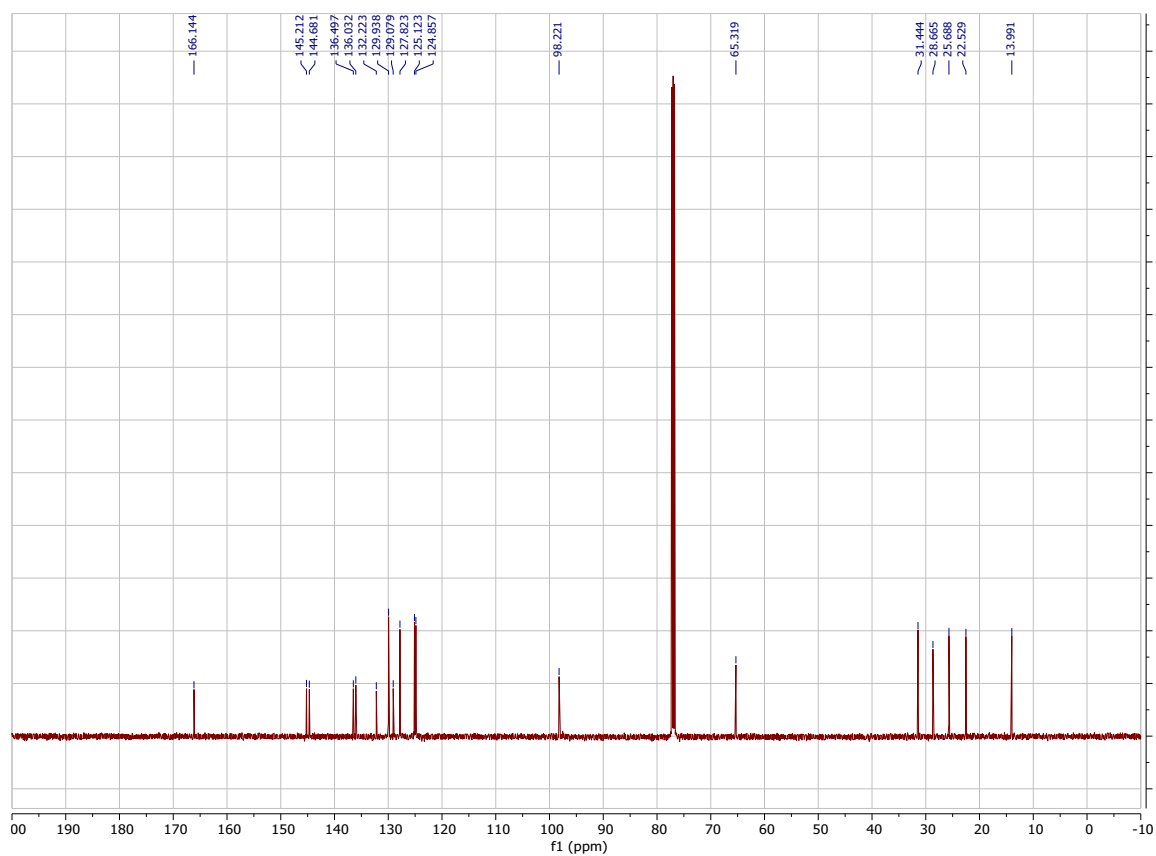
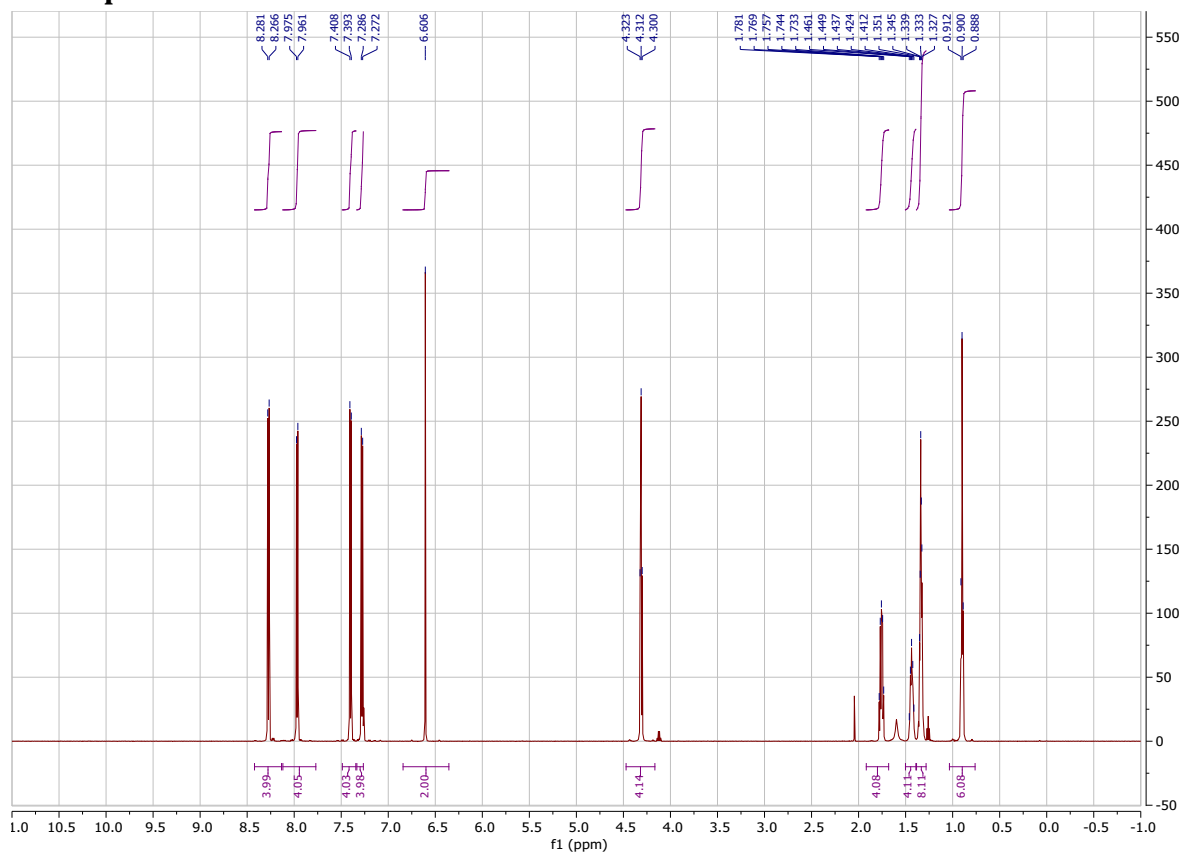
## NMR spectra of S2



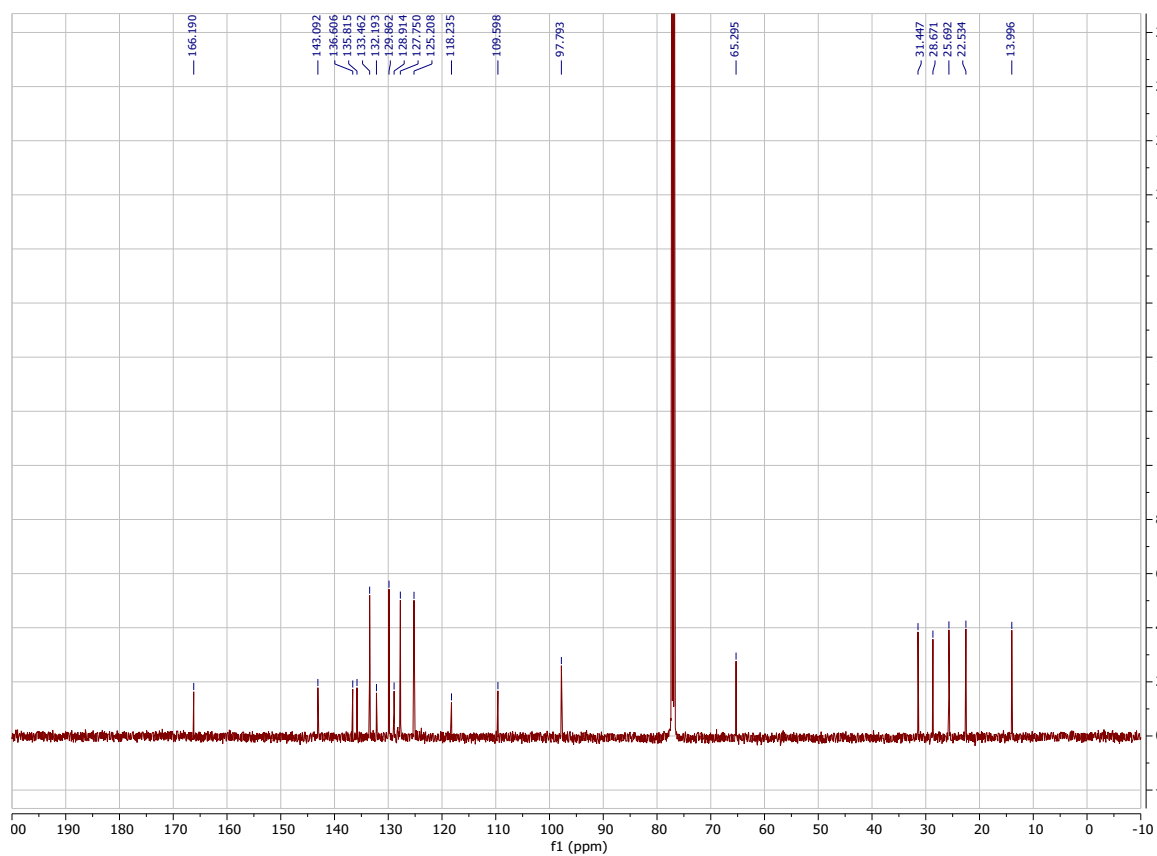
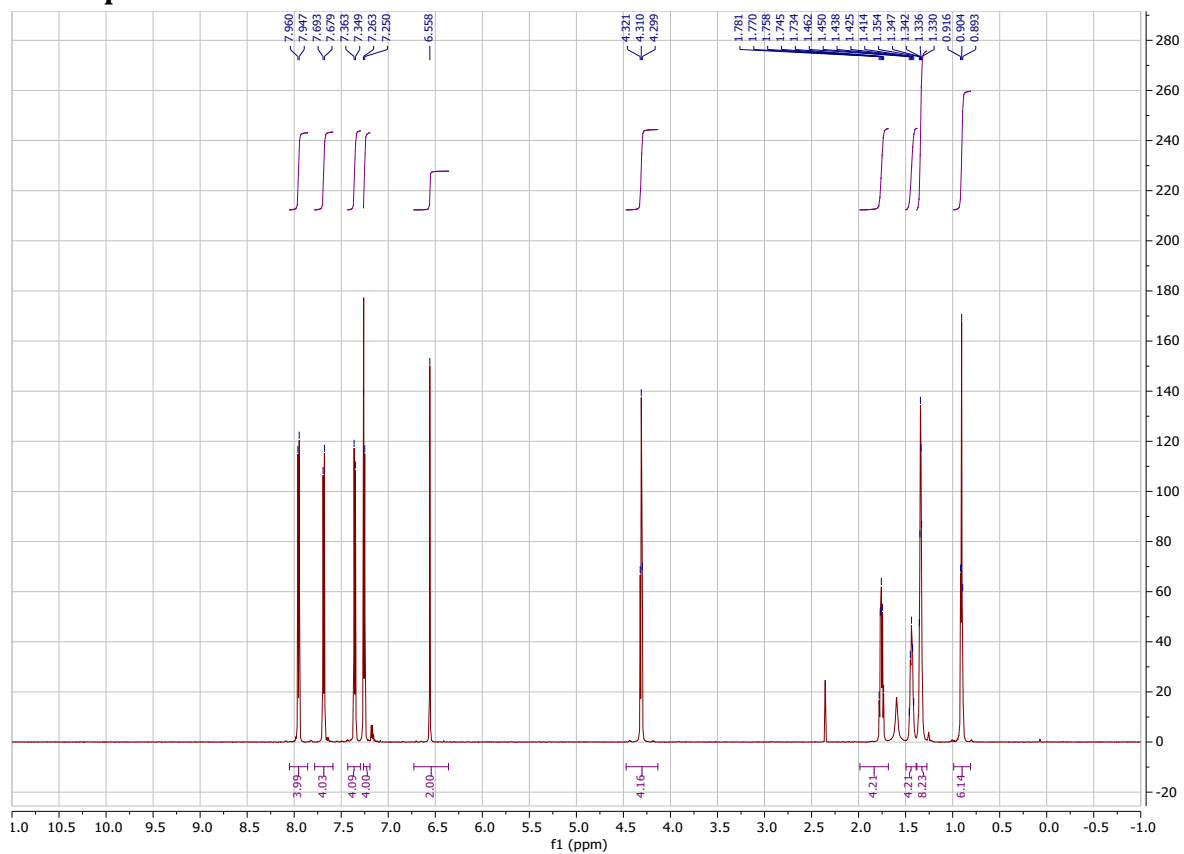
# NMR spectra of S3

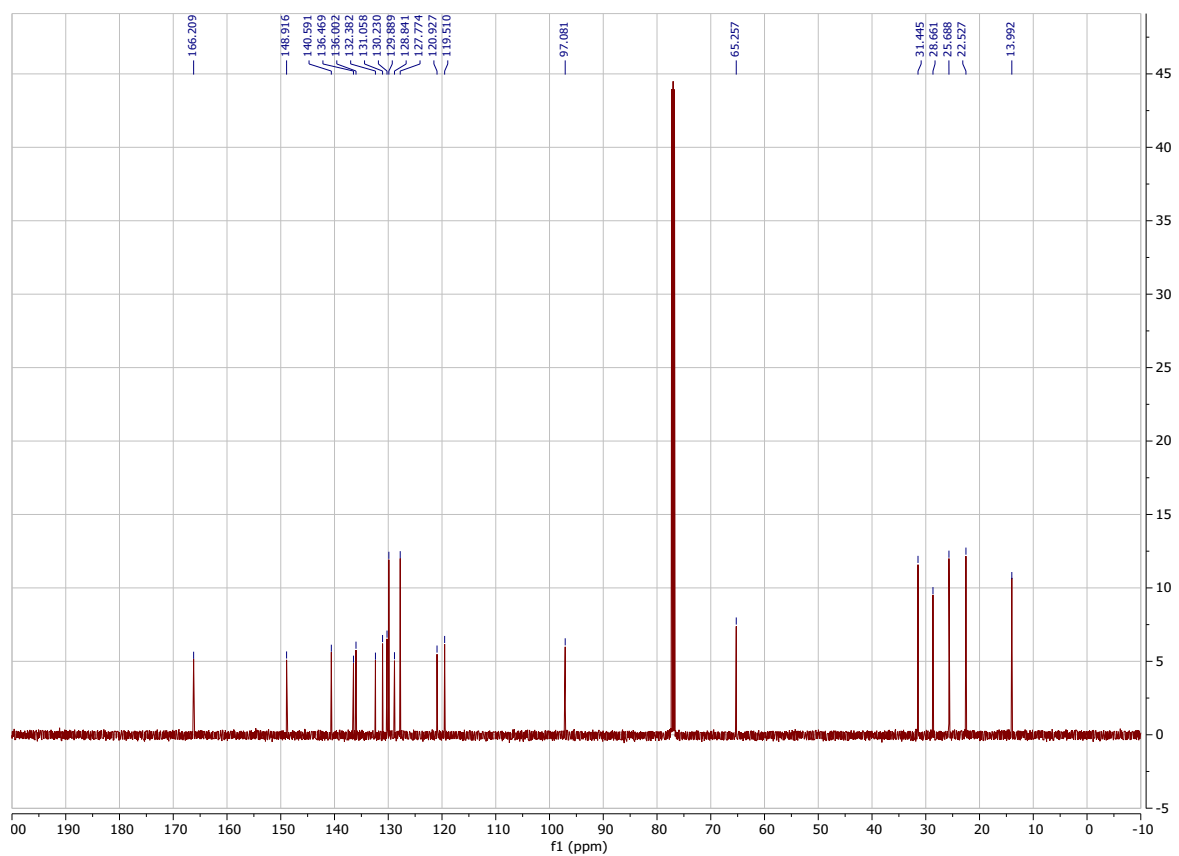


# NMR spectra of **1**

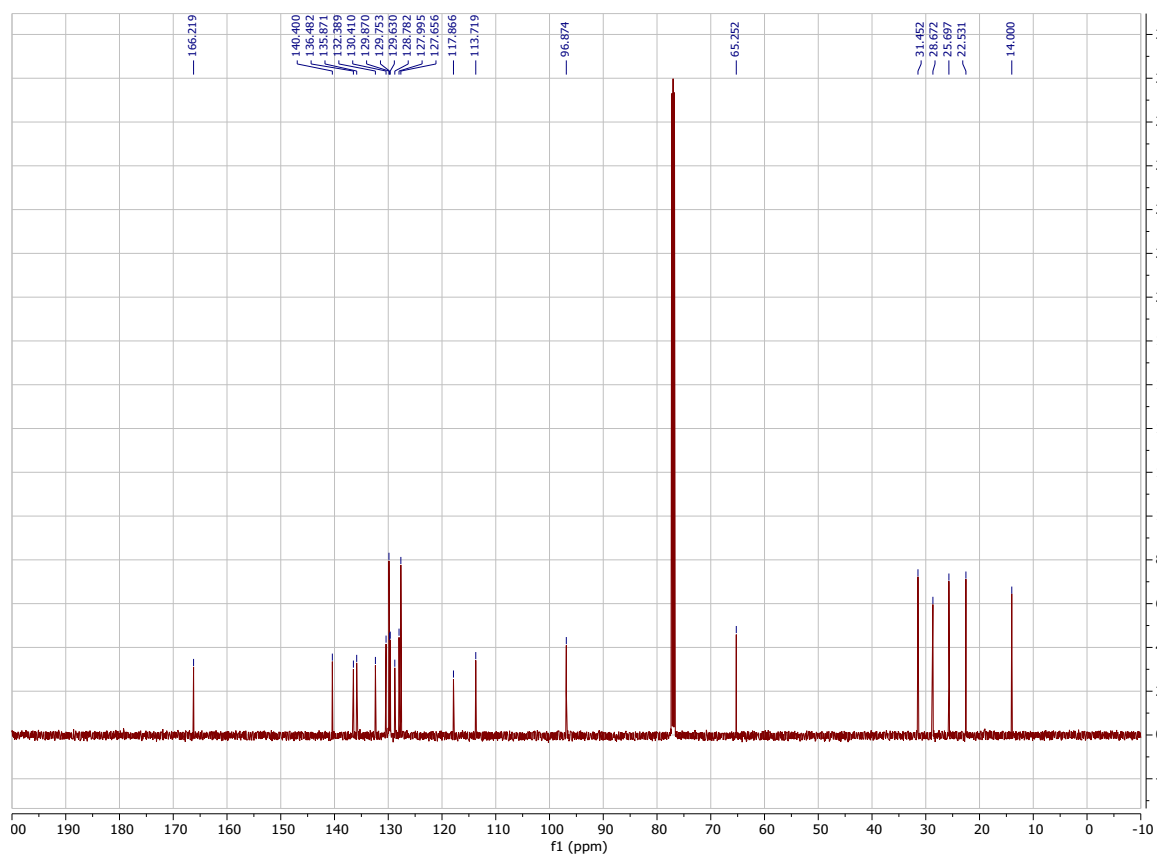
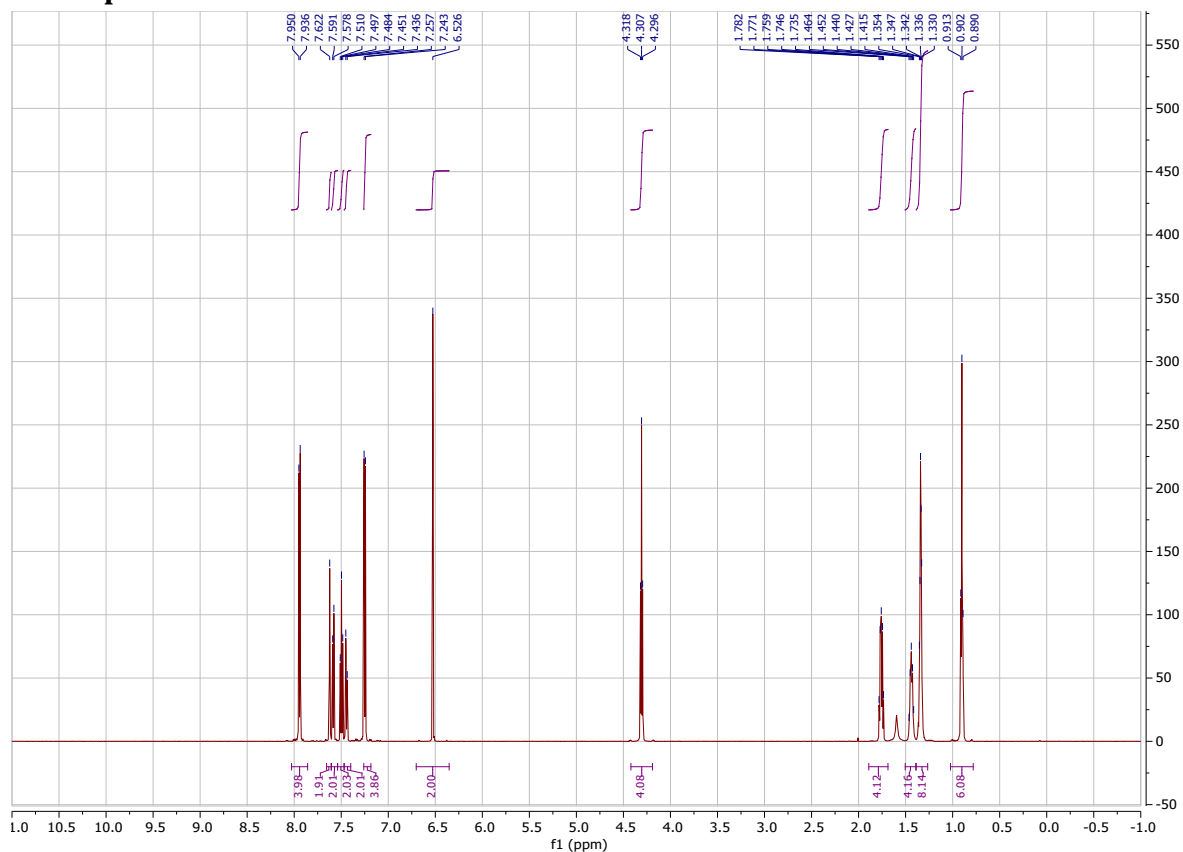


# NMR spectra of 2



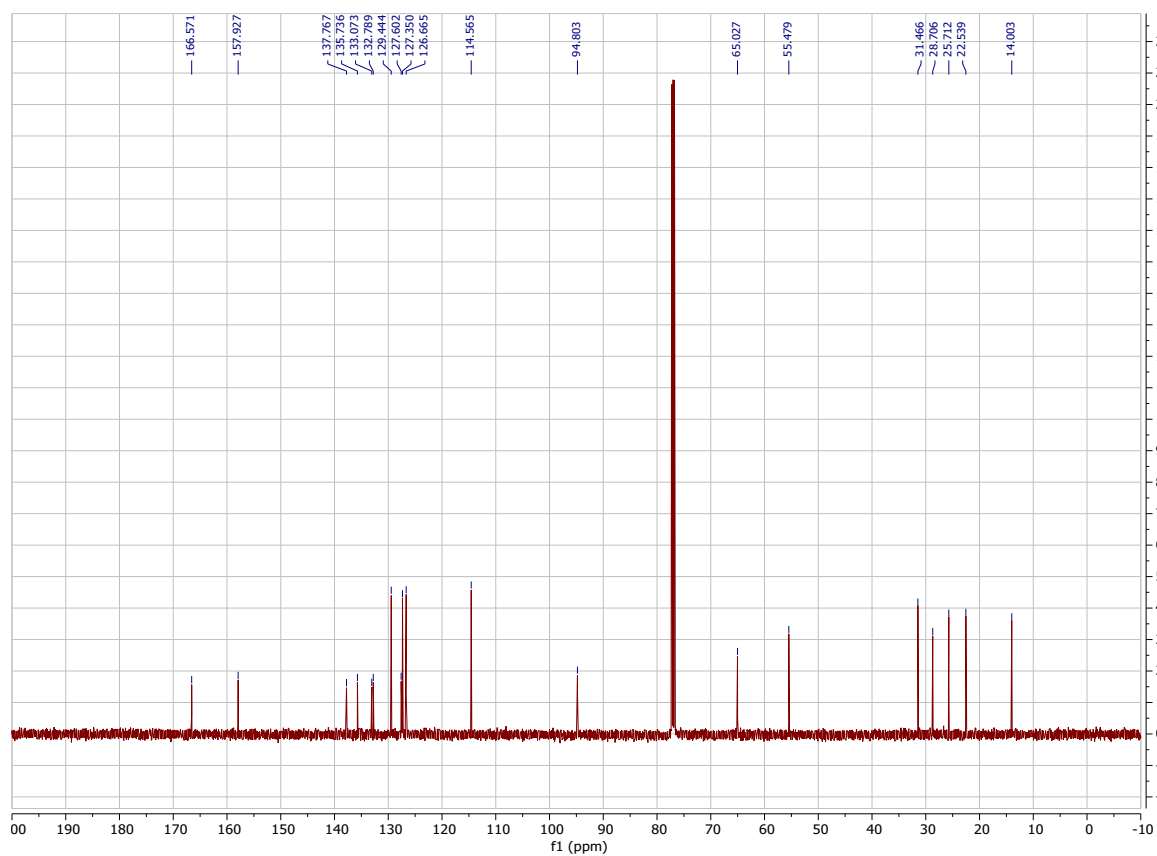
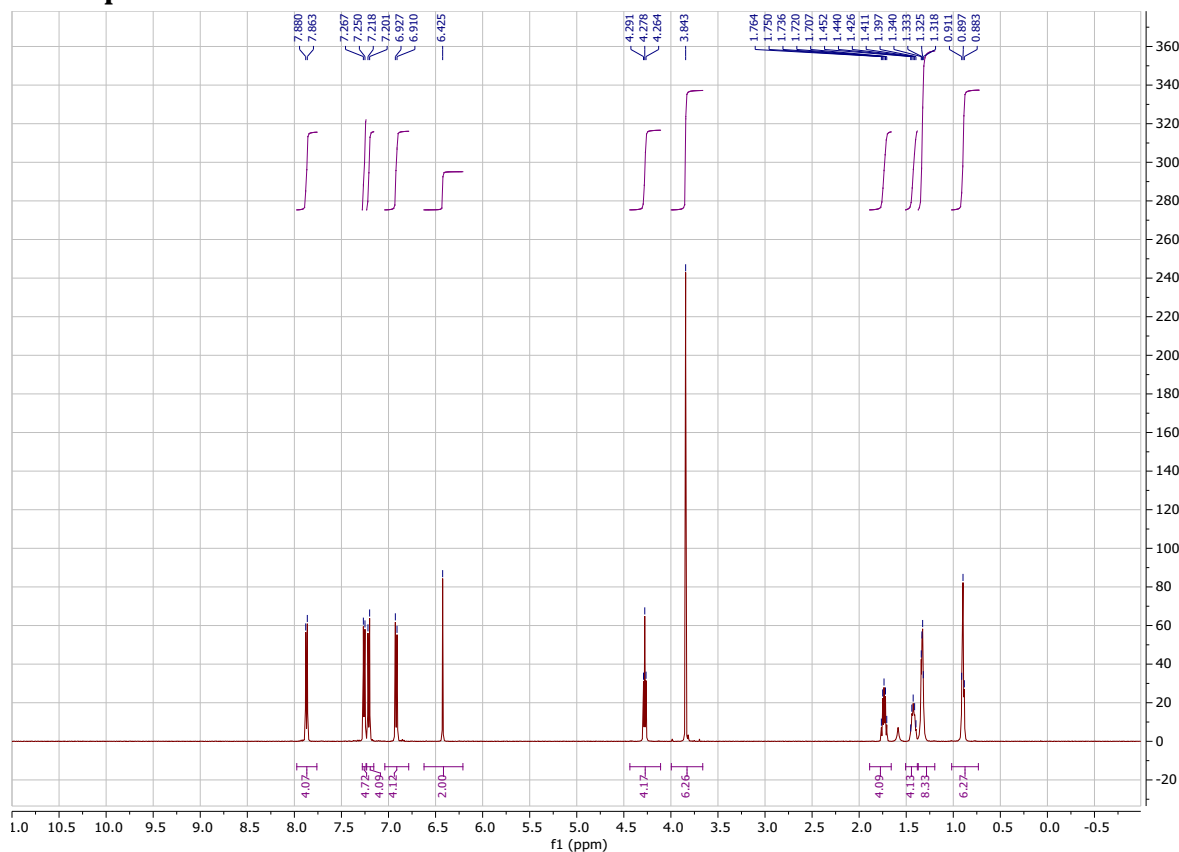


# NMR spectra of 4

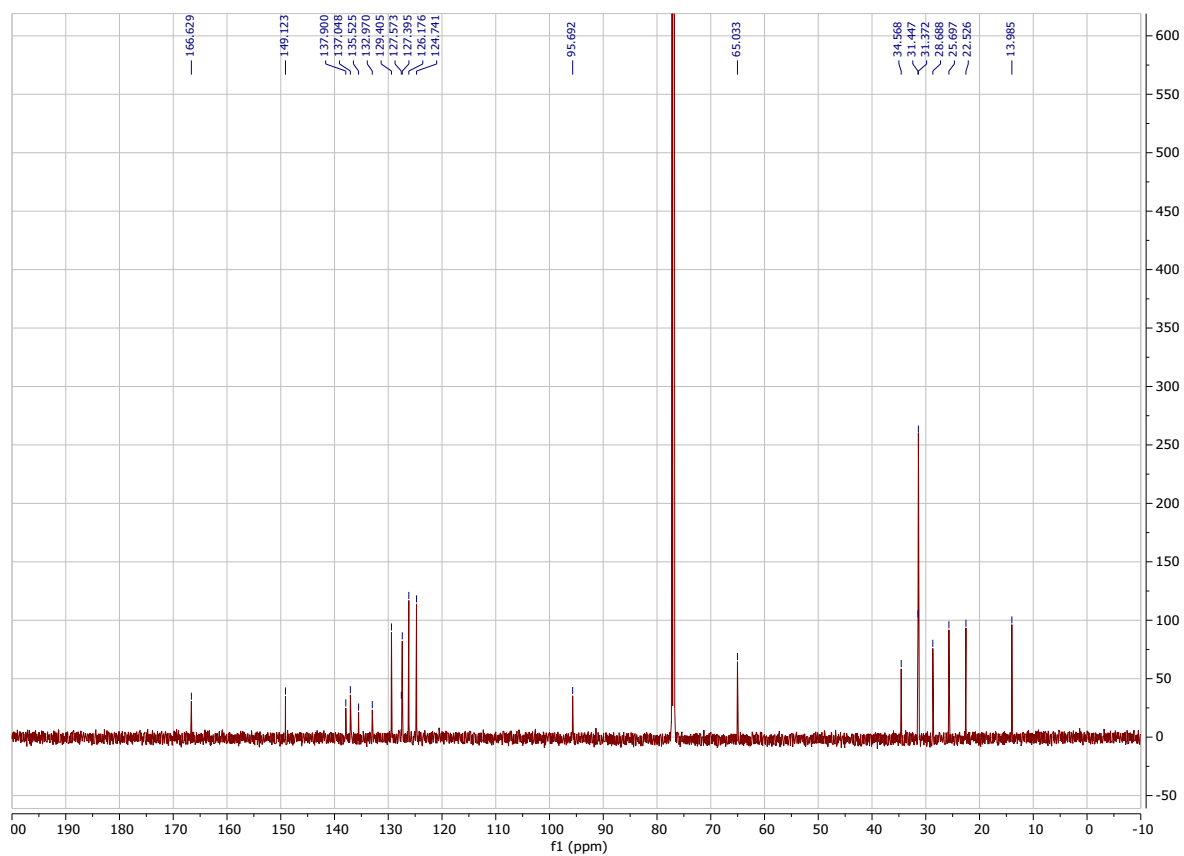
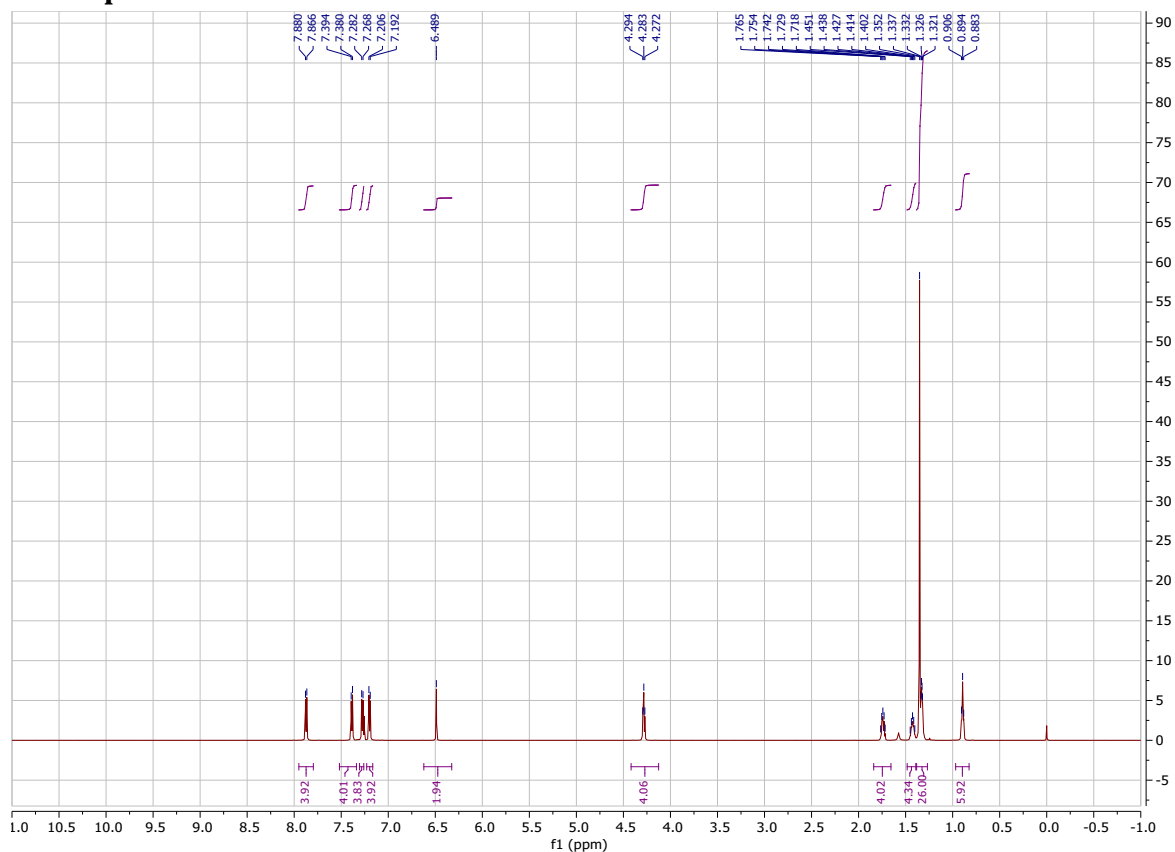




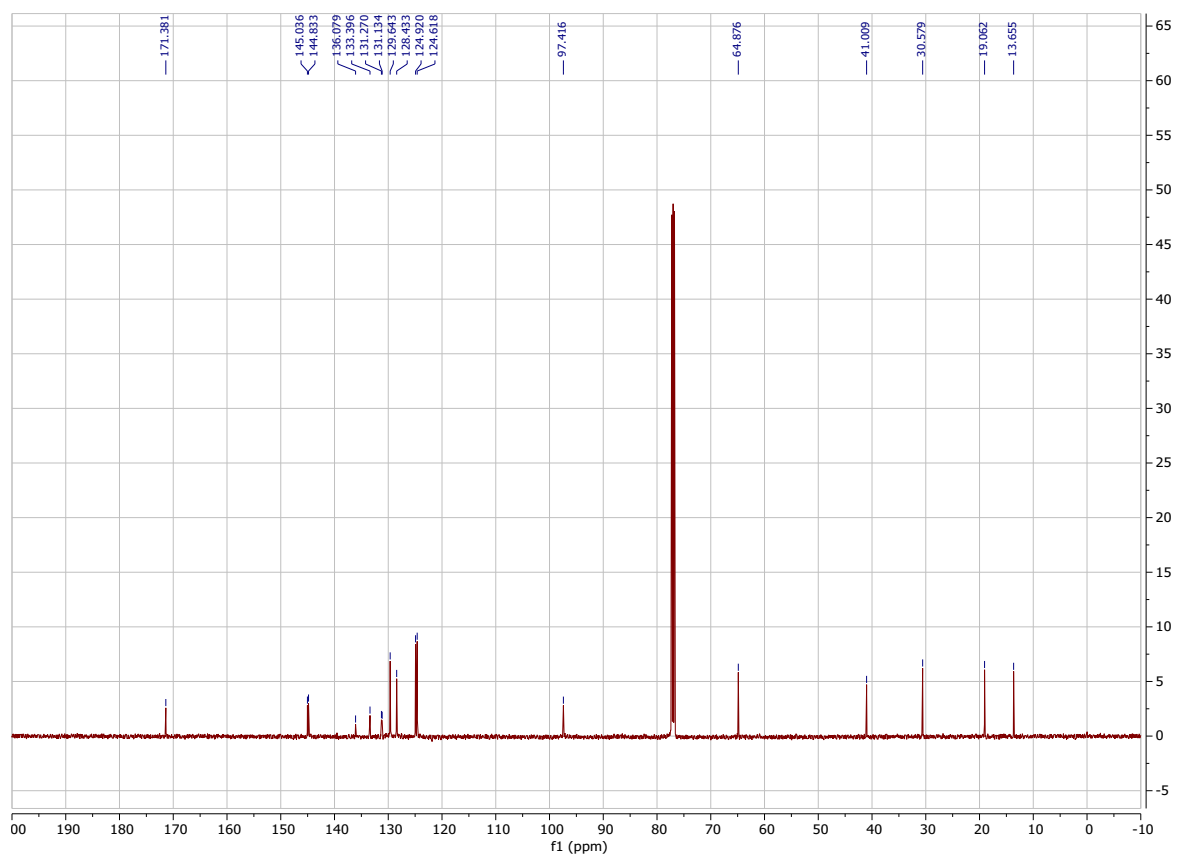
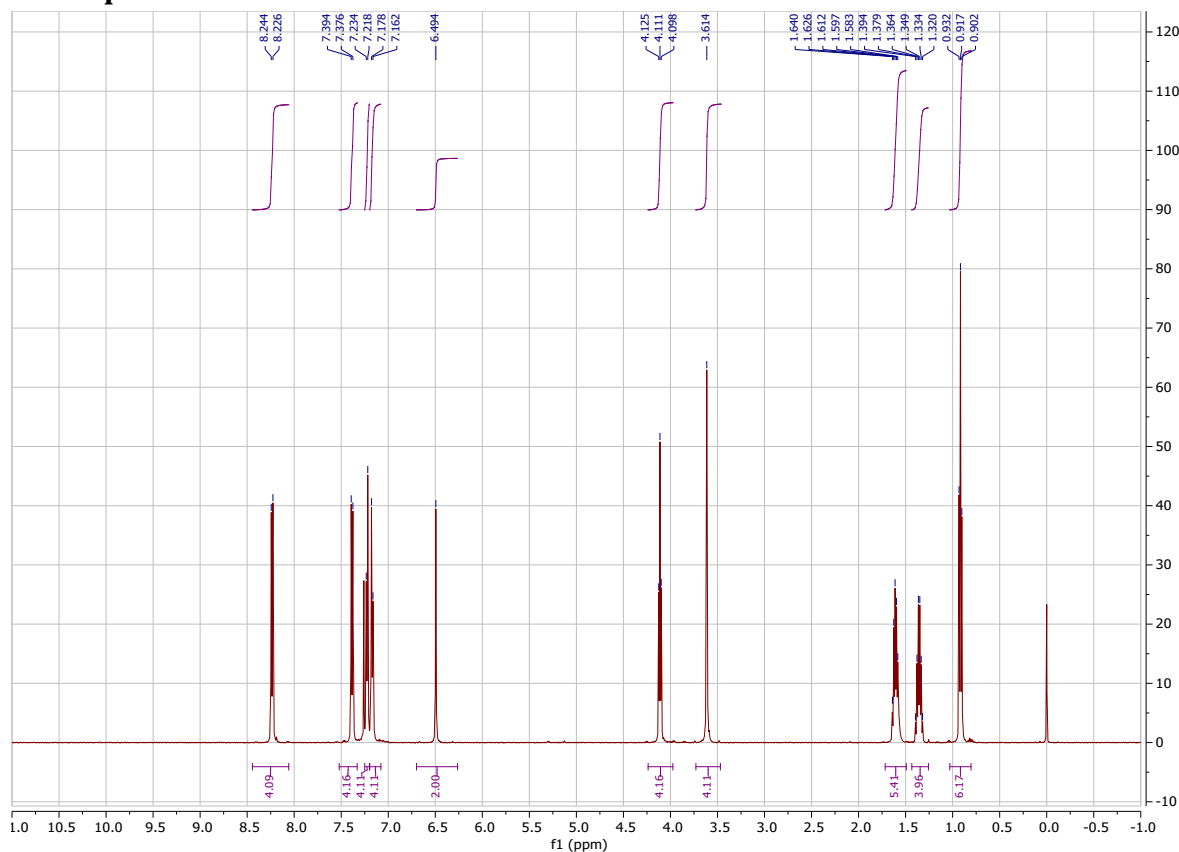
# NMR spectra of 5



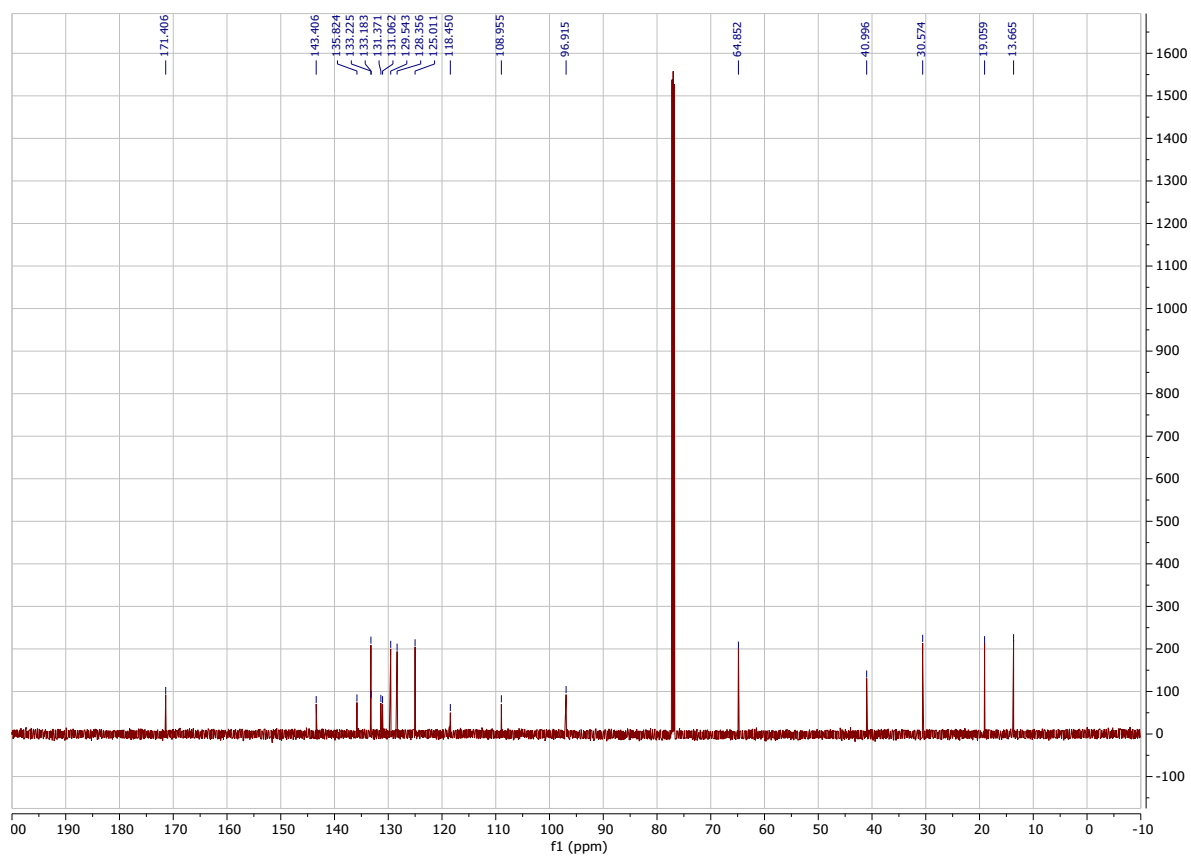
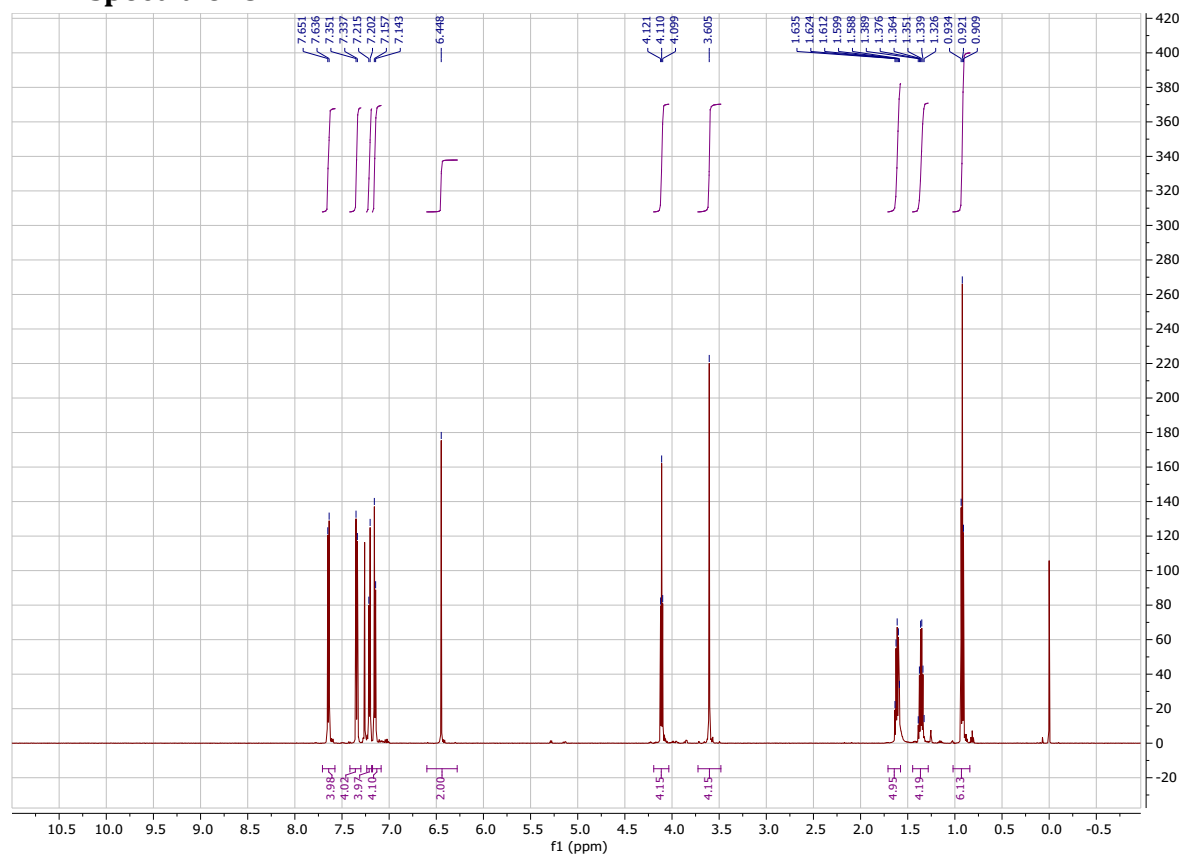
# NMR spectra of 6



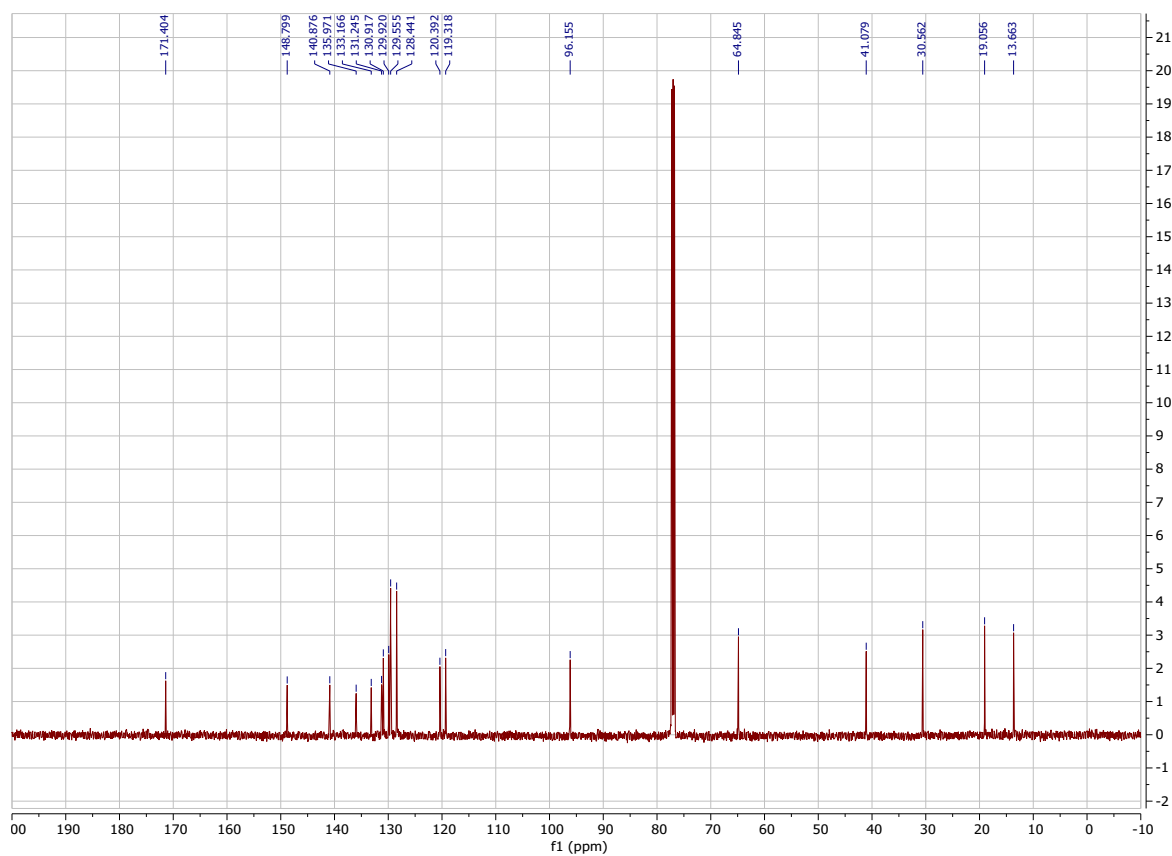
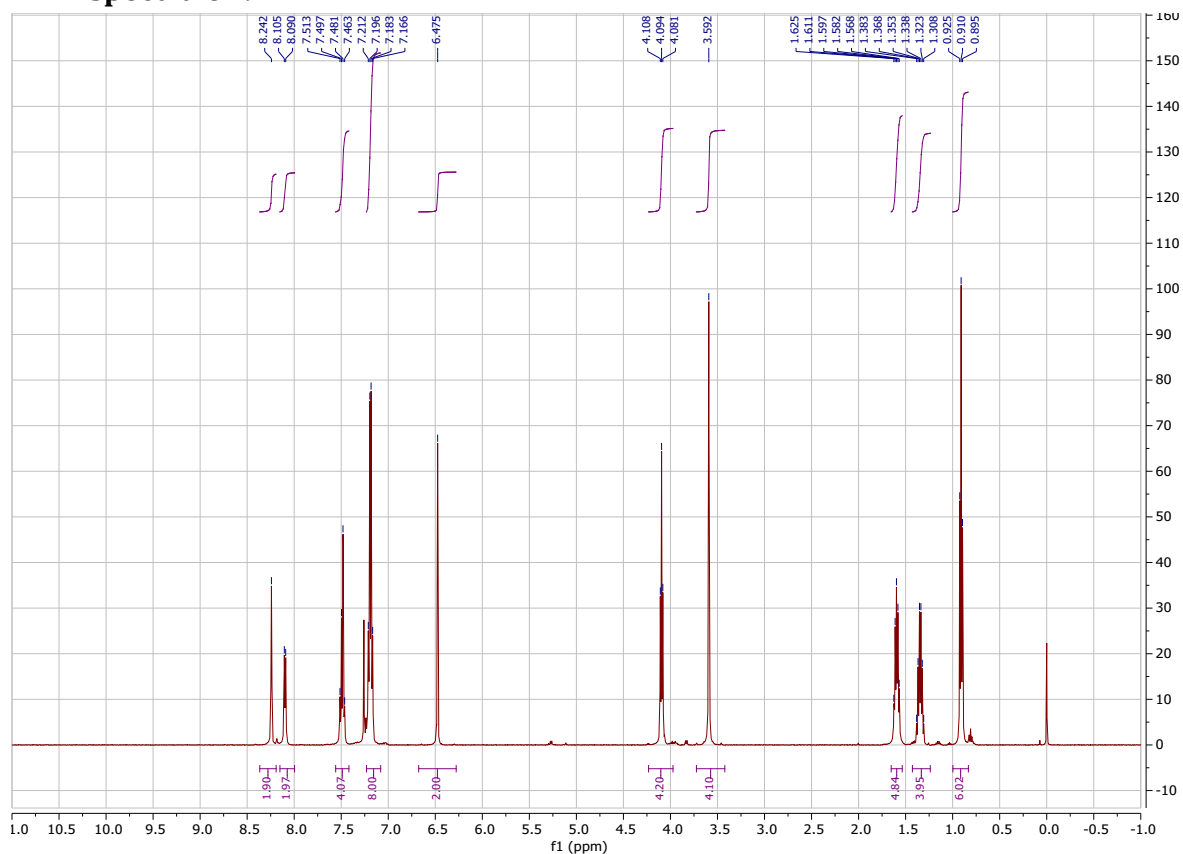
# NMR spectra of 7



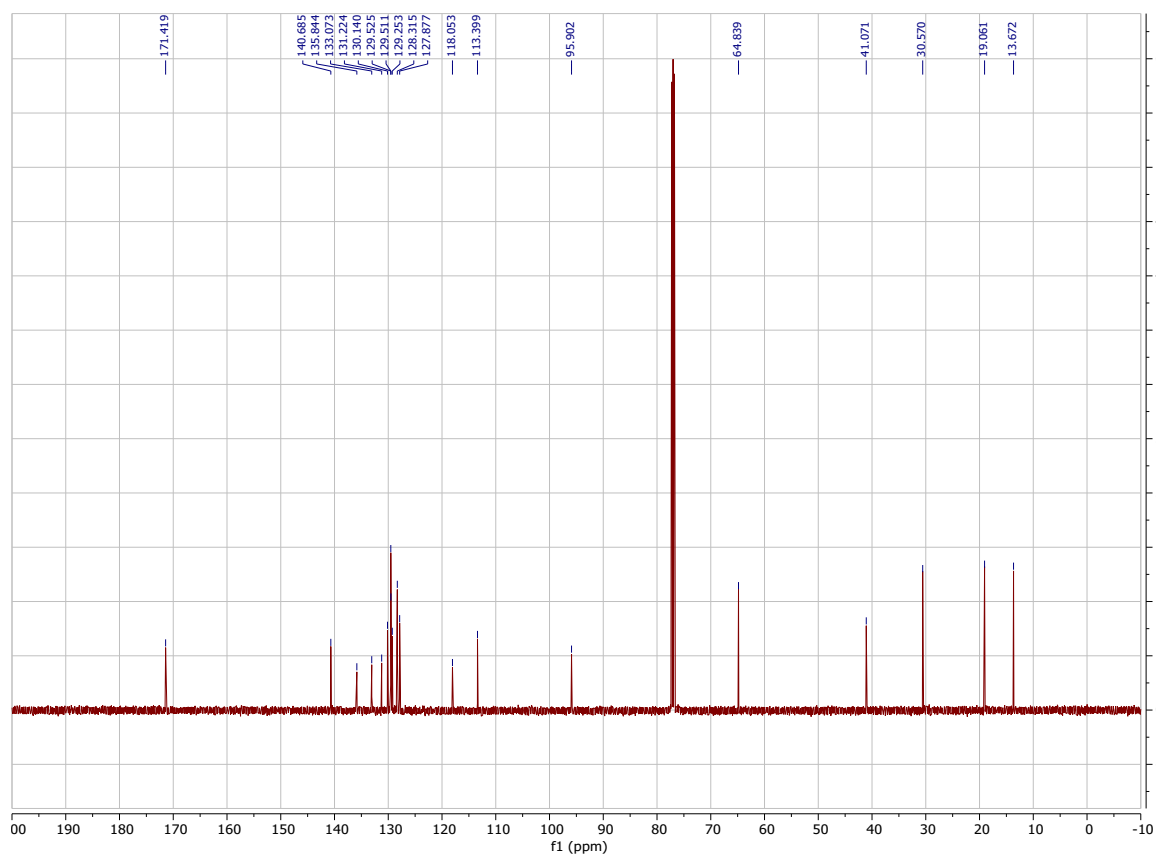
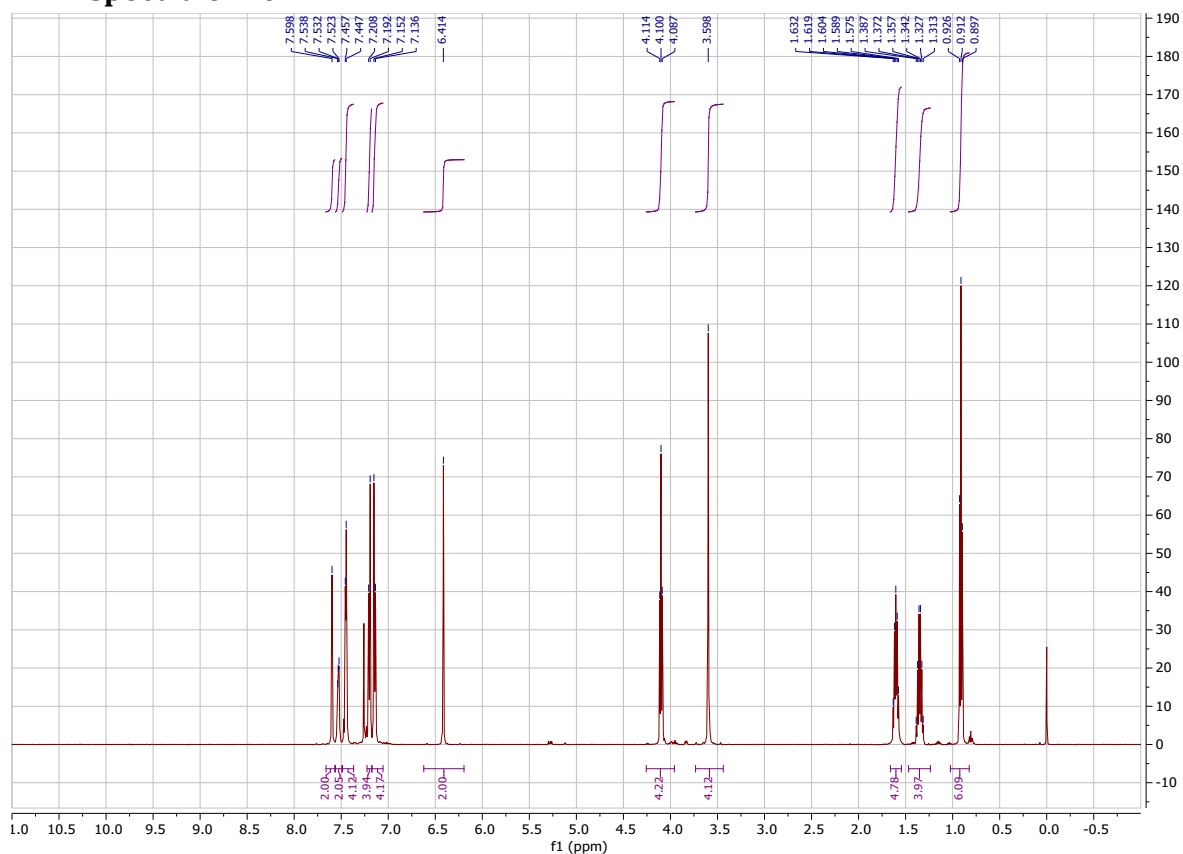
# NMR spectra of 8



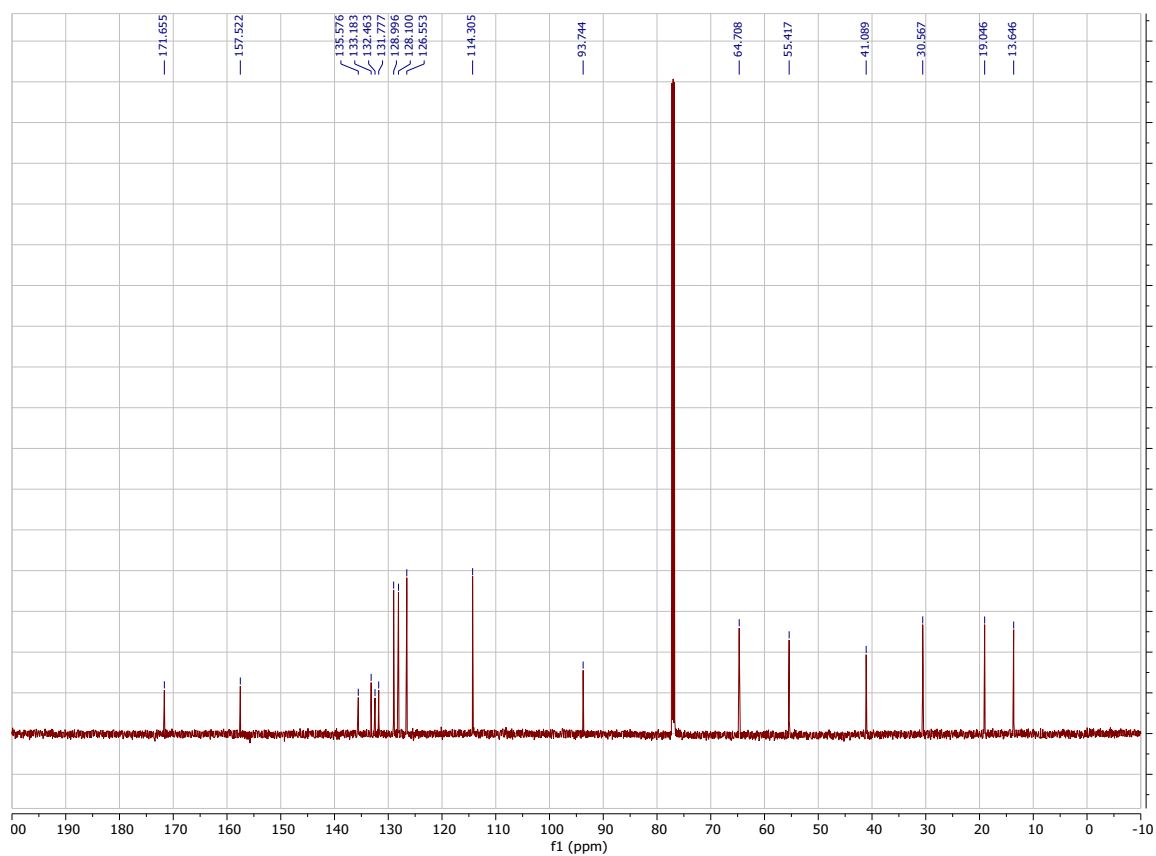
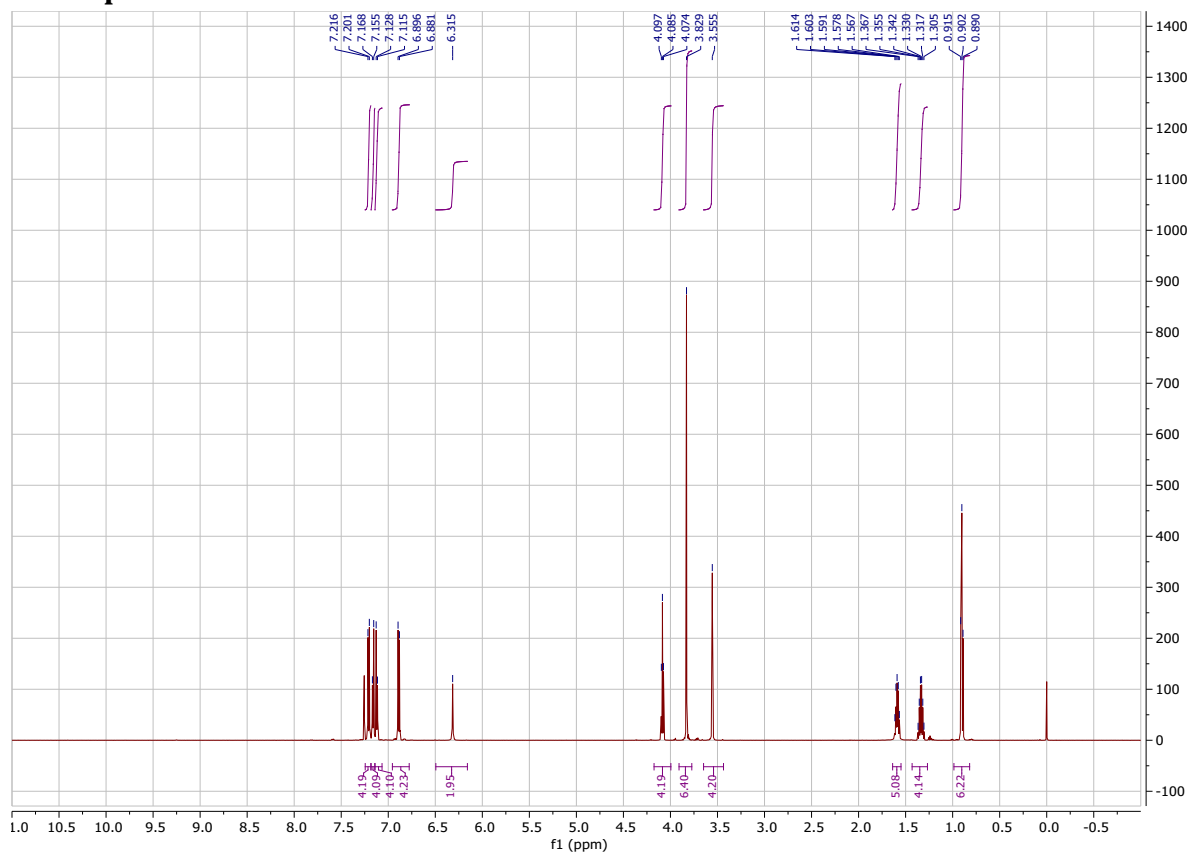
# NMR spectra of 9



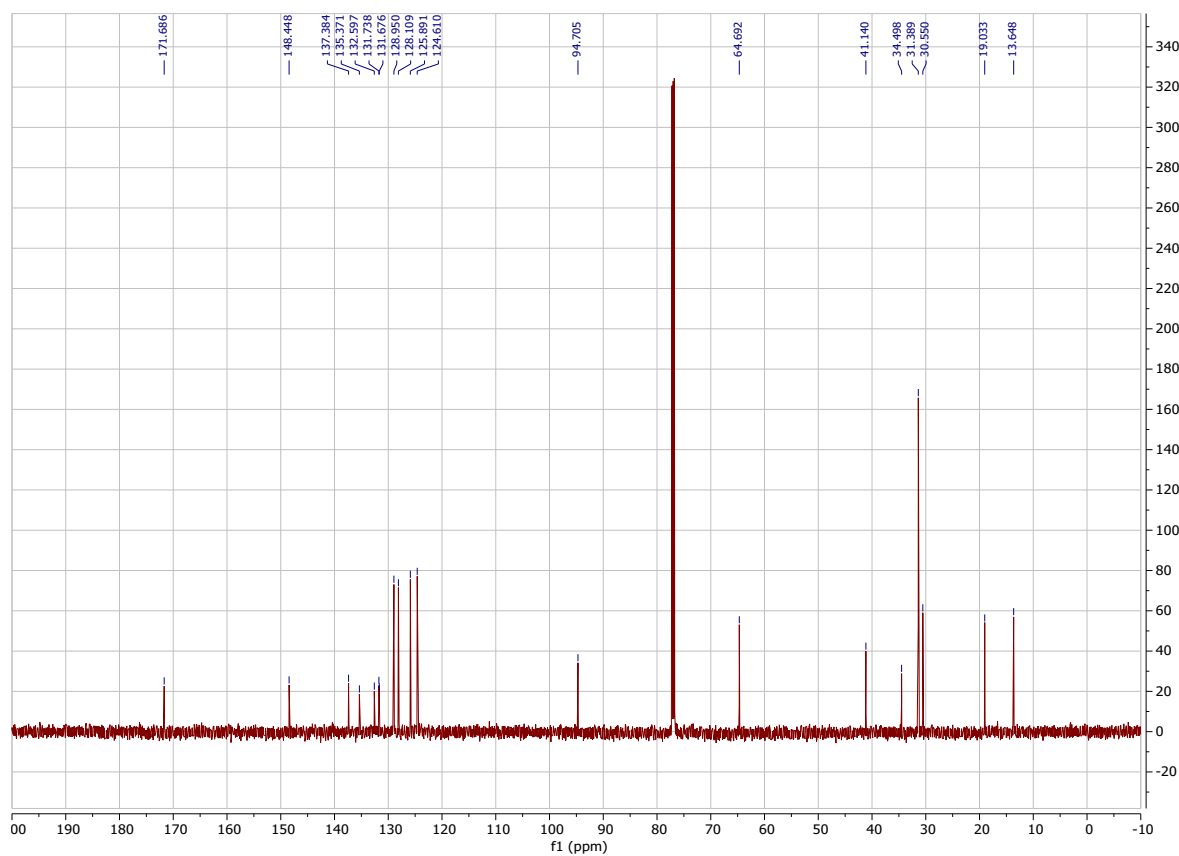
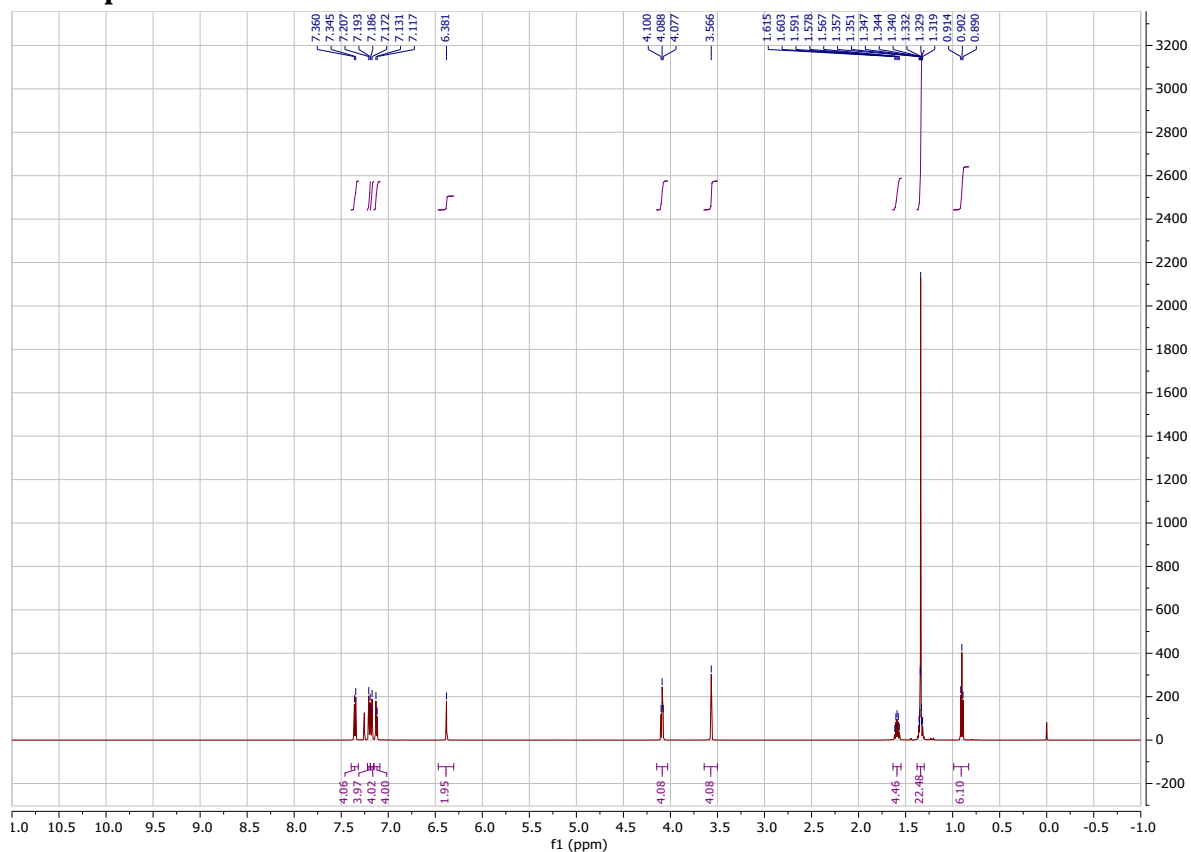
# NMR spectra of 10



# NMR spectra of 11



## NMR spectra of 12





## 7. References

1. Shao, X.-B., Jiang, X.-K., Wang, X.-Z., Li, Z.-T., Zhu, S.-Z. A novel strapped porphyrin receptor for molecular recognition. *Tetrahedron* **59**, 26, 4881–4889 (2003).
2. Omura, K., Swern, D. Oxidation of alcohols by “activated” dimethyl sulfoxide. a preparative, steric and mechanistic study. *Tetrahedron* **34**, 11, 1651–1660 (1978).
3. Tasior, M., Vakuliuk, O., Koga, D., Koszarna, B., Górski, K., Grzybowski, M., Kielesiński, Ł., Krzeszewski, M., Gryko, D. T. Method for the Large-Scale Synthesis of Multifunctional 1,4-Dihydro-pyrrolo[3,2-*b*]pyrroles. *J. Org. Chem.* **85**, 21, 13529–13543 (2020).
4. TURBOMOLE V7.2. <http://www.turbomole.com>, 2017; Last accessed 11 March 2025.
5. Burow, A. M., Sierka, M., Mohamed, F. Resolution of identity approximation for the Coulomb term in molecular and periodic systems. *J. Chem. Phys.* **131**, 21, 214101 (2009).
6. Dunning, T. H. Gaussian basis sets for use in correlated molecular calculations. I. The atoms boron through neon and hydrogen. *J. Chem. Phys.* **90**, 2, 1007–1023 (1989).
7. Weigend, F. RI-MP2: first derivatives and global consistency. *Theor. Chem. Acc.* **97**, 331–340 (1997).
8. Schirmer, J. Beyond the random-phase approximation: A new approximation scheme for the polarization propagator. *Phys. Rev. A* **26**, 5, 2395–2416 (1982).
9. Trofimov, A. B., Schirmer, J. An efficient polarization propagator approach to valence electron excitation spectra. *J. Phys. B At. Mol. Opt. Phys.* **28**, 12, 2299–2324 (1995).
10. Hättig, C. Structure Optimizations for Excited States with Correlated Second-Order Methods: CC2 and ADC(2). in *Advances in Quantum Chemistry* vol. 50 37–60 (Elsevier, 2005).
11. Klamt, A., Schüürmann, G. COSMO: a new approach to dielectric screening in solvents with explicit expressions for the screening energy and its gradient. *J Chem Soc Perkin Trans 2* **5**, 799–805 (1993) doi:10.1039/P29930000799.
12. McRae, E. G. Theory of Solvent Effects on Molecular Electronic Spectra. Frequency Shifts. *J. Phys. Chem.* **61**, 5, 562–572 (1957).
13. Kumar, J., Kumar, N., Hota, P. K. Optical properties of 3-substituted indoles. *RSC Adv.* **10**, 47, 28213–28224 (2020).